Supporting Information

Solid-state Molecular Organometallic Catalysis in Gas/Solid Flow (Flow-SMOM) as Demonstrated by Efficient Room Temperature and Pressure 1–Butene Isomerization

Antonio J. Martínez-Martínez,[a†] Cameron G. Royle,[a,b] Samantha K. Furfari,[a,b] Kongkiat Suriye,[c] Andrew S. Weller[a,b]*

[a] Department of Chemistry, Chemistry Research Laboratories, University of Oxford, Oxford, OX1 3TA, U. K

[b] Department of Chemistry, University of York, Heslington, York, YO10 5DD, U. K.

[c] SCG Chemicals, 1 Siam Cement Road, Bangsue, Bangkok 10800, Thailand.

†Present Address: CIQSO– Centre for Research in Sustainable Chemistry, CIQSO, University of Huelva, 21007 Huelva, Spain

Email: andrew.weller@york.ac.uk

Table of Contents

S1 Experimental Details

S1.1 General Methods and Reagents

All manipulations, unless otherwise stated, were performed under an atmosphere of argon using standard Schlenk techniques on a dual vacuum/inlet manifold or by employment of an MBraun glovebox. Evacuation refers to a pressure equal or lower than 1×10^{-2} mbar, measured with a vacuum gauge and display fitted to a Schlenk line. Glassware was dried in an oven at 130 °C overnight prior to use.

n-pentane, *n*-hexane, and CH_2Cl_2 were dried using an MBraun SPS-800 solvent purification system and degassed by three freeze-pump-thaw cycles. CD_2Cl_2 was dried by stirring over CaH_2 overnight before vacuum distillation, degassed by three freeze-pump-thaw cycles and stored over activated molecular sieves (3 Å). 1,2-difluorobenzene and fluorobenzene were stirred over Al_2O_3 for two hours before stirring over CaH_2 overnight, vacuum distillation, and subsequent three-fold freeze-pump-thawing. CD_3CN was distilled over a small amount of P_2O_5 before subsequent three-fold freeze-pump-thawing. 2,5-norbornadine (bicyclo[2.2.1]hepta-2,5-diene, NBD) was purchased from Sigma-Aldrich, distilled over freshly cut small pieces of sodium metal before subsequent three-fold freeze-pump thawing. Neat 1-butene and isobutene were supplied by CK Special Gases Ltd. (UK) and used as received. *Cis*-2-butene and *trans*-2-butene (2% balanced with N_2) were supplied by Air Liquide (UK) and used as received. High purity hydrogen gas (≥99.9%) was employed in the gas/solid and gas/solution transformations. All other chemicals were purchased from commercial sources and used as received. $RhCl_3 \cdot (H_2O)_n$ was purchased from Precious Metals Online PMO Pty Ltd and used as received. Complexes **1**, **2**, **4**, **5**,[123] $[(COD)RhCl]_2$,[4] and 1,2-bis(di-*tert*-butylphosphino)ethane (*dtbpe*)[5] were synthesised according to pre-existing procedures. $Na[BAr^F_4]$ was prepared according to an improved synthetic protocol.[6]

Elemental microanalyses were all carried out by Dr Stephen Boyer of London Metropolitan University.

S1.2 Solution NMR Spectroscopic Data

Solution NMR data were collected on either a Bruker Avance III NMR spectrometer (equipped with a 11.75 T magnet) or a Bruker Avance III HD nanobay NMR spectrometer (equipped with a 9.4 T magnet) at the specified temperatures. The temperature for NMR experiments was externally calibrated to observe the chemical-shift separation between the OH and CH_3 resonances in methanol. Non-deuterated solvents and gas-phase samples were locked to standard external neat CD_2Cl_2 or 10% fluorobenzene in C_6D_6 sample solutions. $^{31}P\{^1H\}$ NMR spectra were referenced externally to 85% H_3PO_4 in D_2O. All chemical shifts (δ) are quoted in ppm and coupling constants (*J*) in Hz. In general, solution ^{19}F and ^{11}B NMR resonances for all the compounds reported are not represented pictorially since they comprise of a single resonance at $\delta_F = -62.9$ ppm and $\delta_B = -6.6$ ppm respectively, corresponding the $[BAr^F_4]^-$ anion.

Spin simulations were conducted using MestReNova's built-in spin simulation facility (version 11.0.2-18153, © 2016 Mestrelab Research S.L.).

S1.3 Solid-State NMR Spectroscopic Data

Solid-state NMR samples were prepared in an argon-filled glovebox, by pre-loading *c.* 35 mg of the crushed crystalline sample in question into a 4.0 or 3.2 mm zirconia solid-state rotor. The custom glassware used for *in situ* solid-gas transformations inspected *via* solid-state NMR has been detailed elsewhere.[2]

Solid-state NMR spectra were obtained on a Bruker Avance III HD spectrometer equipped with a 9.4 T magnet, operating at 100.56 MHz (^{13}C) or 161.89 MHz (^{31}P), with a MAS rate (ν) of 10 kHz. For ^{13}C{^{1}H} CP/MAS SSNMR a sequence with a variable X-amplitude spin-lock pulse[7] and spinal64 proton decoupling was used. 4500 transients were acquired using a contact time of 2.5 ms, an acquisition time of 25 ms (2048 data points zero-filled to 32 K) and a recycle delay of 2.0 s. All ^{13}C{^{1}H} spectra were referenced to adamantane where the upfield methane resonance was taken to be δ_C = 29.5 ppm[8] on a scale secondarily referenced to $\delta_C(SiMe_4)$ = 0.0 ppm. Relaxation times for ^{1}H and contact time for ^{31}P{^{1}H} CP/MAS, ^{13}C{^{1}H} CP/MAS, and FSLG-HETCOR NMR experiments were optimised for each compound as appropriate. The temperature for variable temperature NMR experiments at low temperatures was calibrated externally using $PbNO_3$.

S1.4 Gas-Phase NMR Spectroscopic Data

Gas phase ^{1}H NMR spectra were obtained using either a Bruker Avance III NMR spectrometer (equipped with a 11.75 T magnet) or a Bruker Avance III HD nanobay NMR spectrometer (equipped with a 9.4 T magnet) at room temperature and referenced to reported gas phase data for methane with T_1 = 1.0 s.[9] Pressurisation of medium wall NMR tubes (2 mL) fitted with a controlled atmosphere PTFE (polytetrafluorethylene, Teflon) valve using the appropriate gaseous substrate was achieved by evacuation and backfilling at the appropriate pressure using custom glassware detailed in previous work.[2] The spectrometer was pre-locked and pre-shimmed to a separate sample of 10% fluorobenzene in C_6D_6 solutions before NMR study of the gaseous NMR sample.

S1.5 Mass Spectrometry Data

Electrospray ionisation mass spectrometry (ESI-MS) was carried out using a Bruker MicrOTOF instrument directly connected to a modified Innovative Technology glovebox.[10] The spectrometer was calibrated using a mixture of tetra alkyl ammonium bromides $[N(C_nH_{2n+1})_4]Br$ (n = 2–8, 12, 16, and 18). Samples were diluted to a concentration of at most 10^{-6} mol dm^{-3} before mass spectrometry. Samples were typically acquired with a 4 µL min^{-1} flow rate, a 0.4 bar nebuliser gas pressure, a flow of argon at 333 K with a 4 L min^{-1} flow rate to act as a drying gas, a capillary voltage of 4.5 kV, and an exit voltage of 60 V.

S1.6 Scanning Electron Microscopy Data

Scanning electron microscopy (SEM) was performed using a Carl Zeiss Merlin-Analytical instrument, with an operating voltage of 3.0 kV, and carried out by Dr Dana-Georgiana Crivoi. The samples were prepared by adding the material directly on the carbon tape, under an atmosphere of argon. The samples were analysed without metal or carbon coating. Energy dispersive X-ray spectroscopy (EDX) was carried out on a Carl Zeiss Merlin-Analytical instrument with an operating voltage of 3.0 kV.

S1.7 Powder X-ray Diffraction Data

Powder X-ray diffraction data were collected on a PANAnalytical X'Pert Pro Diffractometer in scanning mode using Cu Kα radiation (α_1 = 1.540598 Å, α_2 = 1.54426 Å, weighted average = 1.541847 Å). Scans were recorded between 2θ = 3.0 – 80 °, with step size 0.017 ° and scan step time 26.67 s. The samples were mounted on stainless steel holders that gave rise to peaks at 2θ = 43.36, 44.29, and 50.51 ° (these did not interfere with the analysis).

S1.8 Gas Chromatography Data

Analyses by gas chromatography for the alkene gas mixtures (either from batch or flow experiment) were performed using a Shimadzu GC-2014 gas chromatograph equipped with a Flame Ionization Detector (FID) and a Restek alumina (BOND MAPD) capillary column (50 m × 0.53 mm × 10.0 μm) using a gas sampling loop (50 μL). To obtain gaseous sample aliquots, the loop was opened for a period of 60 seconds, and the contents passed *via* the Restek alumina column at a constant temperature of 80 °C (oven operating temperature), 87.4 operating pressure, 9.57 mL min^{-1} operating flow rate, and 60.0 split ratio. Hydrogen and helium were passed through an on-stream oxygen and moisture trap. Sampling from catalytic runs under flow conditions were done by injection of a gas aliquot (50 μL) onto the gas chromatograph using an automated gas sampling valve every 15 min. Gas flow rates are reported as measured at 298 K and atmospheric pressure. External calibration using unique butene samples proved comparable GC response factors for the butenes analysed in this study with reproducible GC traces.

S1.9 Protocol for Gas/Solid Batch Experiments: Sample Preparation and Gas Analyses

Gas samples from batch experiments corresponding to neat gas reagents and/or gas mixtures were diluted to an approximately 100-fold with argon gas before being analysed by gas chromatography using a custom glassware heavy wall ampoule ($V \sim 50$ ml) fitted with tubing/Teflon valves (*Figure S1*). The ampoule was fitted with a medium wall NMR tube with a controlled atmosphere Teflon valve (2 mL), containing the gas sample to be analysed, using the tubing adaptor. With the valve on the NMR tube closed at first, the ampoule was evacuated and filled with argon gas to a pressure of 1.5 bar and closed. Then, the ampoule was half-submerged in liquid nitrogen and the NMR tube was opened for 5 min allowing the gas mixture to condense inside the half-submerged ampoule. At this point, the NMR tube gas

closed, and the ampoule was warmed up to room temperature to give an approximately 100-fold dilution of the gas mixture balanced with argon. At this point, the gas mixture was sufficiently diluted for adequate analyses by gas chromatography. The ampoule containing the diluted gas mixture was then fitted to the sampling valve from the chromatograph, using the tubing adaptor. An aliquot of 50 μL was then injected using the automated sampling valve and analysed by gas chromatography as described before. This protocol proved to give reproducible and consistent results.

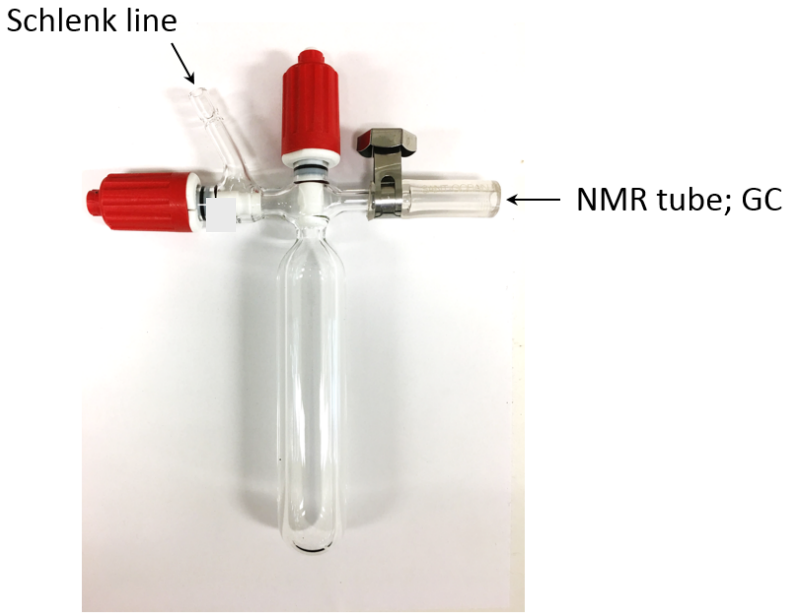

Figure S1: *Custom ampoule (V ~ 50 ml) employed for gaseous sample dilution prior to GC analysis from batch experiments.*

S1.10 Protocols for Gas/Solid Flow Experiments

Samples were prepared by loading an appropriate amount of each catalyst/pre-catalyst supported with inert glass wool inside a stainless-steel column (thickness 6.35 mm, internal diameter 4.0 mm, and length 20.0 cm, *Figure S2*), using a glovebox under an argon atmosphere. The inert glass wool support prevented the catalyst from dislodging from the column and improved the dispersion of the catalyst.

S1.10.1 Sample Preparation: Column Packing

The catalyst or pre-catalyst was crushed in a sample vial and then filtered through a 150 micron Endecott sieves. The fine powder was then grounded further in a glass vial. An initial plug of glass wool (~100 mg) was compacted within the column using a metal rod and then moved back up the column by approximately 2 cm (*Figure S3*, ***A***). A small amount of glass wool (~30 mg) was placed at the top of the column and the powder was added to the glass wool at the top of the column (*Figure S3*, ***B***) which was then compacted lightly on top of the initial glass wool plug (*Figure S3, **C***). This was repeated 5-7 (***B***-***C***) times depending on the catalyst loading (*Figure S3, **D***). Once the column was charged with the supported catalyst/pre-catalyst, it was sealed using the two-way Swagelok gas-tight valves, fitted at each end (*Figure S2*).

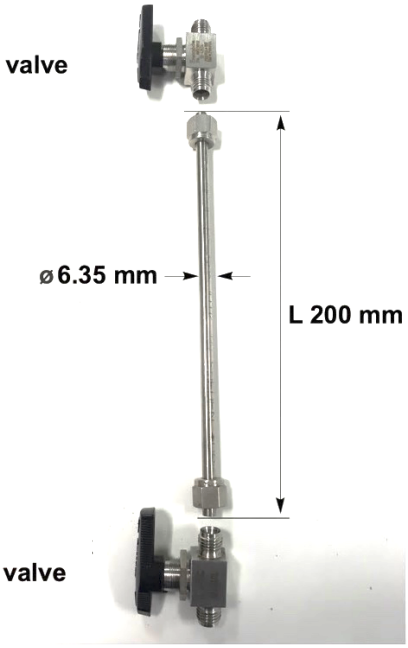

Figure S2: *Stainless steel column fitted with gas-tight valves where either the catalyst or pre-catalyst were charged before the catalytic runs under continuous gas flow conditions. This column was fitted to the continuous gas flow reactor using the upper and lower gas-tight two-way Swagelok valves (Figure S4, **A**).*

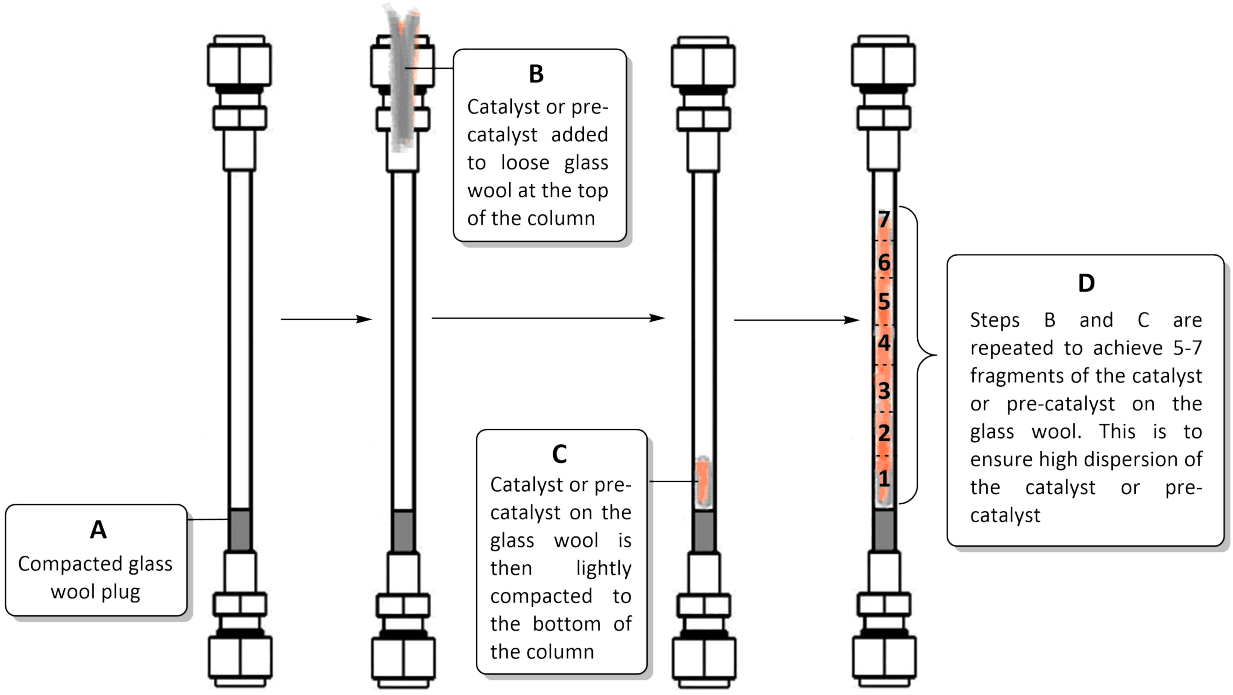

Figure S3: *Packing of the stainless steel column loaded with either the catalyst or pre-catalyst catalytic runs under continuous gas flow conditions. The initial glass wool plug (**A**) followed by the addition of the catalyst or pre-catalyst on glass wool at the top of the column (**B**). The sample is then lightly compacted (**C**) and repeated in small fragments (**D**) to pack the column with the desired amount of catalyst or pre-catalyst.*

S1.10.2 Experimental Monitoring

The pre-loaded column was then fitted to a bespoke continuous gas reactor using the Swagelok valves. Gas flow into the column (*Figure S4, **A***) was controlled with a Brooks Delta Smart II mass-flow meters setup (*Figure S5*). Gas flow out of the column, charged with the corresponding catalyst or pre-catalyst, passed through a loop fitted with a pressure regulator (permitting column pressurisation to ≤ 2 bar; *Figure S4, **B***). Gas aliquots were sampled and analysed every 15 minutes by gas chromatography as described above. Flow rates passing through the loop and thereafter vented were confirmed using an Ellutia 7000 flowmeter.

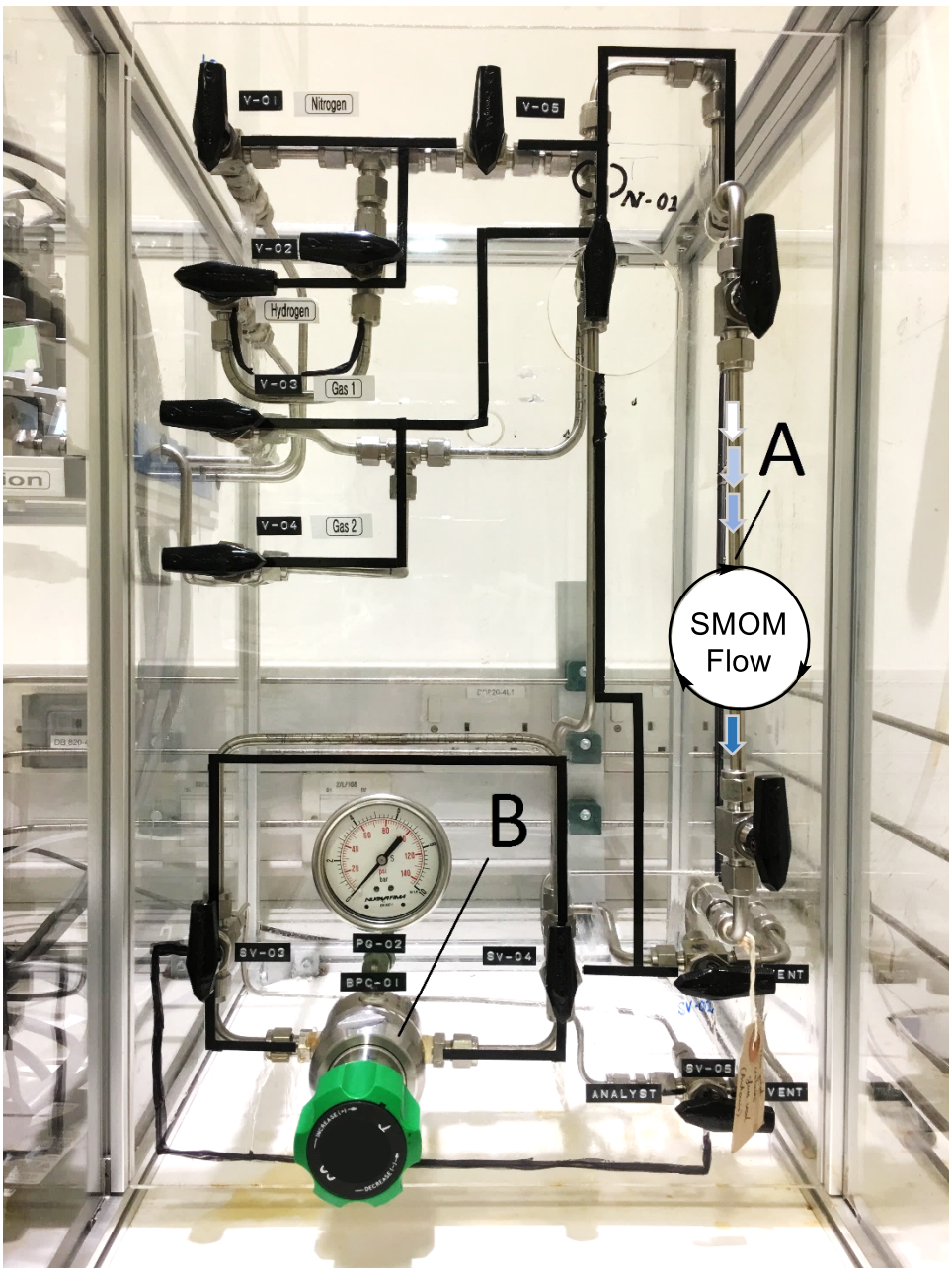

Figure S4: *Bespoke continuous gas flow reactor setup fitted with the pre-loaded stainless-steel column (**A**) containing the catalyst or pre-catalyst, during a catalytic run. Note that the N_2 and H_2 feeds are closed whereas the gas 1 (1-butene) and gas 2 (isobutene) feeds are open and set to pass* via *the column (**A**). The outflow is set to pass* via *the loop, fitted with a regulator (**B**) to allow H_2 pressurisation, and into the gas chromatograph, 'analyst'.*

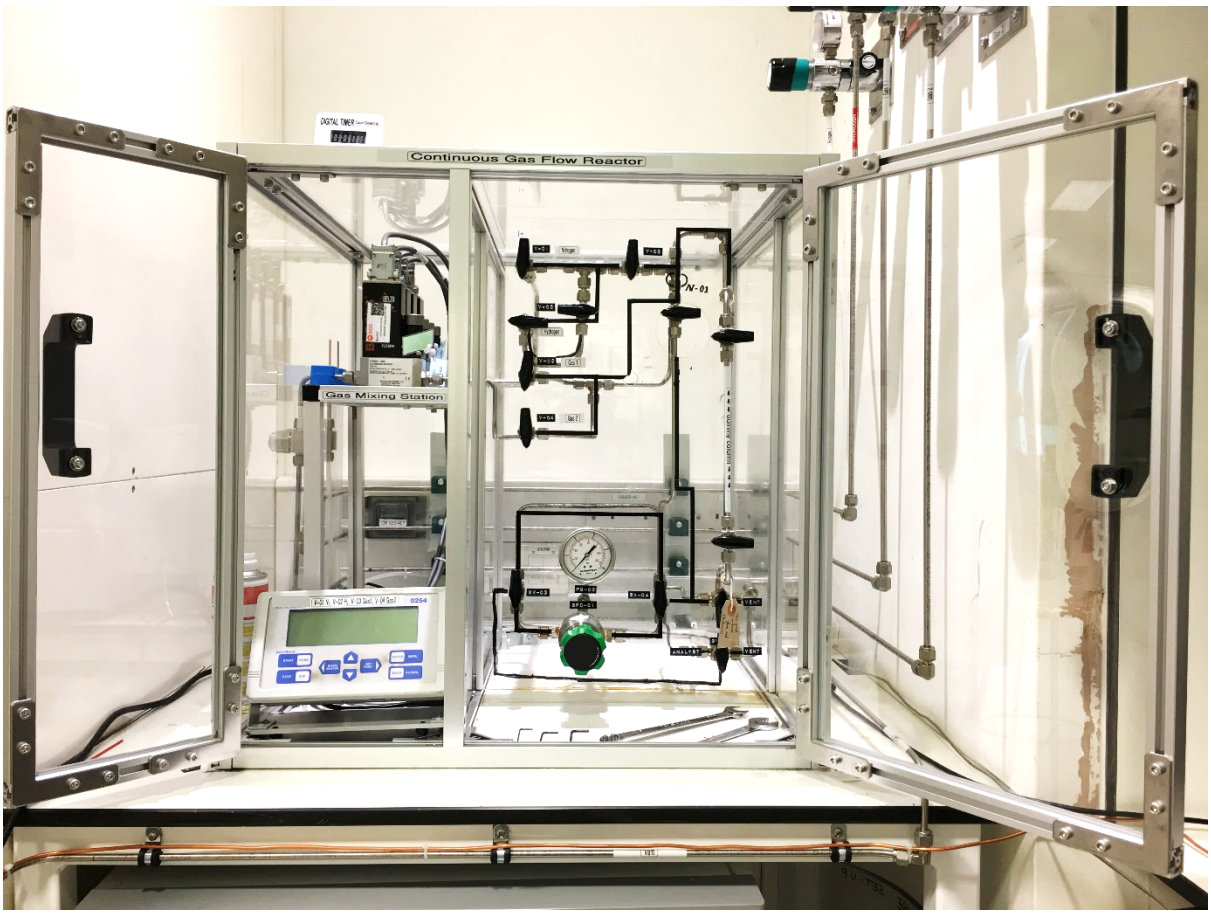

Figure S5: *Bespoke continuous gas flow reactor setup, dormant, fitted with a dummy column: full cabinet view. The mass-flow meters are visible in the leftmost compartment.*

S1.10.3 Typical Procedure for a Continuous Gas Flow Catalytic Experiment

After fitting the packed column into the flow reactor under a 50 mL min^{-1} flow of N_2, tightening all relevant connections, and opening the two-way Swagelok valves at each end of the column, the column was then (1) purged with neat N_2 gas, (2) the pre-catalyst pre-activated with neat H_2 gas (if needed) and (3) the catalytic run was started.

1) Neat N_2 purging – After the column containing the catalyst or pre-catalyst was fitted to the continuous gas flow reactor, the column was purged with neat N_2 gas at 50 mL min^{-1} for 10 min. The N_2 flow passing through the column was immediately vented, bypassing the regulated loop setup. Simultaneously, the substrate diluted gas mixture at their target flow rates were mixed and made to bypass the column, *via* the regulated loop and the gas chromatograph before venting (after the gas chromatograph). After this time, and before the catalytic run started, the N_2 and substrate gas mixture flows were stopped.

2) Pre-activation with H_2 gas (*only for pre-catalysts that require pre-activation with H_2 gas before a catalytic run*) **–** H_2 at 100 mL min^{-1} was passed through the system *via* the column and the regulated loop before venting for 5 min, before pressurisation of the system with H_2 to 1 bar for 10 minutes, using the regulator setup. Then, the pressure was carefully released

and the H_2 flow stopped. A flow of N_2 at 50 mL min^{-1} was resumed and passed *via* the column and the loop before venting for 10 minutes, in order to remove any remaining H_2 gas before the catalytic run was started.

3) Addition of substrate diluted gas mixtures – After the column was charged, fitted, purged with N_2 gas and activated with H_2 gas, the substrate diluted gas mixtures at the target flow rate(s) were passed through the column, *via* the regulated loop and the gas chromatograph before venting (after the gas chromatograph), for the relevant on-stream time(s). Gas aliquots were taken of the outflow and analysed by gas chromatography every 15 minutes *via* the automatic sampling loop installed in the chromatograph as described before.

S2 X-ray Crystallography

S2.1 Crystal Structure Determinations

Single-crystal X-ray diffraction data for the **7**, **9**, **10**, **11**, **12**, **13** and **14** were collected (ω-scans) on Oxford Diffraction/Agilent SuperNova diffractometers with Cu-*Kα* (*λ* = 1.54184 Å) radiation equipped with nitrogen gas Oxford Cryosystems Cryostream unit[11] at the Oxford Chemical Crystallography Service from the University of Oxford. Diffraction images from raw frame data were reduced using CrysAlisPro.[12] The structures were solved using SHELXT[13] and refined to convergence on F^2 and against all independent reflections by full-matrix least-squares using SHELXL[14] (version 2018/3) in combination with the GUI OLEX2[15] program. All non-hydrogen atoms were refined anisotropically and hydrogen atoms were geometrically placed unless otherwise stated (see specific details for each molecular structure in the text) and allowed to ride on their parent atoms. In several structures some of the CF_3 groups on the $BAr^F{}_4^-$ anion were disordered and modelled over two or three main domains, and restrained to maintain sensible geometries. Distances and angles were calculated using the full covariance matrix. Selected crystallographic data and refinement data are summarized in the text (see characterization data in Section 3 Synthetic Procedures) and full details are given in the supplementary deposited CIF files (CCDC 1945264-1945268 and 1945341). These data can be obtained free of charge from the Cambridge Crystallographic Data Centre via http://www.ccdc.cam.ac.uk/data_request/cif.

S3 Synthetic Procedures

S3.1 Synthesis and Characterisation of Single-Crystalline [(dtbpe)Rh(NBD)][BAr^F_4], Complex 7

S3.1.1 Synthesis of [(dtbpe)RhCl]$_2$

[(COD)RhCl]$_2$ (100 mg, 203 µmol) and dtbpe (129 mg, 406 µmol) were introduced to separate Schlenk flasks and separately dissolved in CH_2Cl_2 (10 mL each). The dtbpe solution was then dropwise added to the [(COD)RhCl]$_2$ solution *via* cannula. The reaction mixture was then allowed to stir at room temperature for 60 min before all volatiles were removed *in vacuo*. The resulting dark orange crude was washed with cold hexanes (3 × 10 mL) and dried *in vacuo*. The resulting orange solid was dried *in vacuo* for 12 hours to give [(dtbpe)RhCl]$_2$ (170 mg, 186 µmol, 92%). [(dtbpe)RhCl]$_2$ was used without further purification. Spectroscopic data of this product matched with reported values.[16]

S3.1.2 Synthesis of [(dtbpe)Rh(NBD)][BAr^F_4], Complex 7

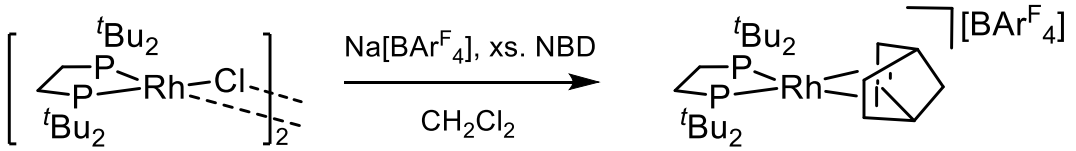

7

In separate Schlenk flasks, [(dtbpe)RhCl]$_2$ (50 mg, 55 µmol) and Na[BAr^F_4] (97 mg, 109 µmol) were dissolved in CH_2Cl_2 (10 mL each). NBD (0.1 mL, 983 µmol, *c.* 9 eq.) was added to the Na[BAr^F_4] solution *via* syringe and stirred for one minute, before the [(dtbpe)RhCl]$_2$ solution was dropwise added *via* cannula with stirring. The reaction mixture was stirred for 30 min at room temperature, and the contents were partially removed *in vacuo* (2.5 mL) to give a claret-coloured solution. The reactions mixture was then filtered *via* cannula, and the filtrate was layered with pentane at 298 K to give red crystalline plates of [(dtbpe)Rh(NBD)][BAr^F_4] **7** after 7 days (120 mg, 79%).

^{1}H NMR (400.1 MHz, CD_2Cl_2, 298 K): δ 1.29 (d, 36 H, $^3J_{HP}$ = 13.0 Hz; ^{t}Bu), 1.75 (s, 2 H; NBD CH_2), 1.82 (m, 4 H; *dtbpe* CH_2), 4.19 (m, 2 H; NBD bridgehead CH), 5.54 (m, 4 H; NBD olefinic CH), 7.56 (s, 4 H; *p*-H), 7.72 (s, 8 H; *o*-H).

^{13}C{^{1}H} NMR (100.6 MHz, CD_2Cl_2, 298 K): δ 23.1 (m; *dtbpe* CH_2), 30.7 (vdd, $J \sim 2.5$ Hz; ^{t}Bu CH_3), 38.5 (ddd, $^1J_{CP}$ = 8.4 Hz, $^2J_{CRh}$ = 6.3 Hz, $^3J_{CP}$ = 1.2 Hz; ^{t}Bu C_Q), 55.0 (m; bridgehead CH), 71.2 (NBD CH_2), 81.1 (m; NBD olefinic CH), 118.1 (septet, $^3J_{CF}$ = 3.8 Hz; *p*-C_{aryl}), 125.1 (q, $^1J_{CF}$ = 272.4 Hz; CF_3), 129.6 (qq, $^2J_{CF}$ = 30.6 Hz, $^4J_{CF}$ = 2.6 Hz; C_{aryl}-CF_3), 135.3 (s; *o*-C_{aryl}), 162.3 (q, $^1J_{CB}$ = 49.4 Hz; *i*-C_{aryl}).

$^{13}C\{^1H\}$ SSNMR (100.6 MHz, 10 kHz spin rate, 298 K): δ 20.8 (*dtbpe* CH_2), 28–39 (^tBu CH_3 + C_Q), 54.0 (NBD CH_2), 67.9 (NBD bridgehead CH), 72.2 (NBD olefinic CH), 85.5 (NBD olefinic CH), 116–137 (BAr^F_4), 162.9 (BAr^F_4 C-B).

$^{13}C\{^1H\}$ SSNMR (100.6 MHz, 10 kHz spin rate, 158 K): δ 19.9 (*dtbpe* CH_2), 23–39 (^tBu CH_3 + C_Q), 53.9 (NBD CH_2), 67.2 (NBD bridgehead CH), 70.6 (NBD olefinic CH), 86.3 (NBD olefinic CH), 116–137 (BAr^F_4), 162.4 (BAr^F_4 C-B).

$^{31}P\{^1H\}$ NMR (161.9 MHz, CD_2Cl_2, 298 K): δ 84.0 ($^1J_{PRh}$ = 154 Hz).

$^{31}P\{^1H\}$ SSNMR (161.9 MHz, 10 kHz spin rate, 298 K): δ 77.7 (d+d, $^1J_{PRh}$ ~ 140 Hz).

$^{31}P\{^1H\}$ SSNMR (161.9 MHz, 10 kHz spin rate, 183 K): δ 75.1 (br. d+d, $\nu_{½}$ ~ 300 Hz).

$^{31}P\{^1H\}$ SSNMR (161.9 MHz, 10 kHz spin rate, 158 K): δ 75.0 (br. d+d, $\nu_{½}$ ~ 325 Hz).

$^{19}F\{^1H\}$ NMR (376.5 MHz, CD_2Cl_2, 298 K): δ –62.8 (Ar^F-CF_3).

$^{11}B\{^1H\}$ NMR (128.4 MHz, CD_2Cl_2, 298 K): δ –6.60 ($BAr^F_4{}^-$).

ESI-MS (CH_2Cl_2) m/z found (calculated) for $C_{25}H_{49}P_2Rh$ $[M]^+$: 514.2394 (514.2414).

Elemental analysis found (calculated) for $C_{57}H_{60}BF_{24}P_2Rh$: C, 49.77% (49.73%); H, 4.44% (4.39%).

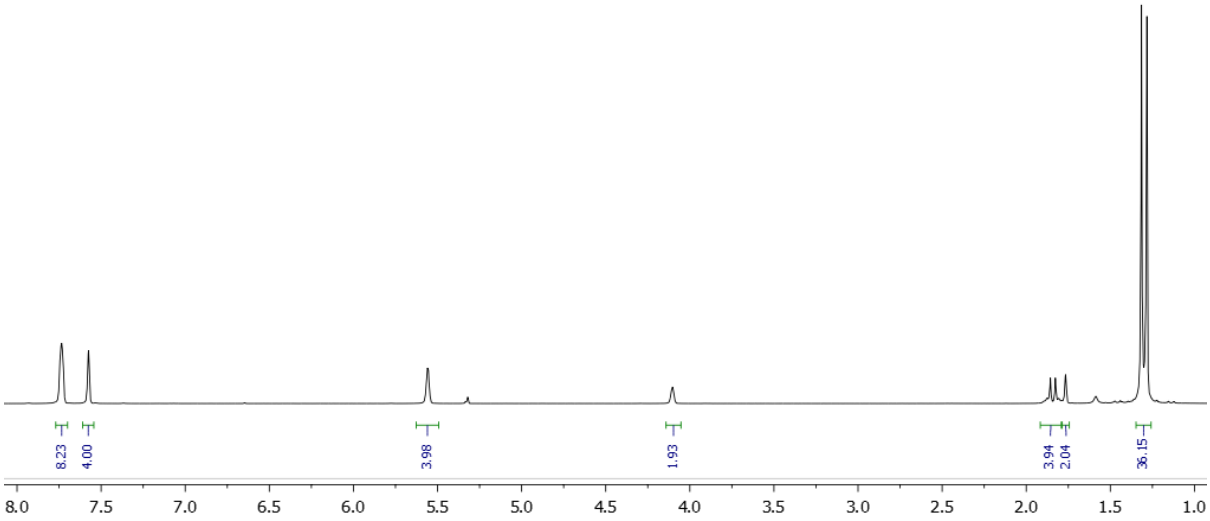

Figure S6: *^{1}H NMR spectrum of complex **7** (400.1 MHz, CD_2Cl_2, 298 K).*

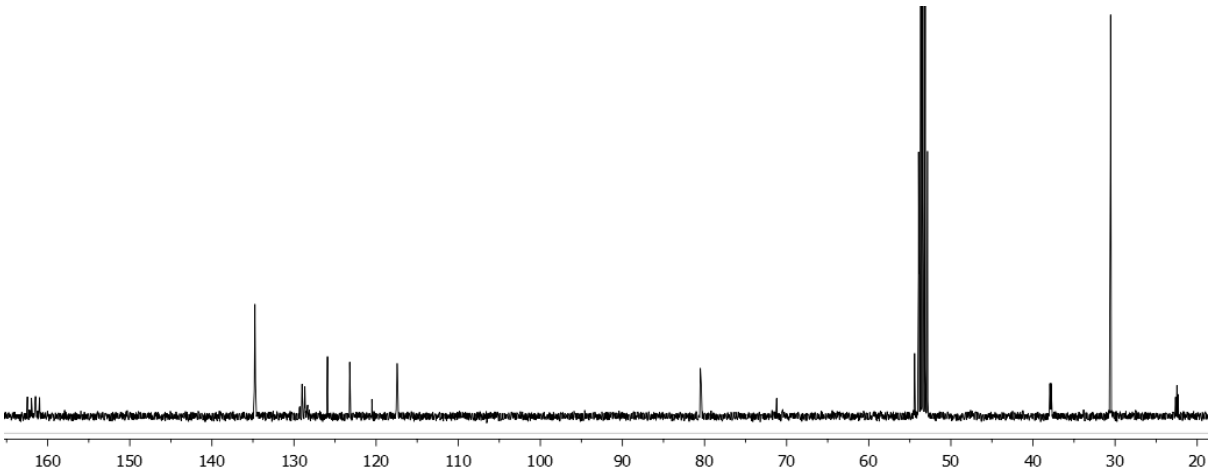

Figure S7: *$^{13}C\{^1H\}$ NMR spectrum of complex **7** (100.6 MHz, 298 K, CD_2Cl_2).*

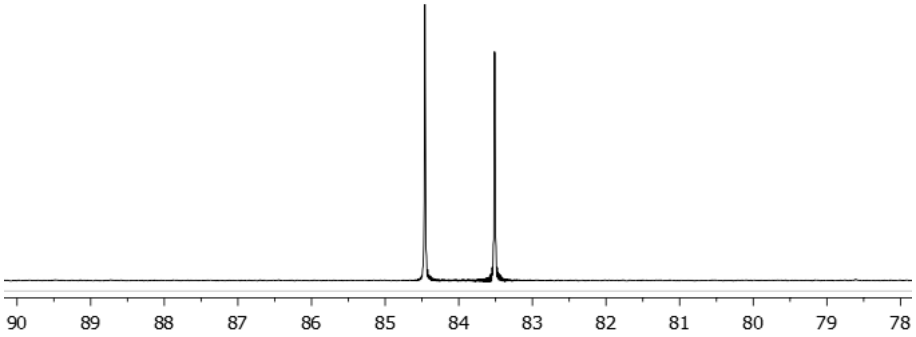

Figure S8: *$^{31}P\{^1H\}$ NMR spectrum of complex **7** (162 MHz, 298 K, CD_2Cl_2).*

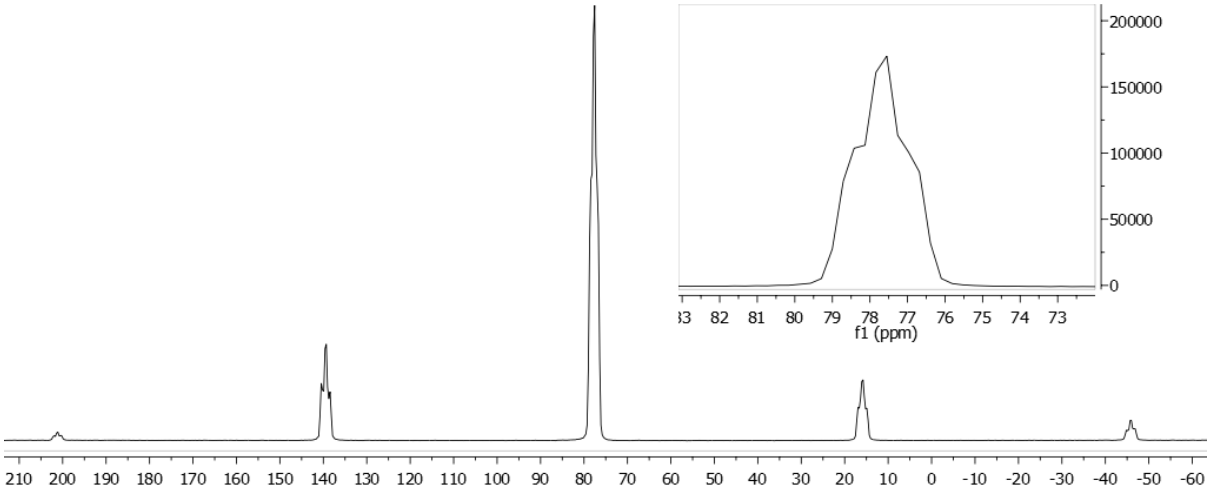

Figure S9: *$^{31}P\{^1H\}$ SSNMR spectrum of complex **7** (161.9 MHz, spinning speed 10 kHz, 298 K).*

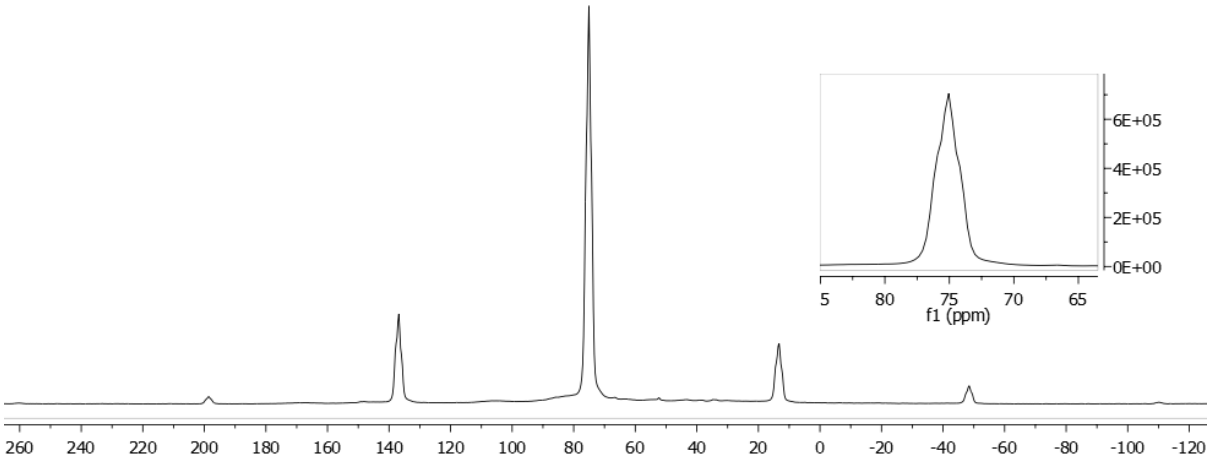

Figure S10: *$^{31}P\{^{1}H\}$ SSNMR spectrum of complex **7** (161.9 MHz, spinning speed 10 kHz, 183 K).*

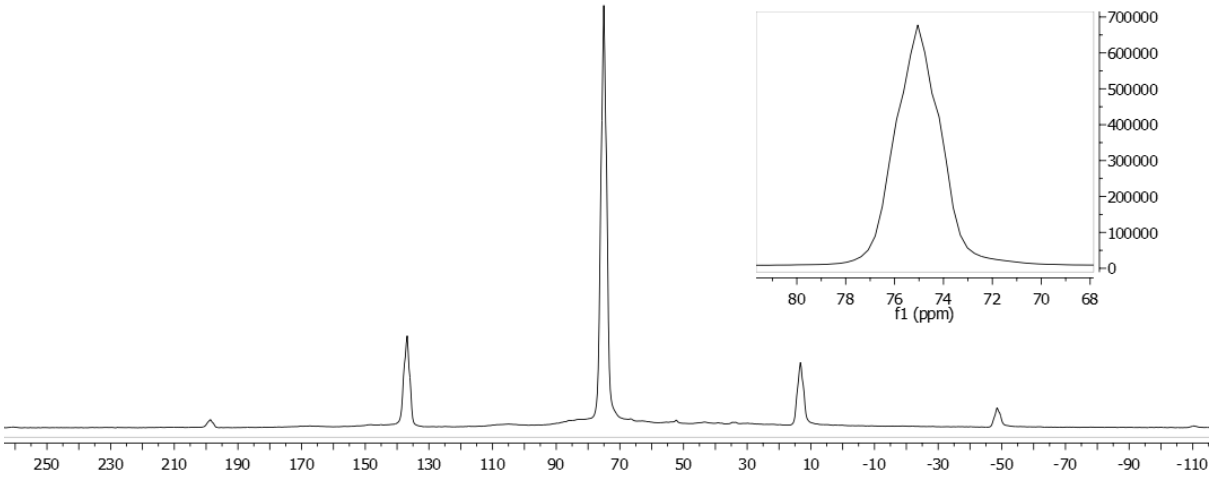

Figure S11: *$^{31}P\{^{1}H\}$ SSNMR spectrum of complex **7** (161.9 MHz, spinning speed 10 kHz, 158 K).*

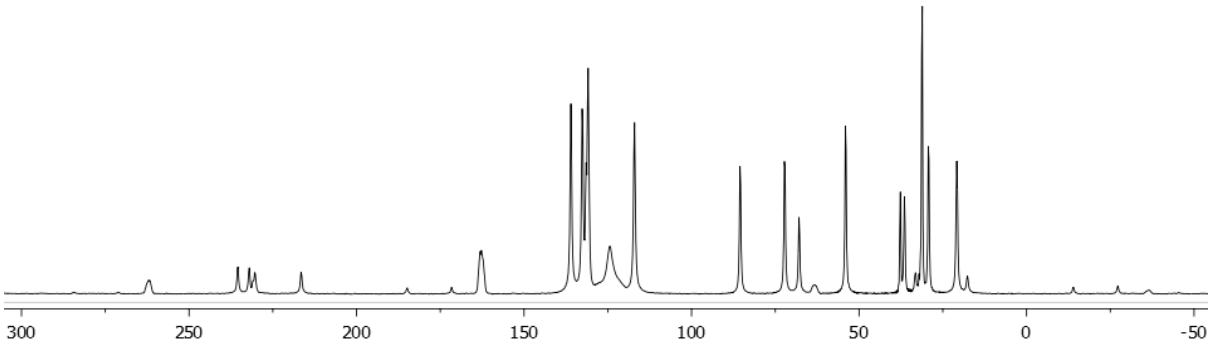

Figure S12: *$^{13}C\{^{1}H\}$ SSNMR spectrum of complex **7** (100.6 MHz, spinning speed 10 kHz, 298 K).*

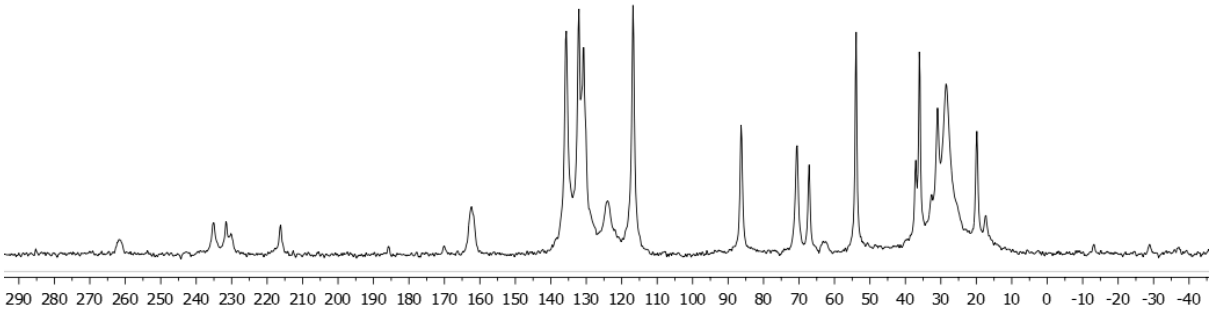

Figure S13: *$^{13}C\{^1H\}$ SSNMR spectrum of complex **7** (100.6 MHz, spinning speed 10 kHz, 158 K).*

S3.1.3 Selected Crystallographic and Refinement Data for Complex 7

Crystal data for 7 (CCDC 1945264): $C_{57}H_{60}BF_{24}P_2Rh$, M = 1376.71 g/mol, monoclinic, *C*2, a = 18.1357(3), b = 18.1424(4), c = 17.9779(4) Å, β = 90.1029(15)°, V = 5915.2(2) Å^3, Z = 4, λ(Cu-Kα) = 1.54184 Å, T = 150(1) K, organge plate, ρ(calcd, g cm^{-3}) = 1.546, μ (mm^{-1}) = 3.869, 43751 reflections collected, 12248 independent measured reflections (R_{int} = 0.0330), F^2 refinement, R_1(obs, I > 2σ(I)) = 0.0269, wR_2(all data) = 0.0711, 12088 independent observed reflections [|F_o| > 4σ(|F_o|), 2ϑ_{max} = 152.4°], 1093 restrains, 994 parameters, GOF = 1.049 and residual electron density (e Å^{-3}) = 0.539/-0.228.

S3.1.4 Supplementary Analysis of the Solid-State Molecular Structure of Complex 7 by Single-Crystal X-ray Diffraction

The cationic fragment [(dtbpe)Rh(NBD)]$^+$ (*Figure S14*) is surrounded by six BAr$^F{}_4^-$ counteranions arranged into a near-perfect octahedron (*Figure S15*). P-symmetric (orthorhombic) and P-asymmetric (monoclinic) solutions were considered for this system. Given the virtual triplet visible in the $^{31}P\{^1H\}$ solid-state NMR spectra at 298 K, 183 K and 158 K, indicating crystallographically distinct P environments, the monoclinic solution was chosen.

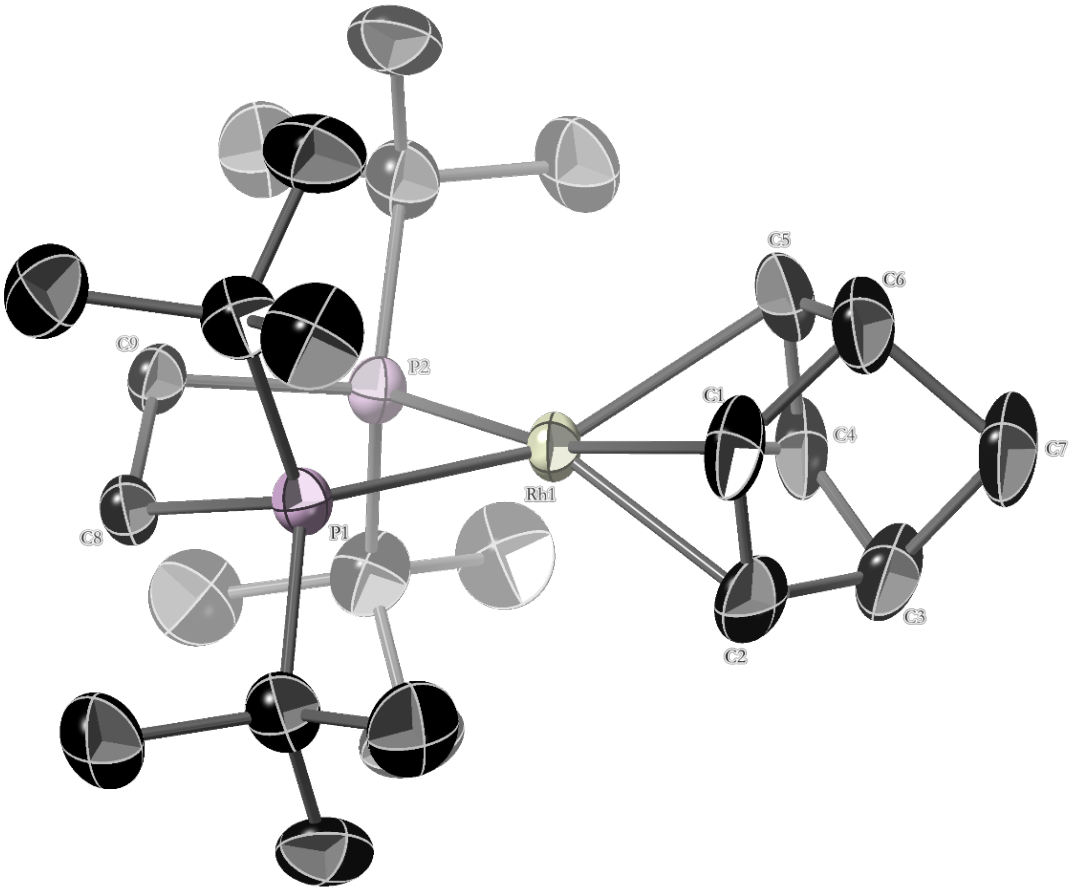

Figure S14: *Cationic fragment [(dtbpe)Rh(NBD)]⁺ of **7**. 50% displacement ellipsoids. H atoms omitted for clarity. Selected bond lengths (Å) and angles (°), where Cent is the centroid of C1–C2 and Cent' is the centroid of C4–C5: Rh1–P1, 2.3517(8); Rh1–P2, 2.3488(8); Rh1–C1, 2.195(4); Rh1–Cent, 2.082(3); Rh1–C2, 2.192(4); Rh1–C4, 2.199(4); Rh1–Cent', 2.085(3); Rh1–C5, 2.192(4); P1–Rh1–P2, 86.34(3); P1–Rh1–Cent, 102.69(10); P2–Rh1–Cent', 102.72(9); C2–Rh1–C4, 65.60(19); Cent–Rh1–Cent', 69.63(13); C1–Rh1–C5, 65.73(19).*

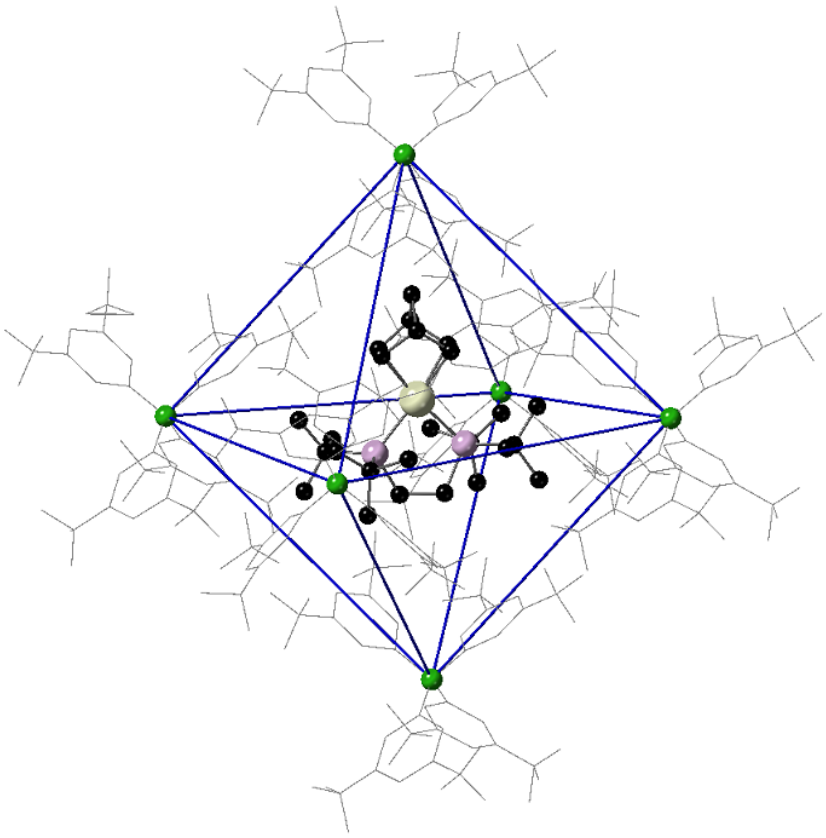

Figure S15: *The regular octahedral packing environment of complex **7**; shown is the coordination of six nearest $BAr^F_4{}^-$ neighbours (modelled as wireframe structures about a B atom ball) about the [(dtbpe)Rh(NBD)]$^+$ cation (modelled as ball-and-stick).*

S3.2 *In Situ* Gas/Solid Synthesis and Characterisation of [(dtbpe)Rh(NBA)][BAr^F_4], Complex 8

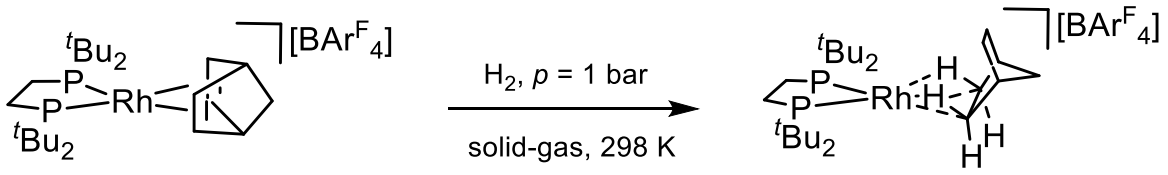

7 **8**, *proposed structure*

A 4.0 mm zirconia solid-state rotor was packed with *c.* 25 mg of **7** (*c.* 20 µmol). Left unsealed, the rotor was exposed[2] to H_2 (1 bar) for 50 min and then the rotor was capped under a flow of H_2 before solid-state NMR studies were undertaken.

Note: Due to the poor area of contact between the packed material and the atmosphere, hydrogenation *in situ* took longer than under *ex situ* conditions (see below).

This material can also be prepared by an *ex situ* solid-gas methodology, from finely powdered complex **7**, by reaction with H_2 gas (1 bar) for 20 min at 298 K in a J. Young's flask. This claret-

coloured material is sensitive to moist air and does not survive in solution, even at 183 K, giving C-Cl activation products in CH_2Cl_2 (converging on complex **13**) or the arene adduct (complex **9**) in 1,2-difluorobenzene. The extent of this reaction has been monitored *via* CD_3CN quenching experiments (*see Section 3.1*). For crushed complex **7**, only *c*. 10 min was necessary for near-quantitative conversion to complex **8** (as determined by $^{31}P\{^1H\}$ NMR spectroscopy).

$^{31}P\{^1H\}$ SSNMR (161.9 MHz, 10 kHz spin rate, 298 K): δ 125.8 (vt, $^1J_{PRh} \sim 190$ Hz).

$^{31}P\{^1H\}$ SSNMR (161.9 MHz, 10 kHz spin rate, 158 K): δ 119.3 (br. s, $\nu_{½} \sim 400$ Hz).

$^{13}C\{^1H\}$ SSNMR (100.6 MHz, 10 kHz spin rate, 298 K): δ 22.4 (dtbpe CH_2), 29.3 (^{t}Bu CH_3), 36.4 (^{t}Bu C_Q), 117–136 ($BAr^F{}_4$), 162.6 ($BAr^F{}_4$ C-B).

$^{13}C\{^1H\}$ SSNMR (100.6 MHz, 10 kHz spin rate, 158 K): δ 22.0 (dtbpe CH_2), 29.1 (^{t}Bu CH_3), 36.1 (^{t}Bu C_Q), 114–140 ($BAr^F{}_4$), 161.5 ($BAr^F{}_4$ C-B).

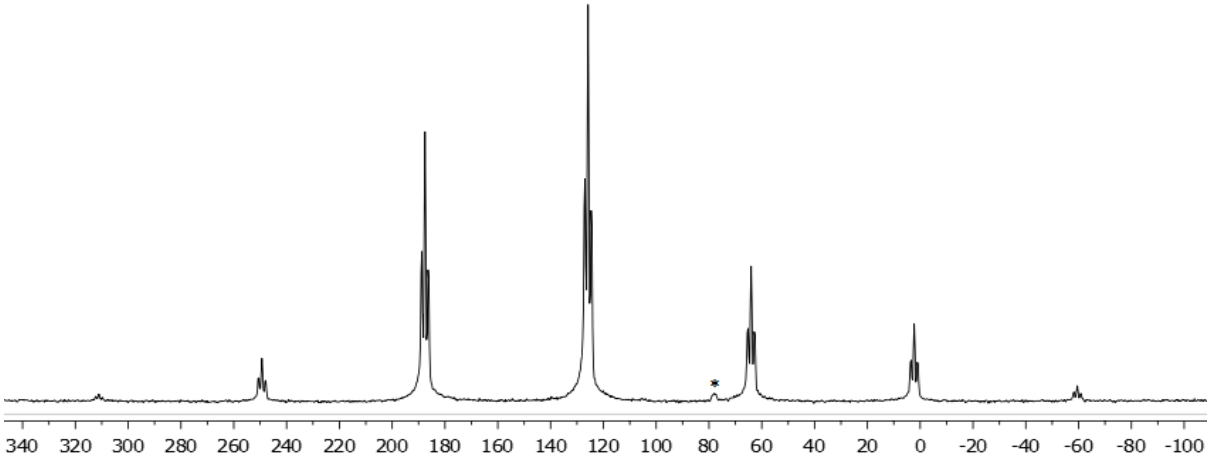

Figure S16: *$^{31}P\{^1H\}$ SSNMR spectrum of complex **8** (161.9 MHz, spinning speed 10 kHz, 298 K).* indicates traces of unreacted complex **7**.*

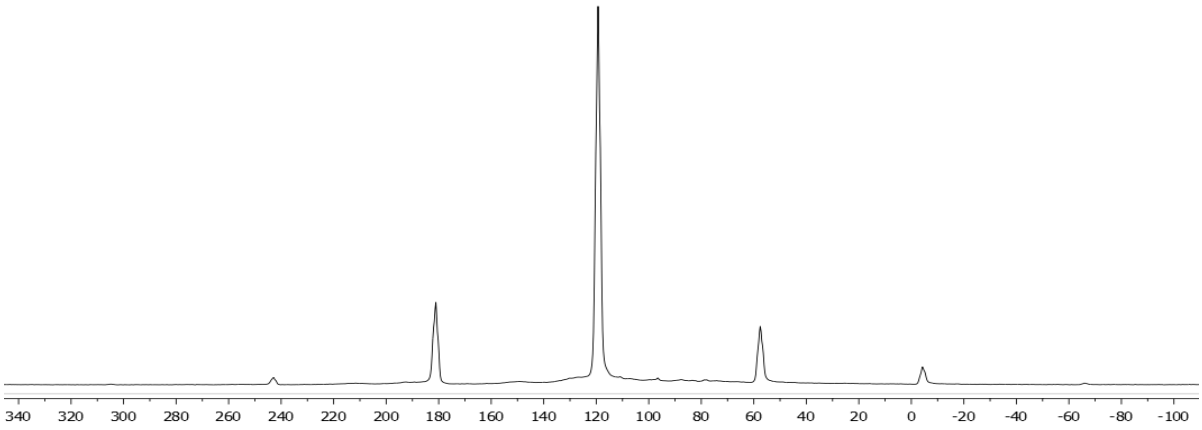

Figure S17: *$^{31}P\{^1H\}$ SSNMR spectrum of complex **8** (161.9 MHz, spinning speed 10 kHz, 158 K).*

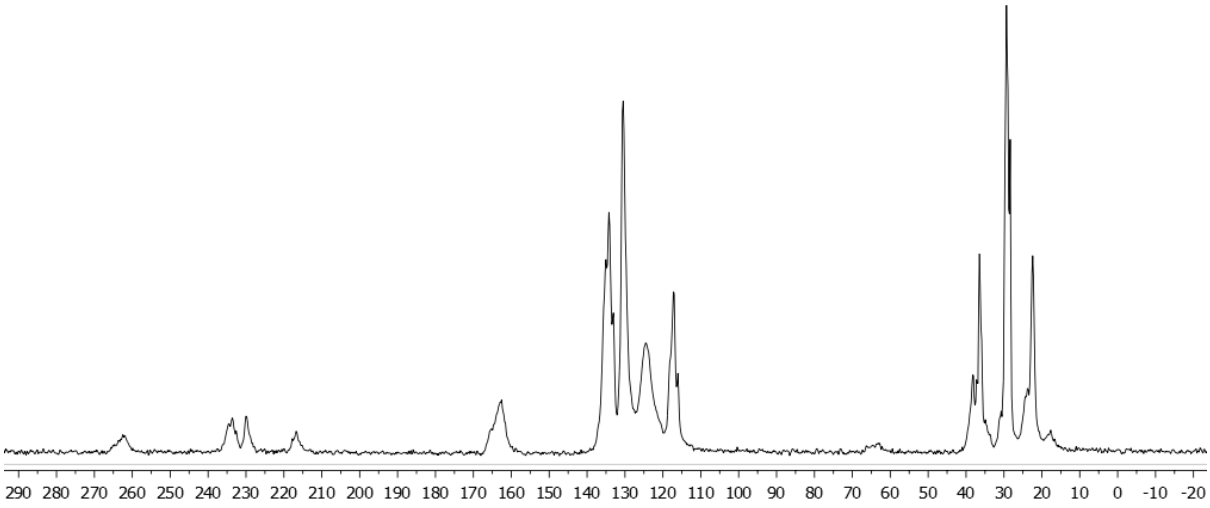

Figure S18: *$^{13}C\{^1H\}$ SSNMR spectrum of complex **8** (100.6 MHz, spinning speed 10 kHz, 298 K).*

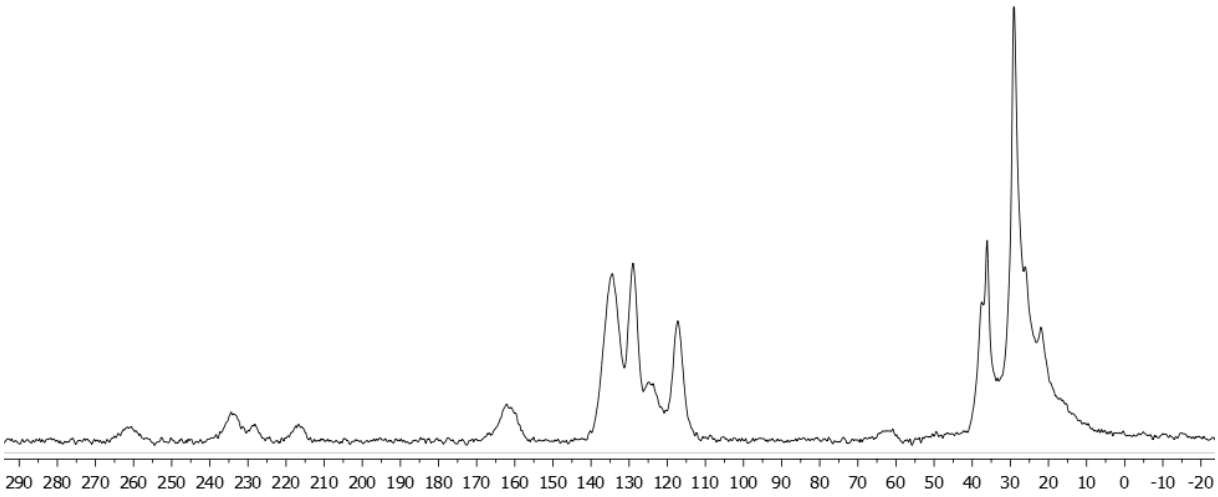

Figure S19: *$^{13}C\{^1H\}$ SSNMR spectrum of complex **8** (100.6 MHz, spinning speed 10 kHz, 158 K).*

S3.2.1 Attempted Single Crystal X-ray Diffraction Characterisation of complex 8

Crystalline samples of **7** (*c.* 2 mg) were loaded into high-pressure NMR tubes fitted with Young's taps (controlled atmosphere valves). These tubes were evacuated and pressurised with H_2 (1 bar) for a time *t*. After this time *t* had elapsed, the tubes were open and their contents immediately interrogated *via* single crystal X-ray diffraction in inert perfluoropolyether oil (Fomblin). In addition to a colour change from red to red-brown, crystals were observed to fracture and burst upon hydrogenation. Crystals for single-crystal x-ray diffraction studies were harvested from intact parts of otherwise split crystals, but diffraction was poor across all *t* considered (*t* = 2, 5, 10, 30 and 60 min) and no diffraction data could be acquired for the postulated σ-alkane complex **8**. Section 3.3 includes the results of this experiment.

S3.3 Synthesis and Characterisation of Single-Crystalline [(dtbpe)Rh(η^6-1,2-$C_6H_4F_2$)][BAr^F_4], Complex 9

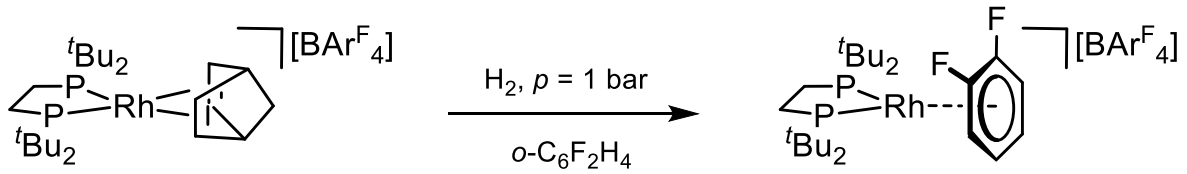

7 **9**

Method I

Powdered crystalline complex **7** (25 mg, 18 µmol) was introduced to a Young's flask and dissolved in 1,2-difluorobenzene (2 mL). The solution was frozen with liquid N_2 before the flask was evacuated and pressurised with H_2 (1 bar). After thawing and 30 min of stirring at room temperature (the solution should lighten significantly to a bright orange), the 1,2-difluorobenzene solution was layered with pentane to give crystals of the 1,2-difluorobenzene complex **9** as orange crystals (17 mg, 12 µmol, 68%) after 24 h.

Method II

Powdered crystalline complex **7** (25 mg, 18 µmol) was introduced to a Young's flask. The flask was evacuated and pressurised with H_2 for 45 min before removal of the H_2 atmosphere and then pressurisation with argon (1 bar). The resulting claret-coloured solid, **8**, was dissolved in 1,2-difluorobenzene (2 mL) and stirred for 30 min at room temperature before removal of all volatiles *in vacuo* to give complex **9** quantitatively as an orange powder.

Repetition of this protocol with a hydrogenation time of just 10 min still provided near-quantitative conversion (*c.* 97% *versus* unreacted complex **7**), verified by $^{31}P\{^1H\}$ NMR studies in 1,2-difluorobenzene, but optimal time for quantitative conversion was confirmed to be 40-50 min under H_2 (1 bar).

^1H NMR (400.1 MHz, CD_2Cl_2, 298 K): δ 1.25 (d, 36 H, $^3J_{HP}$ = 13.6 Hz; ^{t}Bu), 1.78 (d, $^2J_{PP}$ = 13.4 Hz, 4 H; *dtbpe* CH_2), 6.41 (br. m, 2 H; difluorobenzene), 6.86 (m, J = 5.0 Hz, J' = 3.1 Hz, 2 H; difluorobenzene), 7.58 (s, 4 H; *p*-H $BAr^F_4{}^-$), 7.74 (s, 8 H; *o*-H $BAr^F_4{}^-$).

$^{13}C\{^1H\}$ NMR (100.6 MHz, CD_2Cl_2, 298 K): δ 24.1 (m; *dtbpe* CH_2), 30.3 (s; ^{t}Bu CH_3), 38.7 (dm, $^1J_{CP}$ = 19.1 Hz; ^{t}Bu C_Q), 91.5 (m; difluorobenzene), 95.4 (br. m; difluorobenzene), 118.1 (septet, $^3J_{CF}$ = 3.7 Hz; *p*-C_{aryl} $BAr^F_4{}^-$), 123.1 (d, $^1J_{CF}$ = 420.3 Hz; difluorobenzene C-F), 125.2 (q, $^1J_{CF}$ = 272.6 Hz; CF_3 $BAr^F_4{}^-$), 129.5 (qq, $^2J_{CF}$ = 31.7 Hz, $^4J_{CF}$ = 3.0 Hz; C_{aryl}-CF_3 $BAr^F_4{}^-$), 135.4 (s; *o*-C_{aryl}), 162.4 (q, $^1J_{CB}$ = 50.0 Hz; *i*-C_{aryl} $BAr^F_4{}^-$).

$^{31}P\{^1H\}$ NMR (161.9 MHz, CD_2Cl_2, 298 K): δ 117.7 ($^1J_{PRh}$ = 206 Hz).

$^{19}F\{^{1}H\}$ NMR (376.5 MHz, CD_2Cl_2, 298 K): δ –141.2 (1,2-difluorobenzene), –62.8 (Ar^F-CF_3).

$^{11}B\{^{1}H\}$ NMR (128.4 MHz, CD_2Cl_2, 298 K): δ –6.60 ($BAr^F_4^-$).

ESI-MS (CH_2Cl_2) m/z found (calculated) for $C_{24}H_{44}F_2P_2Rh$ $[M]^+$: 535.1974 (535.1936).

Elemental analysis found (calculated) for $C_{56}H_{56}BF_{26}P_2Rh$: C, 48.03% (48.09%); H, 4.13% (4.04%).

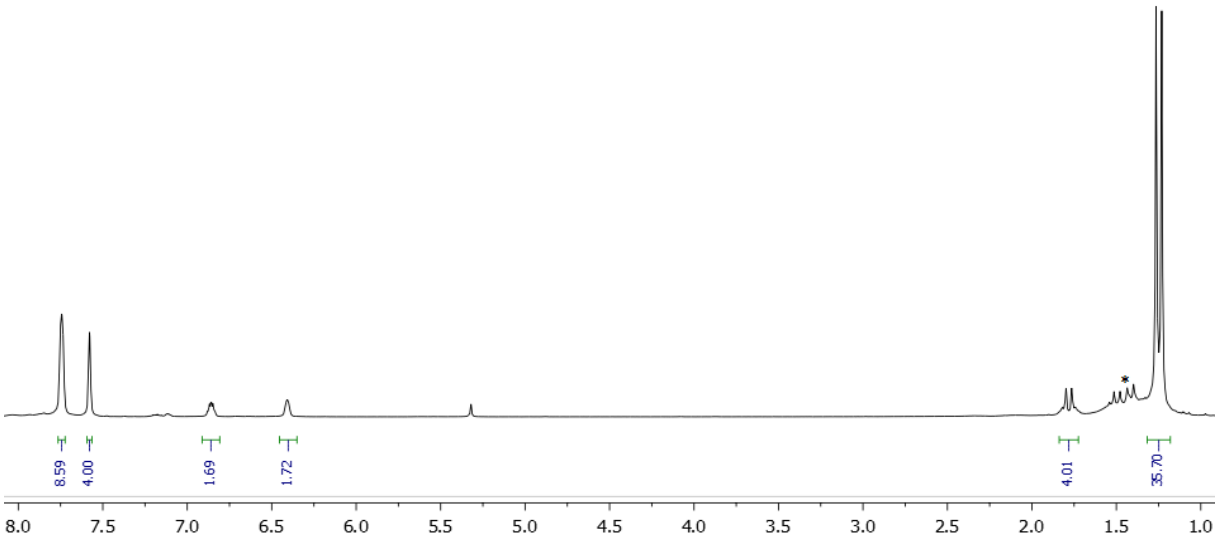

Figure S20: *^{1}H NMR spectrum of complex **9** (400.1 MHz, 298 K, CD_2Cl_2). * indicates unknown degradation products.*

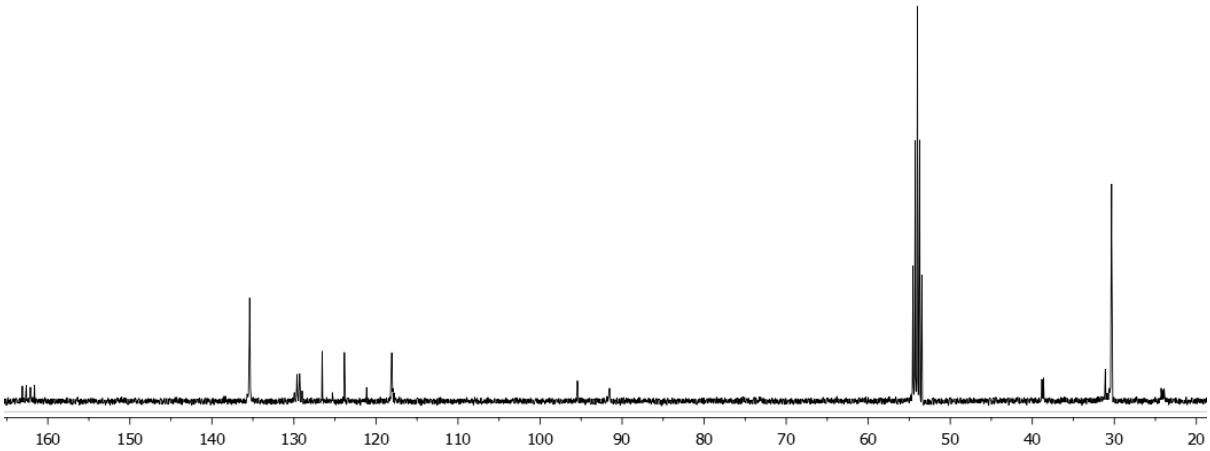

Figure S21: *$^{13}C\{^{1}H\}$ NMR spectrum of complex **9** (100.6 MHz, 298 K, CD_2Cl_2).*

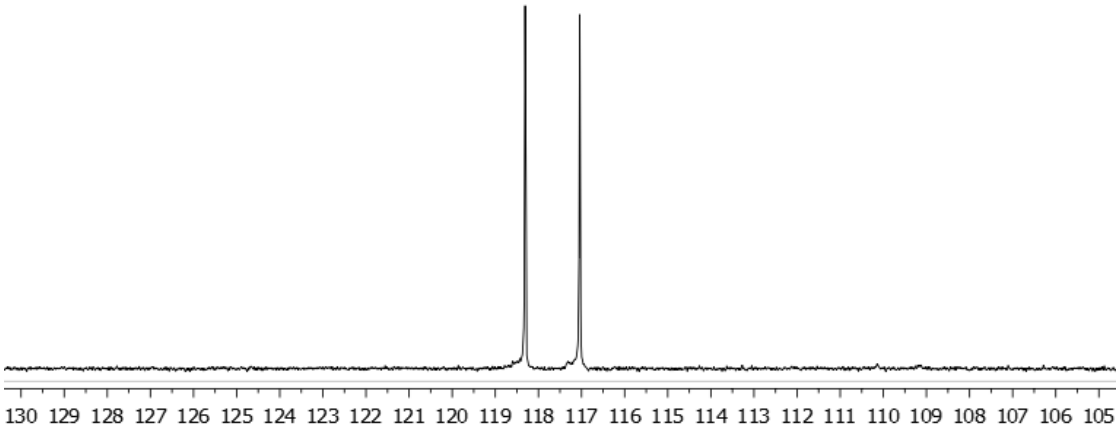

Figure S22: *$^{31}P\{^{1}H\}$ NMR spectrum of complex **9** (161.9 MHz, 298 K, CD_2Cl_2).*

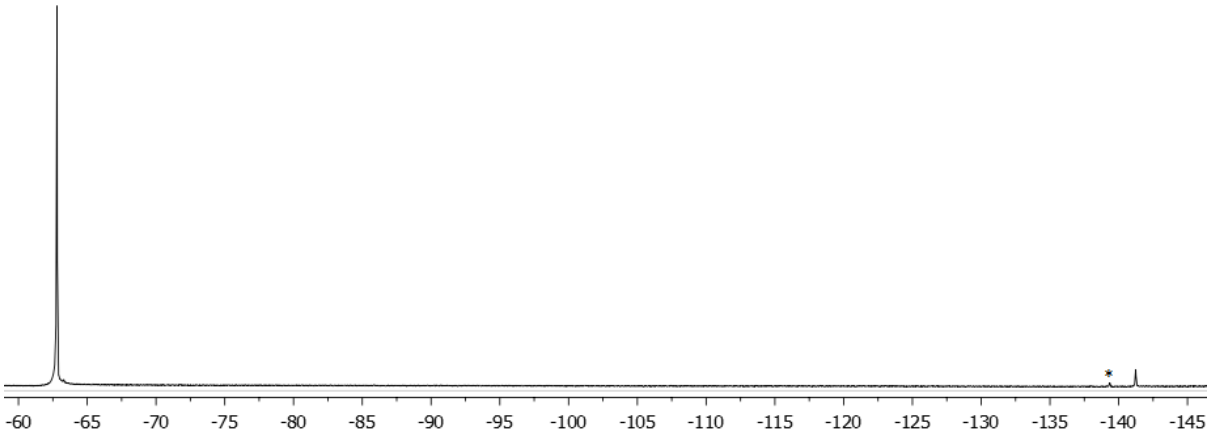

Figure S23: *$^{19}F\{^{1}H\}$ NMR spectrum of complex **9** (376.5 MHz, 298 K, CD_2Cl_2). * indicates free 1,2-difluorobenzene.*

S3.3.1 Selected Crystallographic and Refinement Data for Complex 9

Crystal data for 9 (CCDC 1945265): $C_{56}H_{56}BF_{26}P_2Rh$, M = 1398.66 g/mol, orthorhombic, *P*ccn, a = 35.5500(5), b = 17.7103(2), c = 18.7565(3) Å, α = β = γ = 90°, V = 11809.1(3) Å^3, Z = 8, λ(Cu-Kα) = 1.54184 Å, T = 150(1) K, yellow plate, ρ(calcd, g cm^{-3}) = 1.573, μ (mm^{-1}) = 3.937, 46114 reflections collected, 12210 independent measured reflections (R_{int} = 0.0586), F^2 refinement, R_1(obs, I > 2σ(I)) = 0.1069, wR_2(all data) = 0.2856, 10373 independent observed reflections [|F_o| > 4σ(|F_o|), 2ϑ_{max} = 152.1°], 1749 restrains, 1161 parameters, GOF = 1.032 and residual electron density (e Å^{-3}) = 1.449/-1.249.

S3.3.2 Supplementary Analysis of the Solid-State Molecular Structure of Complex 9 by Single-Crystal X-ray Diffraction

The cationic fragment [(dtbpe)Rh(1,2-difluorobenzene)]$^{+}$ (*Figure S24*) is surrounded by six $BAr^{F}_{4}{}^{-}$ counteranions arranged into a near-perfect octahedron (*Figure S25*). The cationic fragment is disordered over two symmetry-unrelated positions where the minor (*c.* 22% refined chemical occupancies) and major (*c.* 78%) components are differentiated by a *c.* 83° tilt of the P1–Rh1–P2 plane.

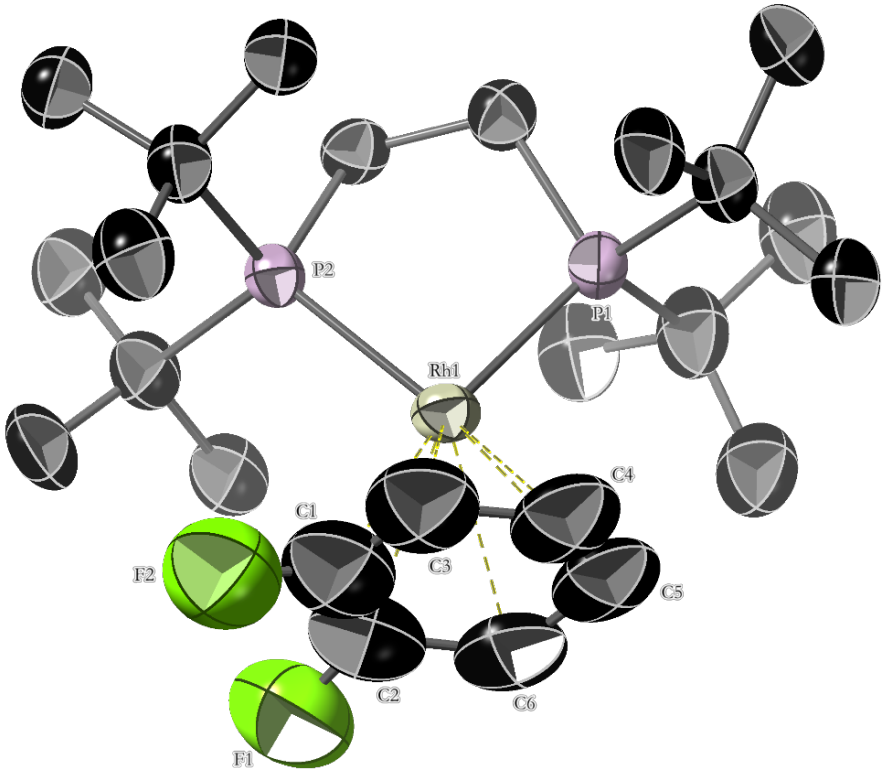

Figure S24: *Cationic fragment [(dtbpe)Rh(1,2-difluorobenzene)]$^{+}$ of* ***9****, major (*c. *78%) disordered component. 50% displacement ellipsoids. H atoms omitted for clarity. Selected bond lengths (Å) and angles (°), where Cent is the centroid of the arene: Rh1–P1, 2.285(3); Rh1–P2, 2.300(2); Rh1–Cent, 1.862(7); C1–C2, 1.21(3); C2–C6, 1.46(3); C6–C5, 1.37(3); C5–C4, 1.31(3); C4–C3, 1.46(3); C3–C1, 1.34(3); C1–F2, 1.23(2); C2–F1, 1.30(2); P1–Rh1–P2, 86.93(9); C1–C2–C6, 120(2); C2–C6–C5, 117.0(17); C6–C5–C4, 117.9(16); C5–C4–C3, 124.5(17); C4–C3–C1, 111.4(19); C3–C1–C2, 129(2).*

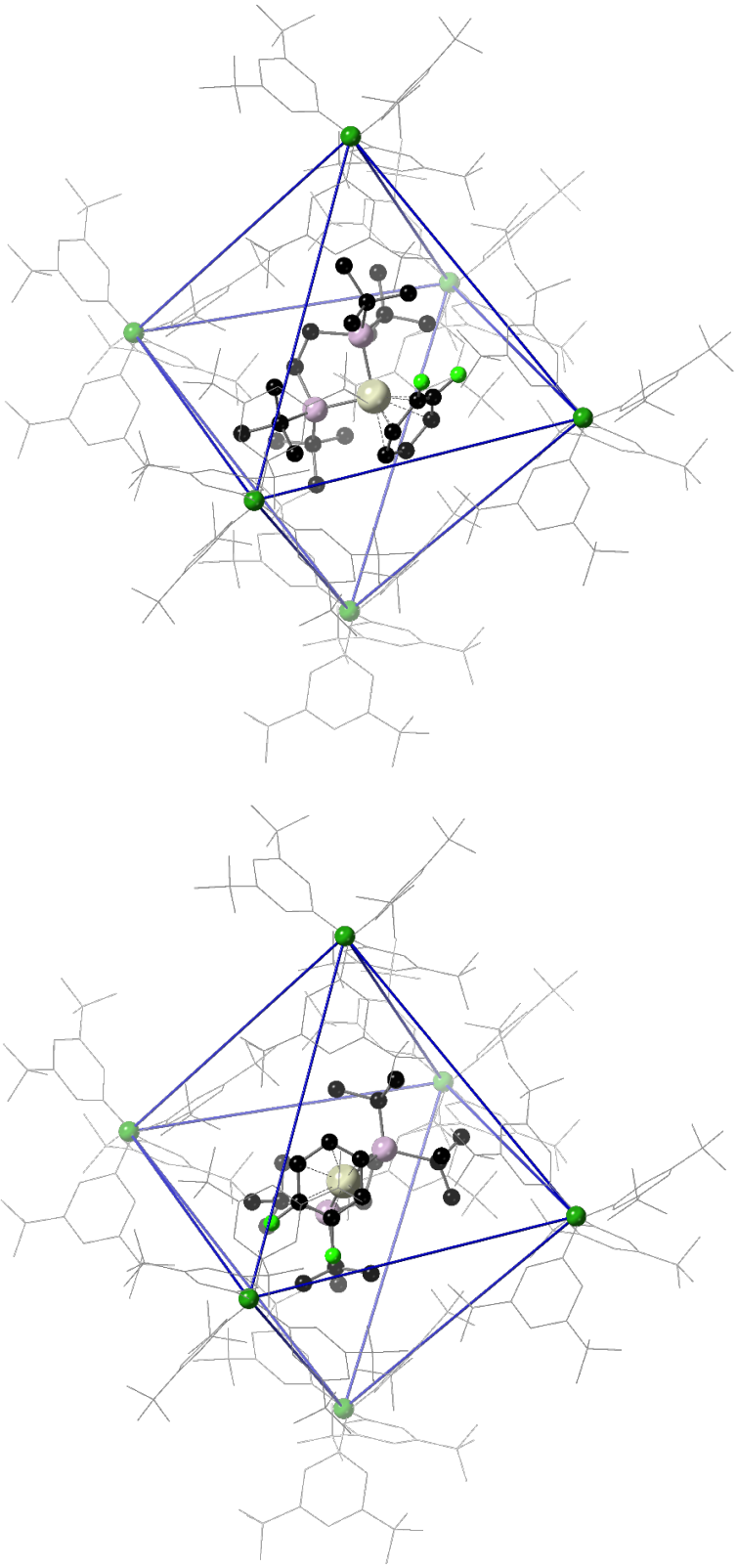

Figure S25: *The packing environment of [(dtbpe)Rh(1,2-difluorobenzene)][BAr$^{F}_{4}$] (**9**), of which both the major (*c. *78%, top) and minor (*c. *22%, bottom) disordered components are shown (modelled as ball-and-stick), and their six mutual nearest BAr$^{F}_{4}{}^{-}$ neighbours (modelled as wireframes with B atom balls).*

S3.4 Synthesis and Characterisation of Single-Crystalline [(dtbpe)Rh(*butenes*)][BAr$^F_4$] (butenes = 1-butene, *cis*-2-butene), Complex 10/11

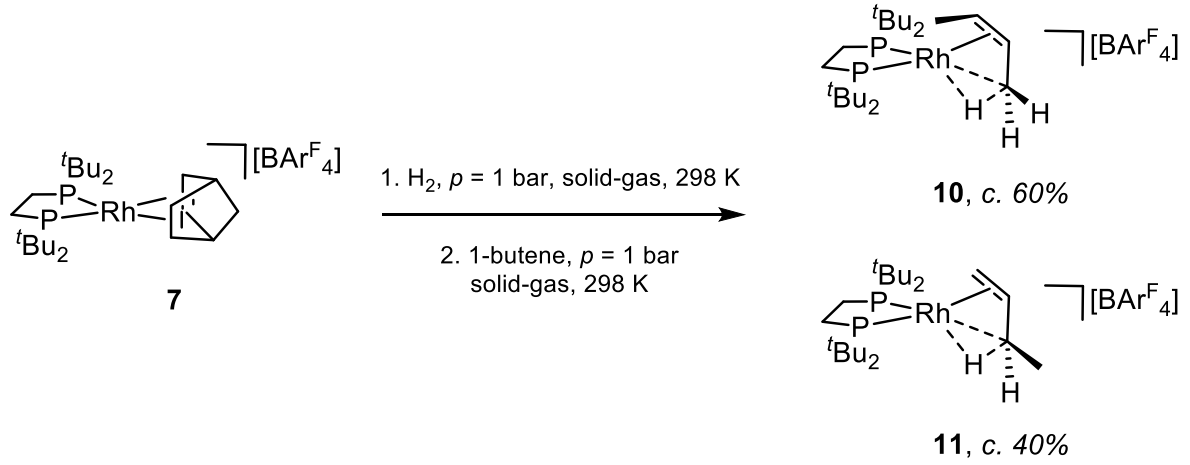

Crystalline complex **7** (*c.* 2 mg) was introduced to a high-pressure NMR tube fitted with a Young's tap (controlled atmosphere valve), before the tube was evacuated and pressurised with H_2 (1 bar) to form complex **8**. After 45 min, the NMR tube was again evacuated, and pressurised with 1-butene (1 bar) for 48 hours. The resulting air-sensitive orange crystals of [(dtbpe)Rh(*butenes*)][BAr$^F_4$], complexes **10** ([(dtbpe)Rh(*cis*-2-butene)][BAr$^F_4$], *c.* 60%) and **11** ([(dtbpe)Rh(1-butene)][BAr$^F_4$], *c.* 40%, proportions in the solid state ascertained from single-crystal x-ray diffraction) are stable indefinitely under an argon atmosphere and for at least seven days under an atmosphere of butenes.

Samples for solid-state NMR analysis were prepared *in situ*. A 4.0 mm zirconia solid-state rotor was packed with *c.* 25 mg of **7** (*c.* 20 µmol). Left unsealed, the rotor was introduced[2] to H_2 (1 bar) for 50 min, followed by evacuation and re-pressurisation with 1-butene (1 bar) for 48 hours and closure of the rotor under a flow of 1-butene.

Rapid libration and allyl hydride/alkene tautomerism of the olefin complexes has been previously established,[2] and is likely responsible for these species' broadness in their NMR spectra in CD_2Cl_2 at 183 K. Cross-peaks visible in the $^1H/^1H$ COSY NMR spectrum (CD_2Cl_2, 183 K; *Figure S26*) at 183 K confirm the presence of 2-butene olefinic CH coincident with the *protio*-solvent and correlating with CH_3 at δ_H = 0.41 ppm. Comparison with the independently synthesised butadiene complex **12** (*vide infra*) confirms that dehydrogenation to give the butadiene complex does *not* occur appreciably in the solid-state, in contrast to complex **1**.

The ^1H NMR spectrum (CD_2Cl_2, 183 K; *Figure S26*) suggests that the *cis*-2-butene fragment is undergoing a fluxional process, providing a single signal for agostic CH_3 and for olefinic CH. Where two ^1H ^{t}Bu environments are observed for the 1-butene complex, in the *cis*-2-butene complex only one environment is observed. In the ^1H NMR spectrum for the 1-butene complex, agostic CH, allylic non-agostic CH, CH_3, and all three olefinic CH are resolvable. Only one olefinic carbon is resolvable in the $^{13}C\{^1H\}$ NMR spectrum (CD_2Cl_2, 183 K; *Figure S28*).

Where the NBA complex **8** produces a virtual triplet in the $^{31}P\{^{1}H\}$ SSNMR spectrum at 298 K (*Figure S16*), the butenes complex **10**/**11** produces a more complicated resonance from overlapping signals of two doublets of doublets (*Figure S33*). Furthermore, no significant signals are visible in the alkene region of the $^{13}C\{^{1}H\}$ solid-state NMR (*Figure S29*) at 298 K, but signals do emerge in this region upon cooling to 183 K (*Figure S30*). Similar cooling produces a loss of definition in the $^{31}P\{^{1}H\}$ solid-state NMR (*Figure S34*).

^{1}H NMR (400.1 MHz, CD_2Cl_2, 183 K): δ 0.05 (br. s, 0.4 H; agostic CH*), 0.41 (br. s, 3.6 H; agostic $CH_3^{\dagger}$), 1.06 (d, $^{3}J_{HP}$ = 13.8 Hz, *c.* 7 H; ^{t}Bu*), 1.19 (vdd, $^{3}J_{HP}$ = 13.2 Hz, *c.* 22 H; $^{t}Bu^{\dagger}$), 1.27 (d, $^{3}J_{HP}$ = 13.6 Hz, *c.* 7 H; ^{t}Bu*), 1.45 (br. t, $^{3}J_{HH} \sim$ 5.5 Hz, 1.2 H; CH_3*), 1.65–2.02 (m, $\sum$ = 4.0 H; *dtbpe* CH_2*†), 2.09 (br. s, 0.4 H; allylic non-agostic CH*), 3.37 (d, $^{3}J_{HH}$ = 14.0 Hz, 0.4 H; olefinic CH*), 4.74 (m, 0.4 H; olefinic CH*), 4.86 (d, *J* = 7.5 Hz, 0.4 H; olefinic CH*), 7.53 (s, 4 H; *p*-H), 7.71 (s, 8 H, *o*-H). *Olefinic CH† is obscured by the* protio-*solvent, confirmed by COSY experiments.*

$^{13}C\{^{1}H\}$ NMR (100.6 MHz, CD_2Cl_2, 183 K): δ 11.2 (d, $^{2}J_{CRh}$ = 4.8 Hz; agostic CH_n*), 13.3 (br. s†), 18.0 (s; 1-butene CH_3), 20.2 (br. m†), 25.5 (br. m†), 29.7 (m; ^{t}Bu CH_3), 35.9 (d, $^{1}J_{CP} \sim$ 19 Hz; ^{t}Bu $C_Q^{\dagger}$), 36.2 (d, $^{1}J_{CP} \sim$ 18 Hz; ^{t}Bu C_Q*), 36.4 (d, $^{1}J_{CP} \sim$ 18 Hz; ^{t}Bu C_Q*), 37.5 (d, $^{1}J_{CP} \sim$ 18 Hz; ^{t}Bu C_Q*), 37.9 (d, $^{1}J_{CP} \sim$ 18 Hz; ^{t}Bu C_Q*), 38.2 (d, $^{1}J_{CP} \sim$ 19 Hz; ^{t}Bu $C_Q^{\dagger}$), 90.2 (olefinic C*), 90.3 (olefinic C†), 90.4 (olefinic C*), 117.2 (br. sept, $^{3}J_{CF} \sim$ 4 Hz; *p*-C_{aryl}), 124.1 (q, $^{1}J_{CF}$ = 272.6 Hz; CF_3), 128.3 (qm, $^{2}J_{CF} \sim$ 30 Hz; C_{aryl}-CF_3), 134.3 (s; *o*-C_{aryl}), 161.5 (q, $^{1}J_{CB} \approx$ 50 Hz (^{11}B); *i*-C_{aryl}).

* corresponds to [(dtbpe)Rh(1-butene)][BAr^F_4], complex **11** (minor, *c.* 40%); † corresponds to [(dtbpe)Rh(*cis*-2-butene)][BAr^F_4], complex **10** (major, *c.* 60%). All ^{1}H NMR resonances are scaled according to $BAr^F_4{}^-$ aryl C-H integrals normalised to 8H:4H.

$^{13}C\{^{1}H\}$ SSNMR (100.6 MHz, 10 kHz spin rate, 298 K): δ 10–40 (*dtbpe*), 115–140 (BAr^F_4), 163 (BAr^F_4 C-B).

$^{13}C\{^{1}H\}$ SSNMR (100.6 MHz, 10 kHz spin rate, 183 K): δ 10–40 (*dtbpe*), 88.3 (olefinic C), 88.9 (olefinic C), 90.5 (olefinic C), 115–140 (BAr^F_4), 163 (BAr^F_4 C-B).

$^{31}P\{^{1}H\}$ NMR (161.9 MHz, CD_2Cl_2, 183 K): δ 112.9 (dd, $^{2}J_{PRh}$ = 162 Hz, $^{3}J_{PP}$ = 16 Hz; P *trans* to σ*), 114.4 (dd, $^{2}J_{PRh}$ = 162 Hz, $^{3}J_{PP}$ = 16 Hz; P *trans* to σ†), 114.9 (dd, $^{2}J_{PRh}$ = 220 Hz, $^{3}J_{PP}$ = 16 Hz; P *trans* to π†), 116.2 (dd, $^{2}J_{PRh}$ = 205 Hz, $^{3}J_{PP}$ = 15 Hz; P *trans* to π*).

$^{31}P\{^{1}H\}$ SSNMR (161.9 MHz, 10 kHz spin rate, 298 K): δ 113.9 (m, $\nu_{½}$ = 200 Hz).

$^{31}P\{^{1}H\}$ SSNMR (161.9 MHz, 10 kHz spin rate, 183 K): δ 111.1 (br. s, $\nu_{½}$ = 600 Hz).

$^{19}F\{^{1}H\}$ NMR (376.5 MHz, CD_2Cl_2, 298 K): δ –62.8 (Ar^F-CF_3).

$^{19}F\{^{1}H\}$ NMR (376.5 MHz, CD_2Cl_2, 183 K): δ –62.2 (Ar^F-CF_3).

$^{11}B\{^{1}H\}$ NMR (128.4 MHz, CD_2Cl_2, 298 K): δ –6.63 ($BAr^F_4{}^-$).

$^{11}B\{^1H\}$ NMR (128.4 MHz, CD_2Cl_2, 183 K): δ –6.87 ($BAr^F{}_4^-$).

This material does not survive in CH_2Cl_2 solution long enough at 298 K to permit mass spectrometry.

Elemental analysis found (calculated) for $C_{54}H_{60}BF_{24}P_2Rh$: C, 48.27 (48.38); H, 4.40 (4.51)

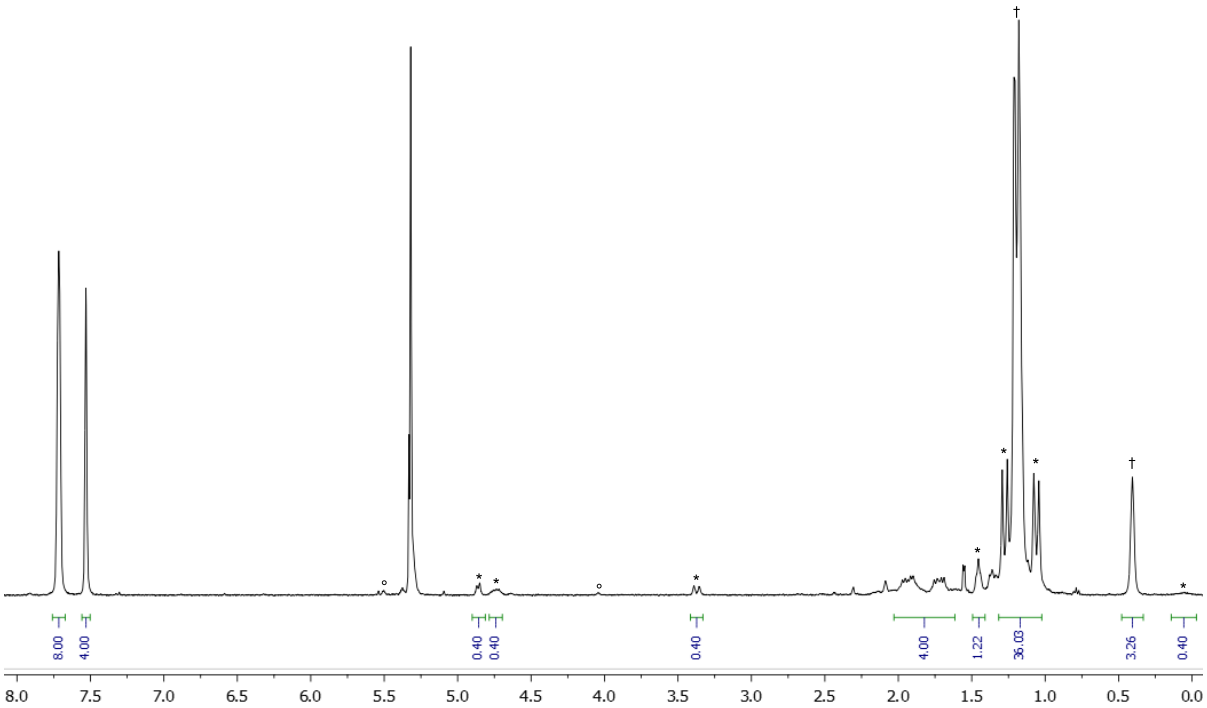

Figure S26: *^1H NMR spectrum of complex **10/11** (400.1 MHz, 183 K, CD_2Cl_2).* * corresponds to [(dtbpe)Rh(1-butene)][$BAr^F{}_4$], complex **11** (minor, *c.* 40%); † corresponds to [(dtbpe)Rh(*cis*-2-butene)][$BAr^F{}_4$], complex **10** (major, *c.* 60%). ° corresponds to unreacted **7** (<4%).

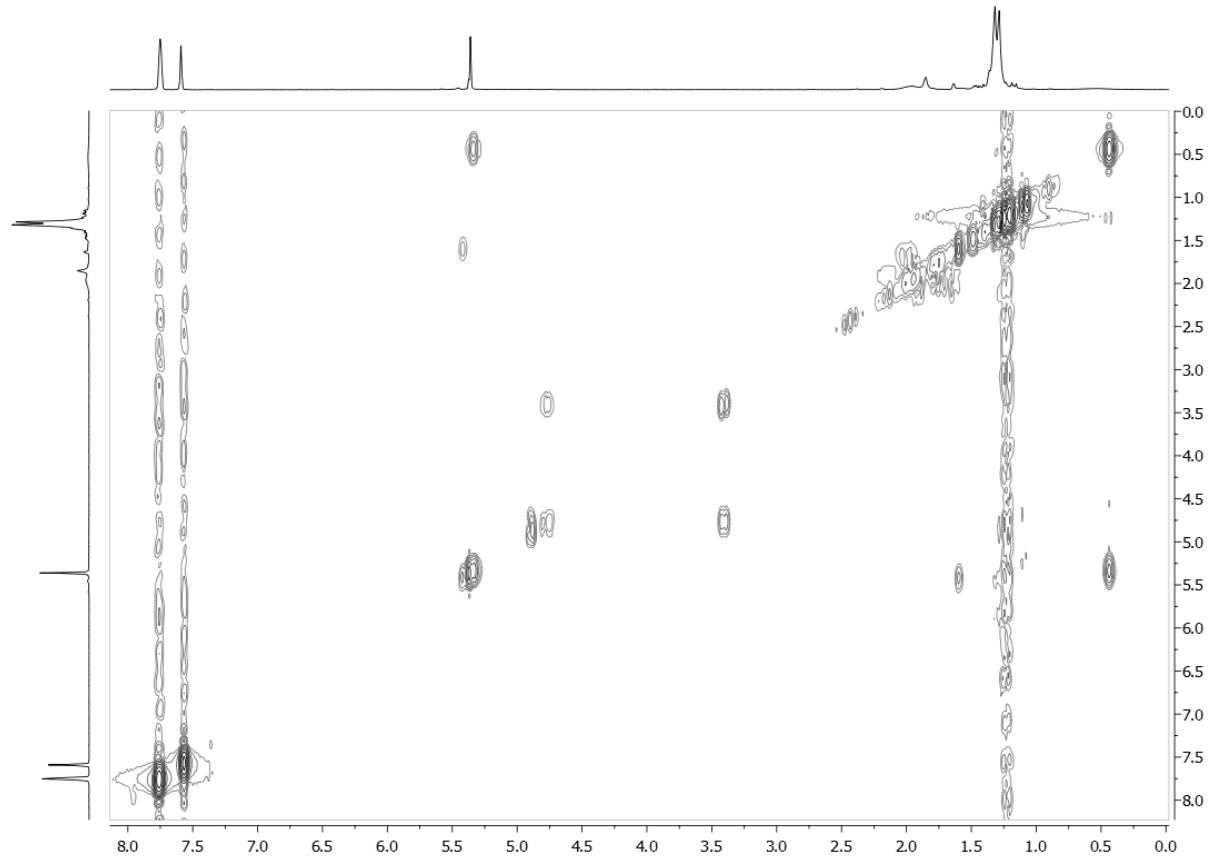

Figure S27: *$^{1}H/^{1}H$ COSY NMR spectrum of complex **10/11** (400.1 MHz, 183 K, CD_2Cl_2).*

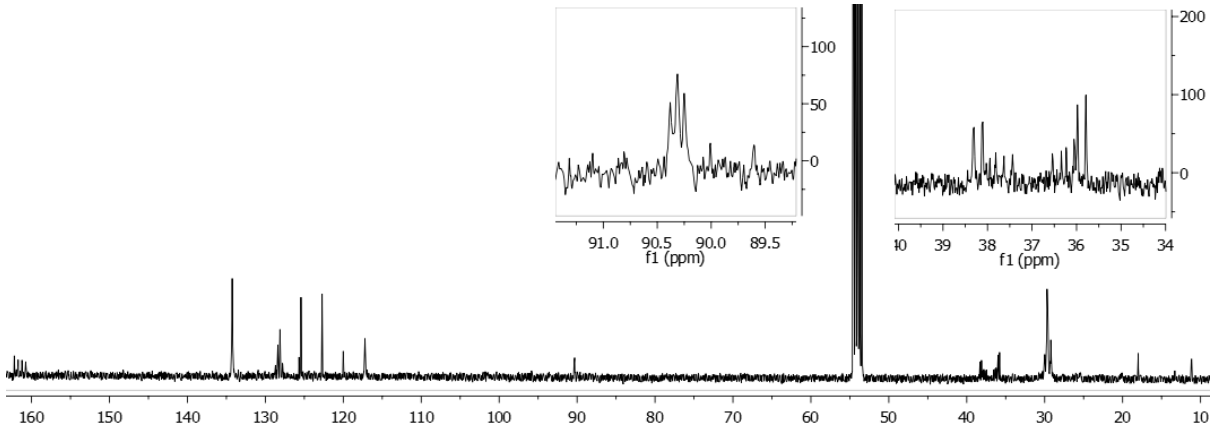

Figure S28: *$^{13}C\{^{1}H\}$ NMR spectrum of complex **10/11** (100.6 MHz, 183 K, CD_2Cl_2).*

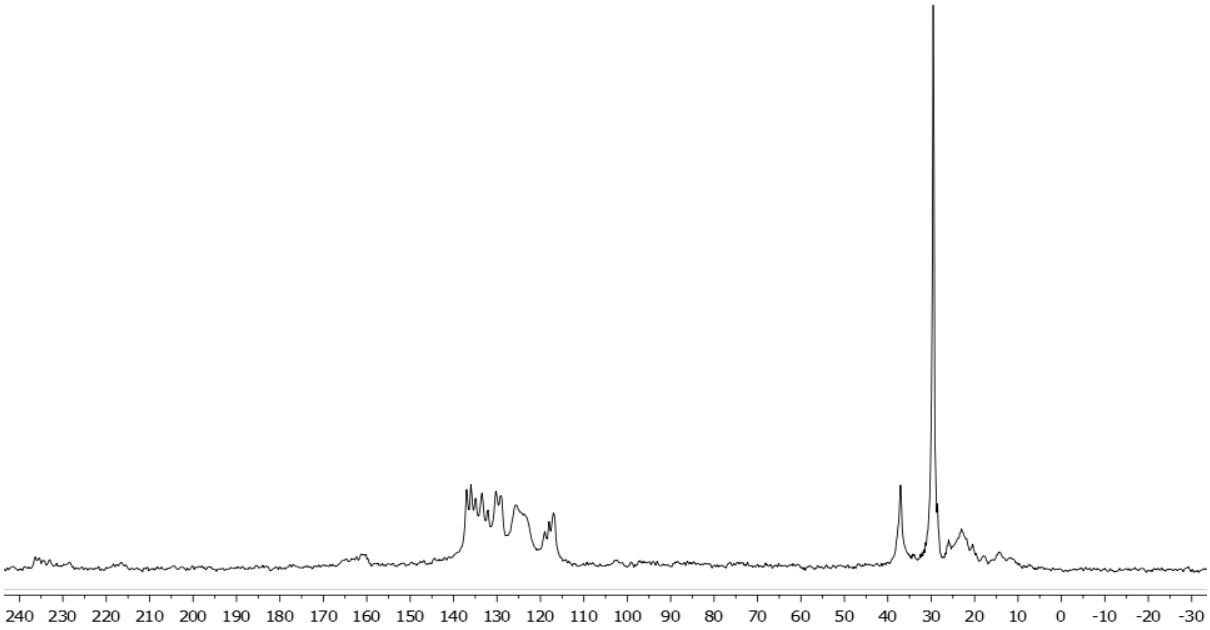

Figure S29: *$^{13}C\{^{1}H\}$ SSNMR spectrum of complex **10/11** (100.6 MHz, spinning speed 10 kHz, 298 K) prepared* in situ *from **8**.*

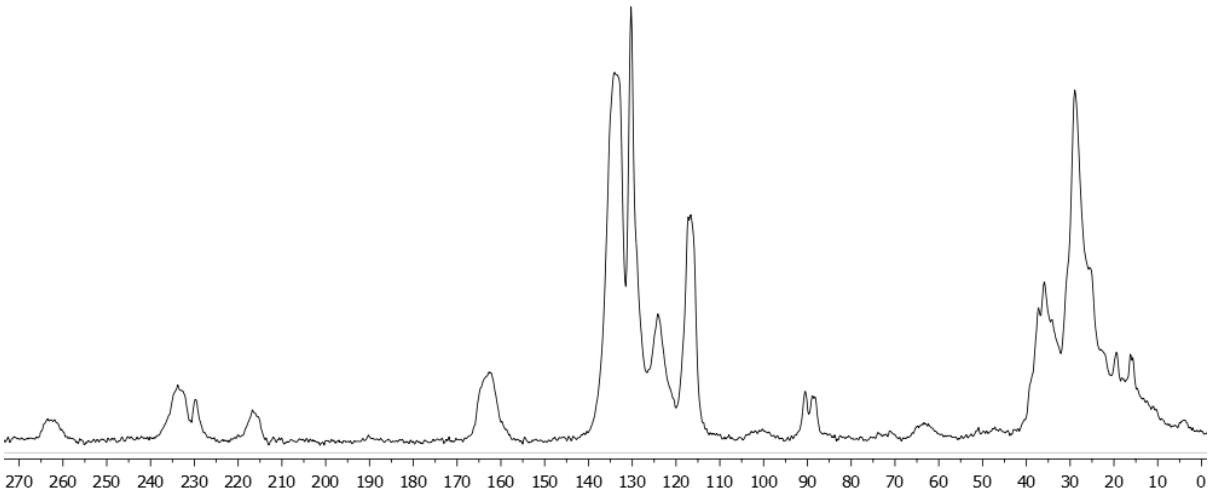

Figure S30: *$^{13}C\{^{1}H\}$ SSNMR spectrum of complex **10/11** (100.6 MHz, spinning speed 10 kHz, 183 K) prepared* in situ *from **8**.*

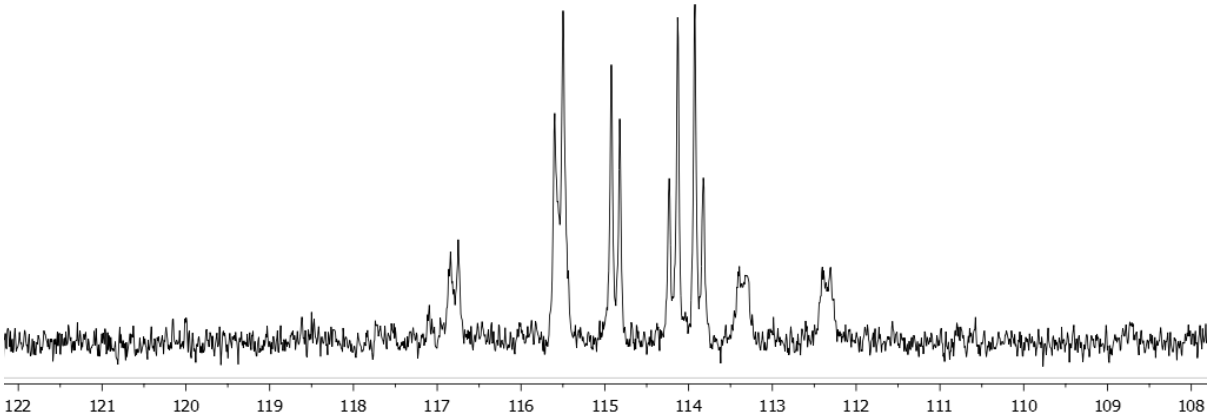

Figure S31: *$^{31}P\{^{1}H\}$ NMR spectrum of complex **10/11** (161.9 MHz, 183 K, CD_2Cl_2)*

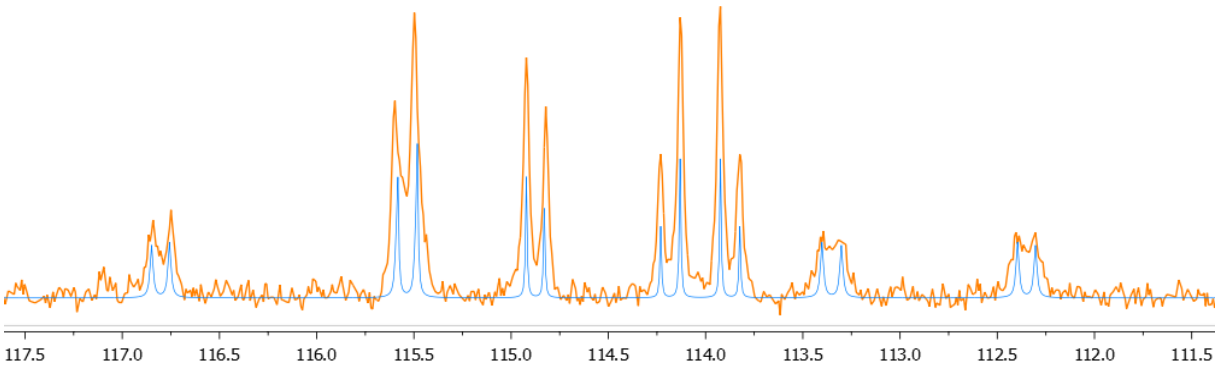

Figure S32: *$^{31}P\{^{1}H\}$ NMR spectrum of complex **10/11** (161.9 MHz, 183 K, CD_2Cl_2; in orange) including a spin simulation (in blue). Complex **10** is modelled as: δ* 114.38 (dd, $^{2}J_{PRh}$ = 162 Hz, $^{3}J_{PP}$ = 16 Hz; P *trans* to σ), 114.85 (dd, $^{2}J_{PRh}$ = 220 Hz, $^{3}J_{PP}$ = 16 Hz; P *trans* to π)*, with a 1.5 Hz linewidth. Complex **11** is modelled as: δ* 112.85 (dd, $^{2}J_{PRh}$ = 162 Hz, $^{3}J_{PP}$ = 16 Hz; P *trans* to σ), 116.17 (dd, $^{2}J_{PRh}$ = 205 Hz, $^{3}J_{PP}$ = 15 Hz; P *trans* to π)*, with a 3.0 Hz linewidth.*

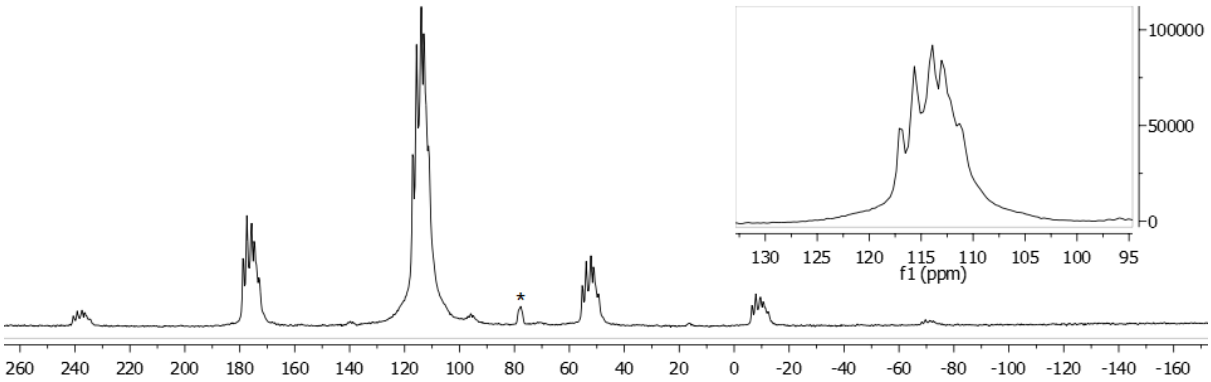

Figure S33: *$^{31}P\{^{1}H\}$ SSNMR spectrum of complex **10/11** (161.9 MHz, spinning speed 10 kHz, 298 K) prepared* in situ *from **8**. * indicates unreacted **7**.*

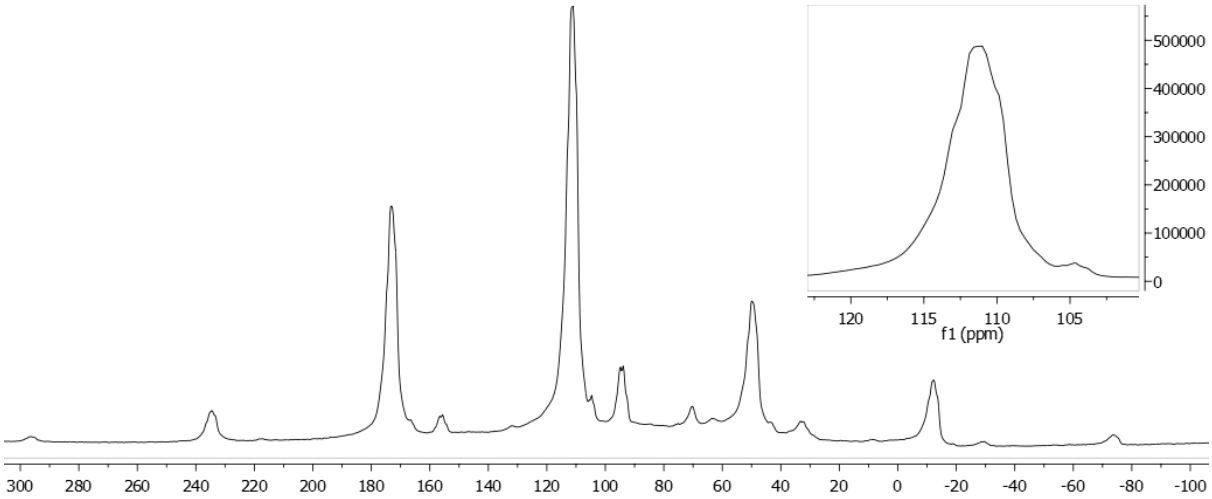

Figure S34: *$^{31}P\{^{1}H\}$ SSNMR spectrum of complex **10/11** (161.9 MHz, spinning speed 10 kHz, 183 K) prepared* in situ *from **8**.*

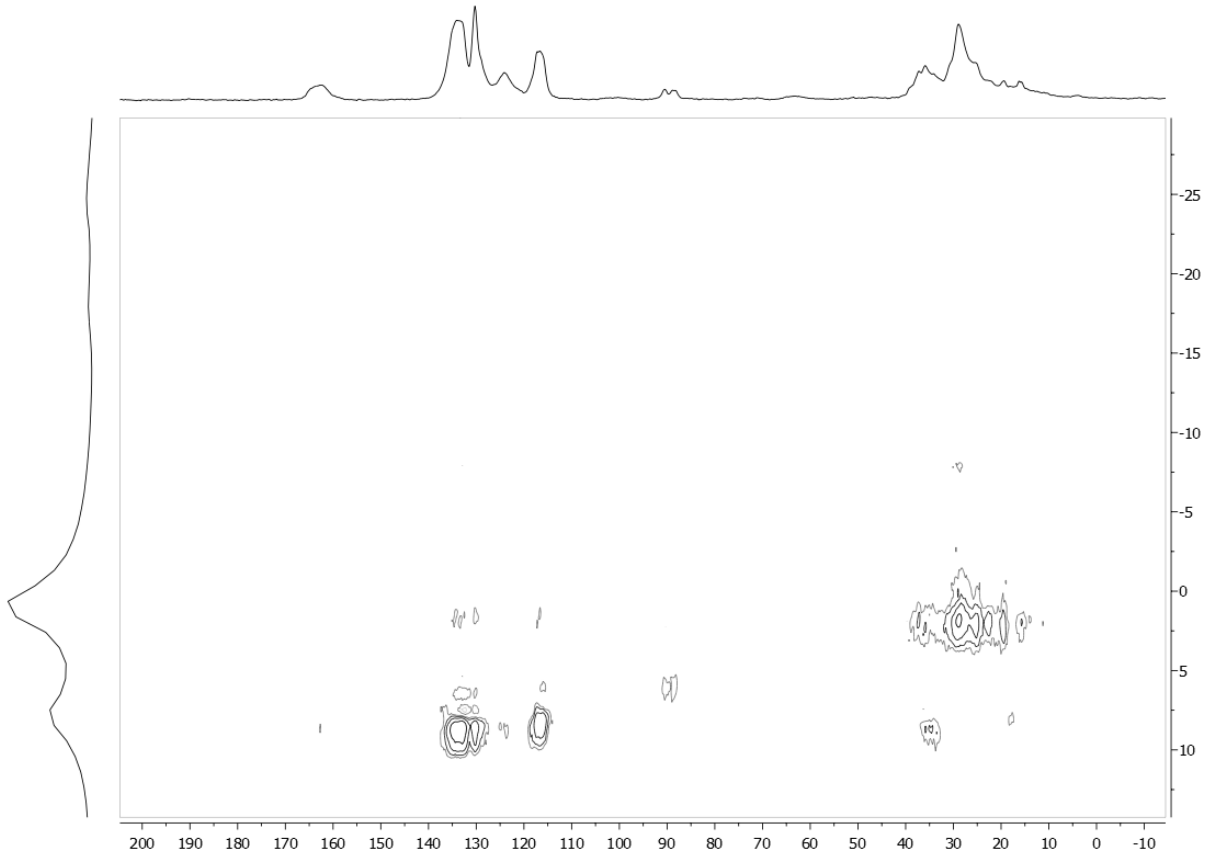

Figure S35: *$^{13}C/^{1}H$ SSNMR HETCOR spectrum of complex **10/11** (spinning speed 10 kHz, 183 K) prepared* in situ *from **8**.*

S3.4.1 Selected Crystallographic and Refinement Data for Complex 10/11

Crystal data for 10 and 11 (CCDC 1945266): $C_{54}H_{60}BF_{26}P_2Rh$, M = 1340.68 g/mol, monoclinic, $P2_1/c$, a = 13.8945(2), b = 17.8193(2), c = 23.5243(4) Å, β = 96.4570(10)°, V = 5887.44(14) Å^3, Z = 4, λ(Cu-Kα) = 1.54184 Å, T = 150(1) K, orange plate, ρ(calcd, g cm^{-3}) = 1.539, μ (mm^{-1}) = 3.936, 55357 reflections collected, 12140 independent measured reflections (R_{int} = 0.0531), F^2 refinement, R_1(obs, $I > 2\sigma(I)$) = 0.0410, wR_2(all data) = 0.1133, 9711 independent observed reflections [$|F_o| > 4\sigma(|F_o|)$, $2\vartheta_{max}$ = 153.4°], 961 restrains, 988 parameters, GOF = 1.025 and residual electron density (e Å^{-3}) = 0.738/-1.021.

S3.4.2 Supplementary Analysis of the Solid-State Molecular Structure of Complex 10/11 by Single-Crystal X-ray Diffraction

The solid-state molecular structures of the two disordered cations of complexes **10** and **11** are shown in *Figure S35*.

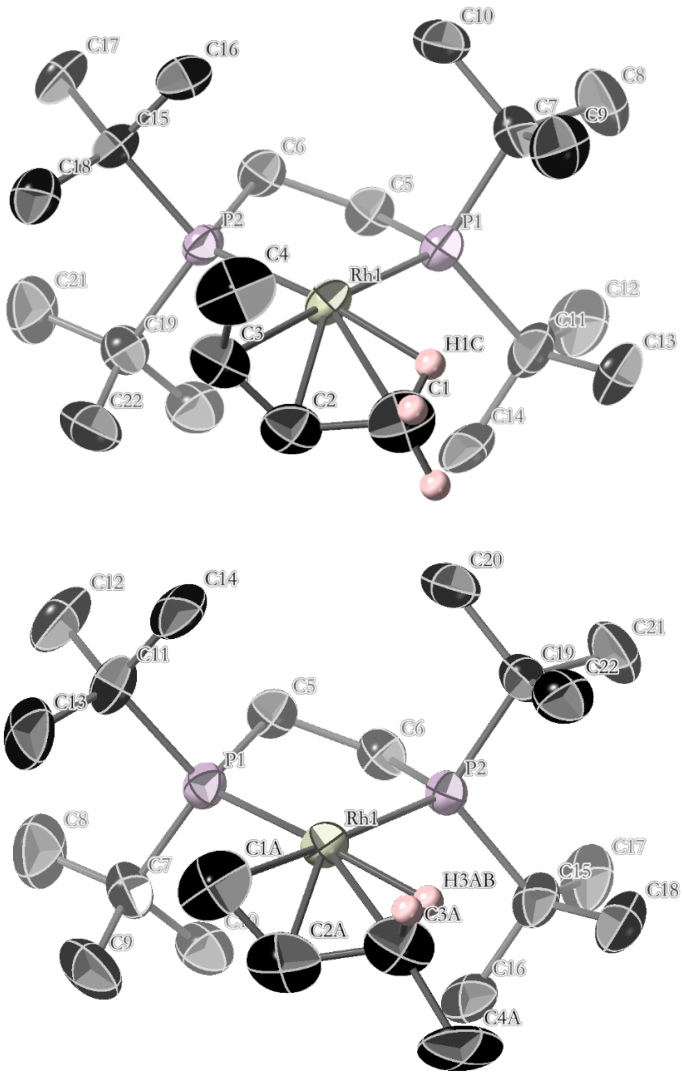

Figure S36: *Cationic fragments [(dtbpe)Rh(*cis*-2-butene)]$^+$ (**10**) and [(dtbpe)Rh(1-butene)]$^+$ (**11**) (top and bottom respectively) of [(dtbpe)Rh(*butenes*)][BAr$^F{}_4$]. 50% displacement ellipsoids. H atoms omitted for clarity excepting those associated with agostic positions. Selected bond lengths (Å) and angles (deg), where Cent1 is the centroid of C1A–C2A and Cent2 is the centroid of C2–C3: Rh1–P1, 2.2652(9); Rh1–P2, 2.2616(8); Rh1–H3AB, 1.8146(4); Rh1–H1C, 1.8953(3); Rh1–C2, 2.167(7); Rh1–C3, 2.356(10); Rh1–C1A, 2.250(10); Rh1–C2A, 2.155(7); Rh1–Cent1, 2.095(7); Rh1–Cent2, 2.161(6); C1–C2, 1.475(13); C2–C3, 1.346(12); C3–C4, 1.467(14); C1A–C2A, 1.362(13); C2A–C3A, 1.525(15); C3A–C4A, 1.541(18); P2–Rh1–C2, 117.26(19); P2–Rh1–Cent2, 106.99(17); P2–Rh1–C3, 96.6(3); P1–Rh1–C2A, 119.8(2); P1–Rh1–Cent1, 108.6(2); P1–Rh1–C1A, 96.8(3).*

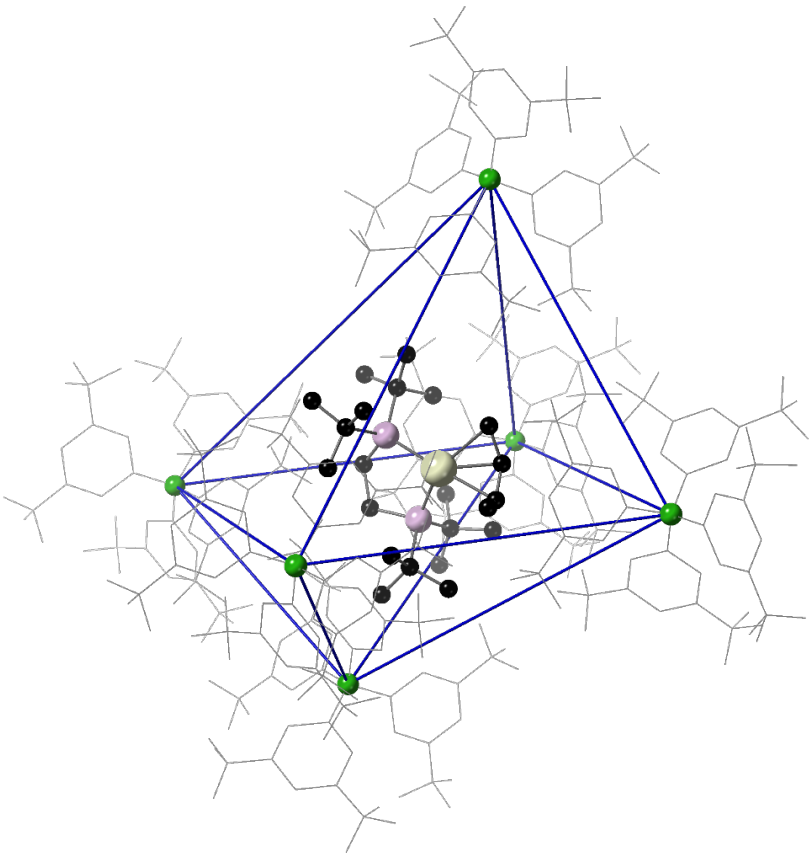

Figure S37: *The packing environment of [(dtbpe)Rh(*butenes*)][BAr$^F_4$] (**10/11**), of which the component L =* cis*-2-butene (**10**) is shown (modelled as ball-and-stick), and its six nearest BAr$^F_4$$^-$ neighbours (modelled as wireframes with B atom balls).*

S3.5 Synthesis and Characterisation of Single-Crystalline C-Cl Activated Product [(dtbpe)Rh(μ-CH$_2$)(μ-Cl)$_2$Rh(dtbpe)][BAr$^F_4$]$_2$, Complex 12

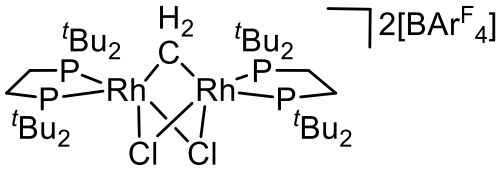

12

Method I

Fine crystalline **14** (5 mg, 2 μmol, as prepared below) was introduced to an NMR tube fitted with a Young's tap and dissolved in CH_2Cl_2 (0.4 mL). After 2 weeks, when only one $^{31}P\{^1H\}$ NMR resonance was observed, the contents of the NMR tube were concentrated by 50% and layered with pentane.

This gave orange crystals of [(dtbpe)Rh(μ-CH_2)(μ-Cl)$_2$Rh(dtbpe)][$BAr^F{}_4$]$_2$, complex **12** (*c.* 0.5 mg, *c.* 10%), after 6 hours. While conversion was quantitative as observed *via* NMR, isolated crystalline yield was poor.

Method II

Crushed complex **7** (*c.* 5 mg) was introduced to an NMR tube fitted with a Young's tap. The tube was evacuated and re-pressurised with H_2 (1 bar) for 45 min to give complex **8**, before the H_2 atmosphere was evacuated and the tube was backfilled with argon. CH_2Cl_2 (0.4 mL) was then introduced at room temperature to dissolve complex **8**. The solution was left for 48 hours before quantitative conversion to complex **12** was obtained, observed *via* $^{31}P\{^1H\}$ NMR; initially, a broad doublet in the $^{31}P\{^1H\}$ NMR was visible at δ_P = 120.3 ppm ($^1J_{PRh} \sim 220$ Hz).

Method III

This complex is likewise generated from the quenching of **10**/**11** in CH_2Cl_2 at room temperature; after 48 hours at 298 K, complex **12** was obtained quantitatively, observed *via* ^1H and $^{31}P\{^1H\}$ NMR.

^1H NMR (400.1 MHz, CD_2Cl_2, 298 K): δ 1.42 (d, 18 H, $^3J_{HP}$ = 14.9 Hz; ^{t}Bu), 1.50 (d, 18 H, $^3J_{HP}$ = 14.2 Hz; ^{t}Bu), 1.94 (m, 2 H; *dtbpe* CH_2), 2.18 (s, 2 H; bridging CH_2), 2.32 (m, 2 H; *dtbpe* CH_2), 7.56 (s, 4 H; *p*-H), 7.71 (s, 8 H; *o*-H).

$^{31}P\{^1H\}$ NMR (162 MHz, CD_2Cl_2, 298 K): δ 98.0 (br. d, $^1J_{PRh} \sim 150$ Hz).

$^{19}F\{^1H\}$ NMR (376.5 MHz, CD_2Cl_2, 298 K): δ –62.8 (Ar^F-CF_3).

$^{11}B\{^1H\}$ NMR (128.39 MHz, CD_2Cl_2, 298 K): δ –6.65 ($BAr^F{}_4^-$).

ESI-MS (CH_2Cl_2) m/z found (calculated) for $C_{37}H_{82}P_4Rh_2Cl_2$ $[M]^{2+}$: 463.1460 (463.1422).

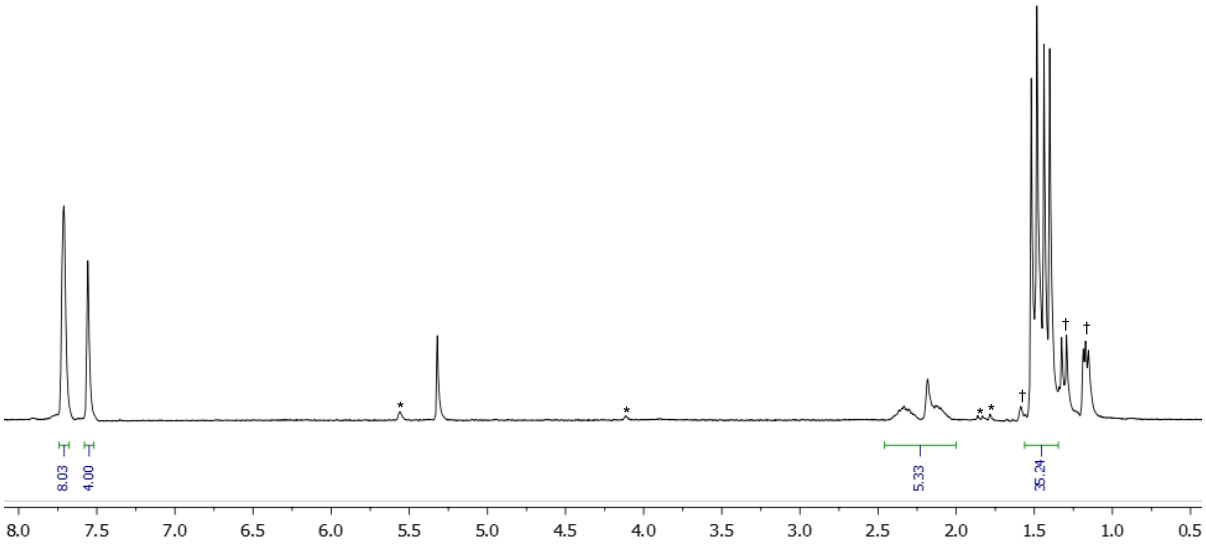

Figure S38: *^{1}H NMR spectrum of complex **12** (400.1 MHz, 298 K, CD_2Cl_2) as generated* in situ via *Method II. As such, * corresponds to unreacted **7** (<5%) and † to free NBA.*

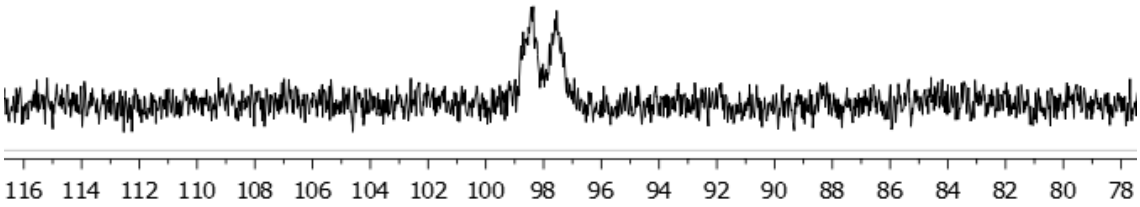

Figure S39: *^{1}H NMR spectrum of complex **12** (161.9 MHz, 298 K, CD_2Cl_2) as generated* in situ via *Method II.*

S3.5.1 Selected Crystallographic and Refinement Data for Complex 12

Crystal data for 12 (CCDC 1945268): $C_{101}H_{106}B_2Cl_2F_{48}P_4Rh_2$, M = 2654.07 g/mol, orthorhombic, $P2_12_12$, a = 24.0564(2), b = 18.6694(2), c = 12.35080(10) Å, α = β = γ = 90°, V = 5546.97(9) Å^3, Z = 2, λ(Cu-Kα) = 1.54184 Å, T = 150(1) K, yellow trapezoid, ρ(calcd, g cm^{-3}) = 1.589, μ (mm^{-1}) = 4.534, 55033 reflections collected, 11519 independent measured reflections (R_{int} = 0.0493), F^2 refinement, R_1(obs, $I > 2\sigma(I)$) = 0.0441, wR_2(all data) = 0.1130, 10839 independent observed reflections [$|F_o| > 4\sigma(|F_o|)$, $2\vartheta_{max}$ = 152.5°], 667 restrains, 869 parameters, GOF = 1.030 and residual electron density (e Å^{-3}) = 1.878/-0.906.

S3.5.2 Supplementary Analysis of the Solid-State Molecular Structure of Complex 12 by Single-Crystal X-ray Diffraction

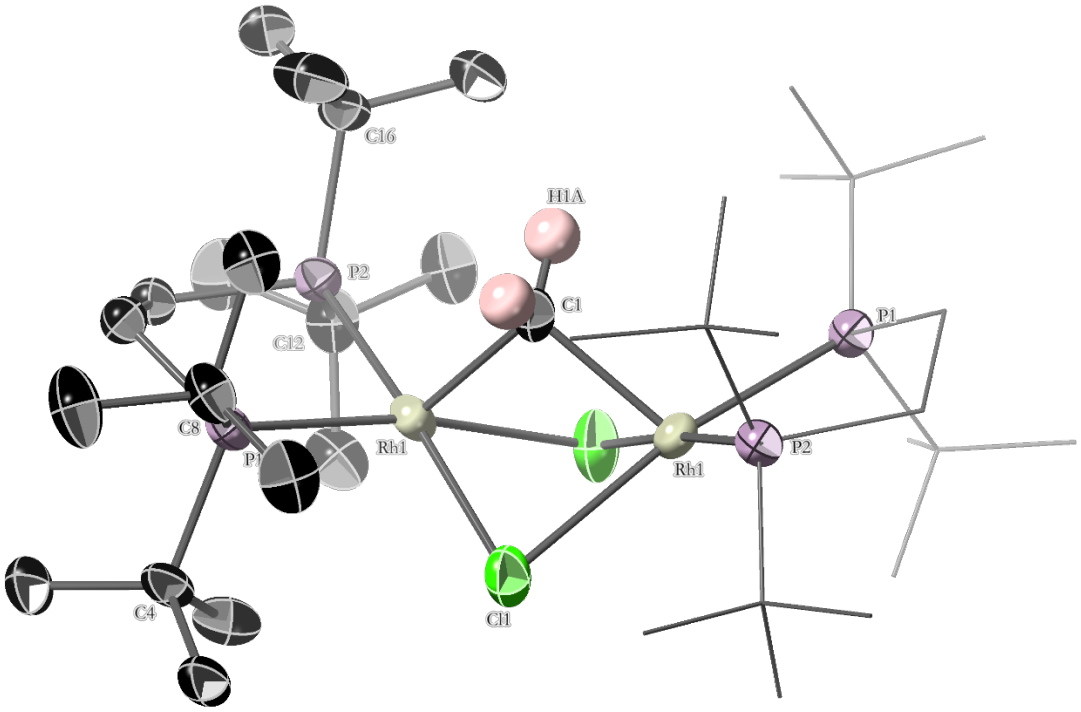

Figure S40: *Cationic fragment [(dtbpe)Rh(μ-CH₂)(μ-Cl)₂Rh(dtbpe)]²⁺ of* ***12****. 50% displacement ellipsoids. H atoms omitted for clarity excepting bridging methylene. Selected bond lengths (Å) and angles (deg): Rh1–Rh1, 3.0312(8); Rh1–C1, 2.045(6); Rh1–Cl1, 2.4431(16); Rh1–P1, 2.3165(14); Rh1–P2, 2.3475(15); P1–Rh1–P2, 86.77(5); P1–Rh1–C1, 109.54(13); P2–Rh1–C1, 104.79(13); C1–Rh1–Cl1, 79.72(14); Rh1–Rh1–Cl1, 51.49(4); Cl1–Rh1–Cl1, 82.61(6).*

S3.6 Synthesis and Characterisation of Single-Crystalline [(dtbpe)Rh(η⁴-C₄H₆)][BArᶠ₄], Complex 13

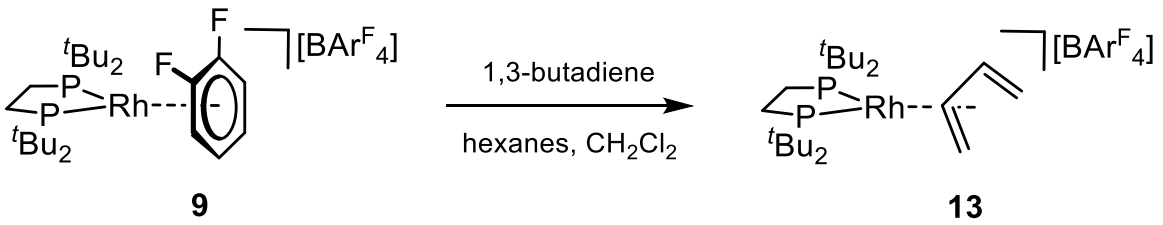

9 **13**

Powdered crystalline complex **7** (25 mg, 18 μmol) was introduced to a Young's flask and dissolved in 1,2-difluorobenzene (2 mL). The solution was frozen with liquid N_2 and the flask was evacuated before re-pressurisation with H_2 (1 bar).

After thawing and 30 min of stirring at room temperature, all volatiles were removed *in vacuo* to give the difluorobenzene adduct [(dtbpe)Rh(η^6-1,2-diflurobenzene)][BAr$^F{}_4$], complex **9**, as an orange solid. This was then re-dissolved in CH_2Cl_2 (2 mL), and a solution of 1,3-butadiene in hexanes (0.5 mL, *c.* 15 wt%, *c.* 1,000 µmol) was introduced.

Stirring was continued for a further 2 hours – over which time the solution turned a deep red – before volatiles were removed *in vacuo*. The product was then redissolved in CH_2Cl_2 (2 mL) and layered with hexane to give dark purple crystals of [(dtbpe)Rh(η^4-C_4H_6)][BAr$^F{}_4$]·CH_2Cl_2, complex **13**·CH_2Cl_2 (17 mg, 13 µmol, 72%) after 48 hours. The butadiene complex **13** degraded in CH_2Cl_2 over time to give unknown products, and, unlike the parent NBD complex **7**, was sensitive to moist air. Hydrogenation of a *c.* 2 mg sample of crushed complex **7** in a high-pressure NMR tube fitted with a Young's tap (controlled atmosphere valve; H_2 1 bar, 45 min) followed by evacuation and pressurisation with 1-butene (1 bar) at 70 °C for 48 hours generates butadiene complex **13** (*c.* 95%), confirmed through ^{1}H and ^{31}P{^{1}H} NMR analysis.

^{1}H NMR (400.1 MHz, CD_2Cl_2, 298 K): *δ* 1.18 (d, 18 H, $^3J_{HP}$ = 13.6 Hz; ^{t}Bu), 1.40 (d, 18 H, $^3J_{HP}$ = 13.6 Hz; ^{t}Bu), 2.02 (m, 4 H; CH_2), 2.71 (dm, 2 H, $^3J_{HH}$ = 14.8 Hz; CH), 4.73 (m, 2 H; CH), 5.52 (m, 2 H; CH), 7.56 (s, 4 H; *p*-H), 7.72 (br. m, 8 H; *o*-H).

^{13}C{^{1}H} NMR (100.6 MHz, CD_2Cl_2, 298 K): *δ* 24.3 (m; *dtbpe* CH_2), 30.2 (s; ^{t}Bu CH_3), 31.6 (s; ^{t}Bu CH_3), 38.8 (m; ^{t}Bu C_Q), 61.9 (q, *J* = 5.5 Hz; butadiene CH_2), 101.8 (d, *J* = 5.8 Hz; butadiene CH), 118.0 (m; *p*-C_{aryl}), 125.1 (q, $^1J_{CF}$ = 273.5 Hz; CF_3), 129.4 (qq, $^2J_{CF}$ = 31.4 Hz, $^4J_{CF}$ = 2.8 Hz; C_{aryl}-CF_3), 135.3 (s; *o*-C_{aryl}), 162.3 (q, $^1J_{CB}$ = 49.9 Hz (^{11}B); *i*-C_{aryl}).

^{13}C{^{1}H} SSNMR (100.6 MHz, 10 kHz spin rate, 298 K): *δ* 23.2 (*dtbpe* CH_2), 29.2 (^{t}Bu CH_3), 37.9 (^{t}Bu C_Q), 58.9 (butadiene CH_2), 61.5 (butadiene CH_2), 99.3 (butadiene CH), 101.4 (butadiene CH), 115–137 (BAr$^F{}_4$), 163.9 (BAr$^F{}_4$ C-B).

^{31}P{^{1}H} NMR (161.9 MHz, CD_2Cl_2, 298 K): *δ* 97.8 (br. d, $^2J_{PRh}$ = 173 Hz).

^{31}P{^{1}H} SSNMR (161.9 MHz, 10 kHz spin rate): *δ* 95.5 (s) ($\nu_{½}$ = 400 Hz).

^{19}F{^{1}H} NMR (376.5 MHz, CD_2Cl_2, 298 K): *δ* –62.9 (Ar^F-CF_3).

^{11}B{^{1}H} NMR (128.9 MHz, CD_2Cl_2, 298 K): *δ* –6.61 (BAr$^F{}_4^-$).

ESI-MS (CH_2Cl_2) m/z found (calculated) for $C_{29}H_{46}P_2Rh$ $[M]^+$: 475.2145 (475.2124).

Elemental analysis found (calculated) for $C_{54}H_{58}BF_{24}P_2Rh$: C, 48.79 (48.45); H, 4.45 (4.37).

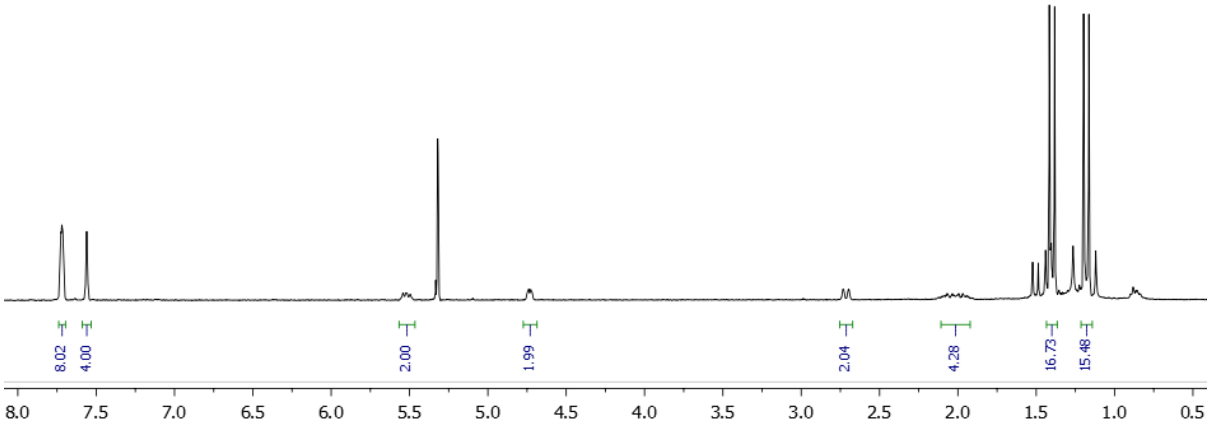

Figure S41: *^{1}H NMR spectrum of complex **13** (400.1 MHz, 298 K, CD_2Cl_2).*

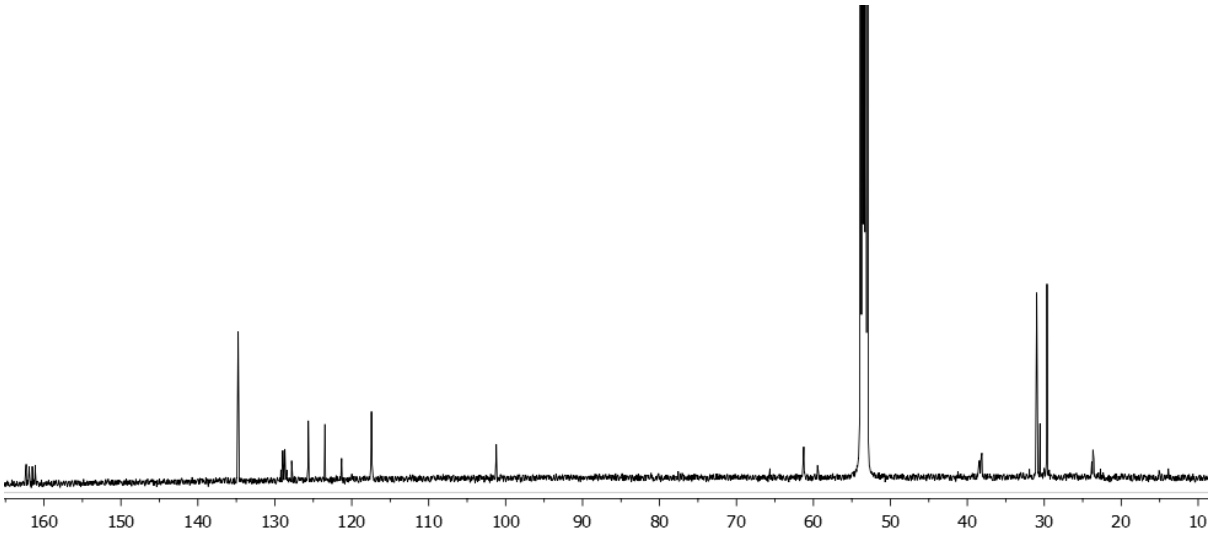

Figure S42: *$^{13}C\{^{1}H\}$ NMR spectrum of complex **13** (100.6 MHz, 298 K, CD_2Cl_2).*

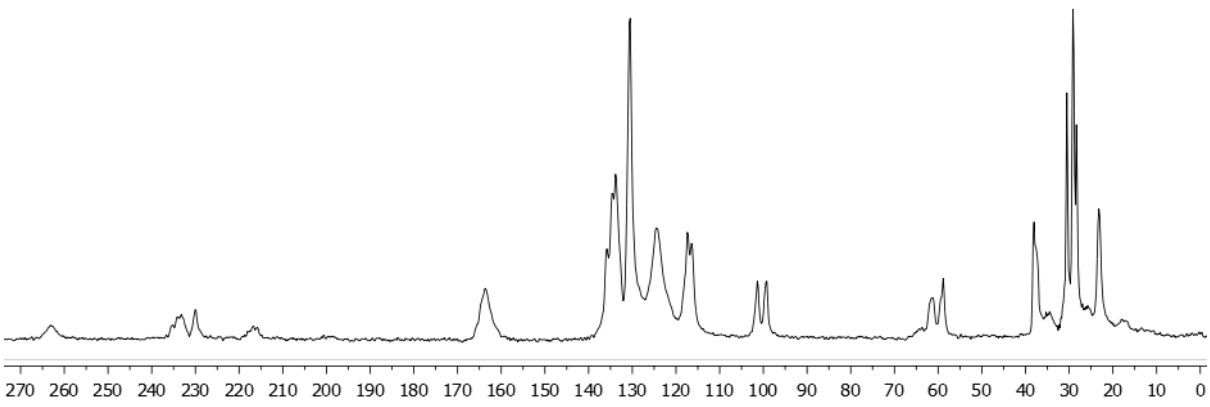

Figure S43: *$^{13}C\{^{1}H\}$ SSNMR spectrum of complex **13** (100.6 MHz, spinning speed 10 kHz, 298 K).*

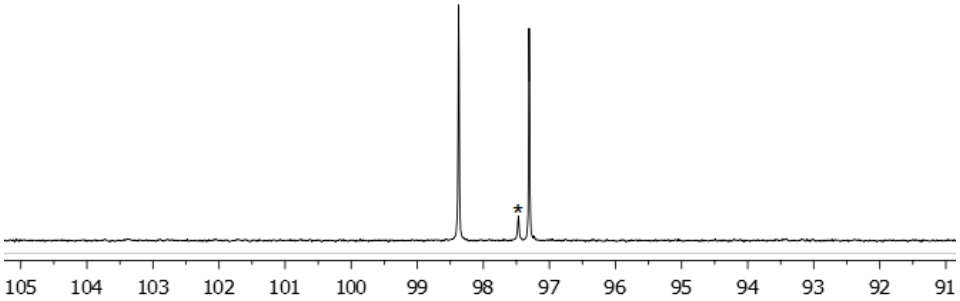

Figure S44: *$^{31}P\{^{1}H\}$ NMR spectrum of complex **13** (161.9 MHz, 298 K, CD_2Cl_2). * indicates an unknown degradation product.*

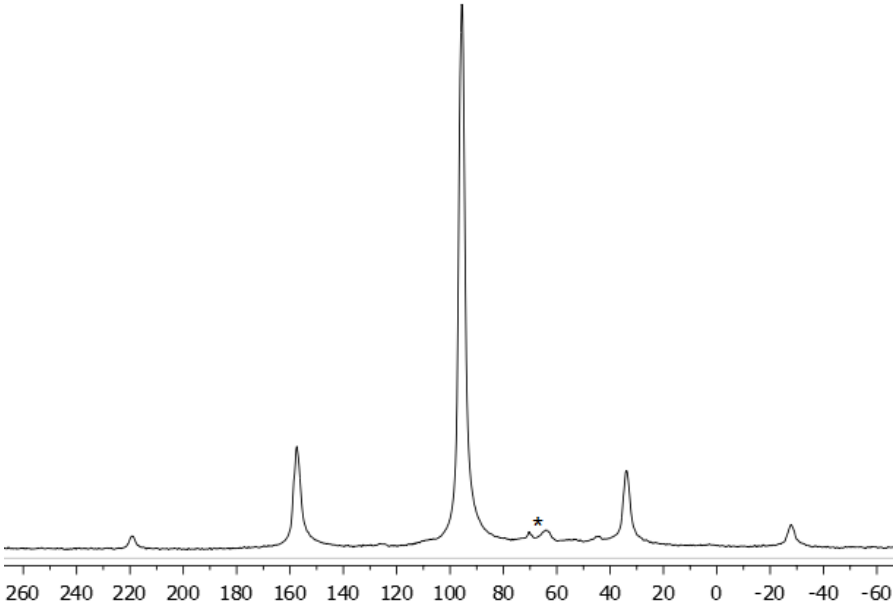

Figure S45: *$^{31}P\{^{1}H\}$ SSNMR spectrum of complex **13** (161.9 MHz, spinning speed 10 kHz, 298 K). * indicates an unknown degradation product(s).*

S3.6.1 Selected Crystallographic and Refinement Data for Complex 13

Crystal data for 13 (CCDC 1945267): $C_{54}H_{58}BF_{24}P_2Rh$, M = 1338.66 g/mol, monoclinic, *P*2/*n*, a = 17.59335(7), b = 18.77356(10), c = 35.33268(14) Å, β = 91.6093(4)°, V = 11665.42(9) Å^3, Z = 8, λ(Cu-Kα) = 1.54184 Å, T = 150(1) K, red plate, ρ(calcd, g cm^{-3}) = 1.524, μ (mm^{-1}) = 3.905, 301140 reflections collected, 24335 independent measured reflections (R_{int} = 0.0482), F^2 refinement, R_1(obs, I > 2σ(I)) = 0.0332, wR_2(all data) = 0.0874, 21819 independent observed reflections [|F_o| > 4σ(|F_o|), 2ϑ_{max} = 153.1°], 1473 restrains, 1827 parameters, GOF = 1.017 and residual electron density (e Å^{-3}) = 0.639/-0.745.

S3.6.2 Supplementary Analysis of the Solid-State Molecular Structure of Complex 13 by Single-Crystal X-ray Diffraction

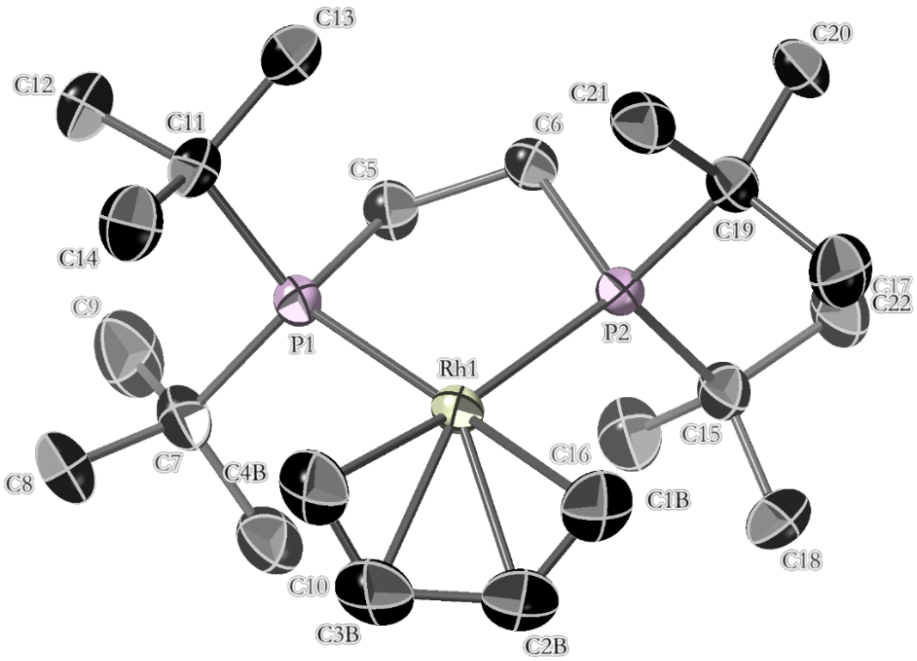

Figure S46: *Cationic fragment [(dtbpe)Rh(η⁴-C₄H₆)]⁺ of* ***13****. 50% displacement ellipsoids. H atoms omitted for clarity. There are two independent fragments [(dtbpe)Rh(η⁴-C₄H₆)]⁺, from which one disordered position of butadiene is shown (C1B-C4B); the alternative position arises from a* c. *180° rotation of the butadiene fragment relative to the [(dtbpe)Rh]⁺ fragment. Selected bond lengths (Å) and angles (deg): Rh1–P1, 2.3316(10); Rh1–P2, 2.3244(7); Rh1–C1B, 2.255(11); Rh1–C2B, 2.193(8); Rh1–C3B, 2.199(10); Rh1–C4B, 2.240(14); C1B–C2B, 1.337(17); C2B–C3B, 1.447(15); C3B–C4B, 1.349(18); P1–Rh1–P2, 87.06(3); C1B–C2B–C3B, 121.8(11); C2B–C3B–C4B, 119.4(10).*

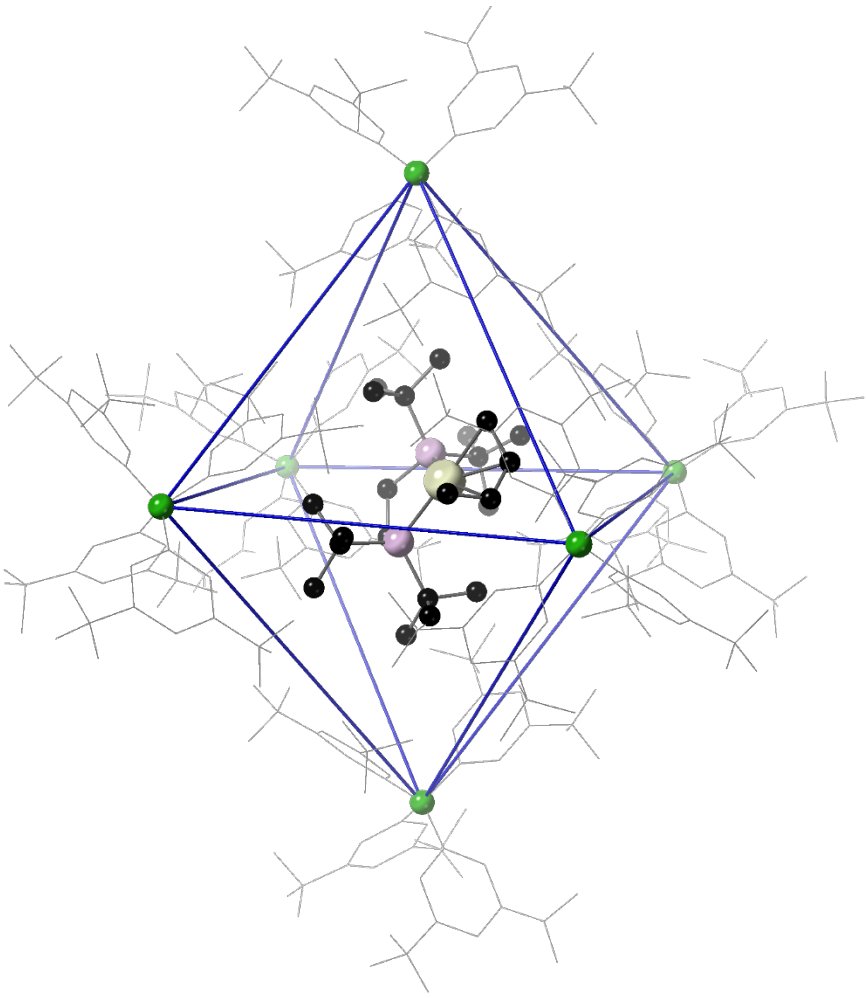

Figure S47: *The octahedral packing environment of [(dtbpe)Rh(η⁴-C₄H₆)][BAr$^F_4$], complex **13**.*

S3.7 Synthesis and Characterisation of Single-Crystalline {[(dtbpe)RhH(μ-H)]$_2$}[BAr$^F_4$]$_2$, Complex 14

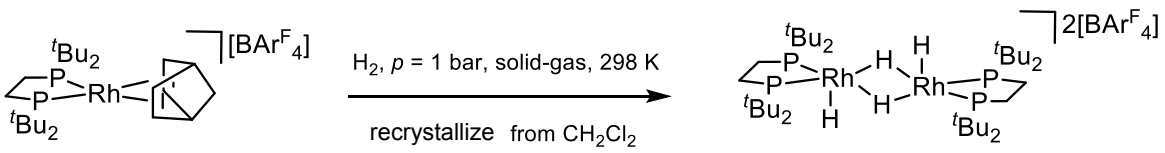

7 **14**

Crushed crystalline **7** (25 mg, 18 μmol) was introduced to a Young's flask before the flask was evacuated and re-pressurised with H_2 (1 bar), initially forming complex **8**. After 24 hours, the material had yellowed significantly: the flask was evacuated ($p < 10^{-2}$ mbar, 5 min) and H_2 (1 bar) was reintroduced; this was repeated after an additional 24 hours.

After a third 24 hour period (72 hours in total), the bright yellow resulting solid was dissolved in CH_2Cl_2 (1 mL) for crystallisation. This solution was immediately frozen with liquid N_2, before the headspace was evacuated and re-pressurised with H_2 (1 bar) to prevent dehydrogenation and formation of C-Cl activated complex **12** upon thawing. Crystallisation was carried out at 2 °C, providing bright yellow crystals of {[(dtbpe)RhH(μ-H)]$_2$}[BAr$^F{}_4$]$_2$, complex **14** (19 mg, 7 μmol, 73%), after 6 hours. The supernatant was removed *via* cannula under pressure of H_2. Once extracted, the crystals can survive indefinitely under an atmosphere of argon, and are not sensitive to vacuum (p = 10^{-3} mbar). Dissolution of crystalline complex **14** in CD_2Cl_2 and immediate NMR interrogation at 183 K produced spectra comparable to the amorphous material produced after 72 hours under H_2 without a crystallisation step. The solution-phase NMR information given below corresponds to this method. This complex was also accessible from the butadiene complex, **13**: a crushed crystalline sample of complex **12** (*c.* 25 mg, *c.* 20 μmol) was introduced to a Young's flask before the flask was evacuated and re-pressurised with H_2 (1 bar). A yellow solid was generated almost immediately; NMR studies conducted on the resulting solid at 183 K after 20 min under H_2 confirmed quantitative conversion to the dihydride **14**. This material was also prepared *in situ* for solid-state NMR studies (crystalline **14** was studied by solid-state NMR separately).

In Situ *Method I* from Butenes Complex **10**/**11**

A 4.0 mm zirconia solid-state rotor was packed with *c.* 25 mg of **7** (*c.* 20 μmol). Left unsealed, the rotor was introduced[2] to H_2 (1 bar) for 50 min to give complex **8**, before evacuation and re-pressurisation with 1-butene (1 bar) for 48 hours to give complex **10**/**11**. Evacuation and re-pressurisation with H_2 (1 bar) for a further 50 min gave complex **14**. The rotor was capped under a flow of H_2 before solid-state NMR studies were undertaken.

In Situ *Method II* Directly from Complex **8**

A 4.0 mm zirconia solid-state rotor was packed with *c.* 25 mg of **7** (*c.* 20 μmol). Left unsealed, the rotor was introduced[2] to H_2 (1 bar) for 50 min to give complex **8**, followed by evacuation and a second charge of H_2 (1 bar) for 16 hours. The rotor was capped under a flow of H_2 before solid-state NMR studies were undertaken.

Due to the tendency of this species to slowly degrade in solution coupled with its generally poor solubility, a clean solution-phase $^{13}C\{^1H\}$ spectrum could not be achieved. Such a tendency to degrade also prevented the acquisition of elemental microanalysis data.

^{1}H NMR (400.1 MHz, CD_2Cl_2, 298 K): δ 1.36 (d, 36 H, $^3J_{HP}$ = 12.8 Hz; ^{t}Bu), 2.23 (d, 4 H, $^2J_{HP}$ = 12.0 Hz; CH_2), 7.56 (s, 4 H; *p*-H), 7.72 (s, 8 H; *o*-H), *Rh-H poorly resolved.*

^{1}H NMR (400.1 MHz, CD_2Cl_2, 183 K): δ –27.6 (br. d, $^1J_{HRh} \sim$ 48 Hz, 2 H; terminal Rh-H), –4.70 (br. tt, $^1J_{HRh} \sim$ 30 Hz, $^2J_{HP} \sim$ 65 Hz, 2 H; bridging Rh-H), 1.17 (br. d, $^3J_{PH} \sim$ 9 Hz, 18H; ^{t}Bu), 1.27

(br. d, $^{3}J_{PH}$ ~ 8 Hz, 18 H; ^{t}Bu), 2.00 (br. s, 2 H; CH_2), 2.12 (br. s, 2 H; CH_2), 7.52 (s, 4 H; *p*-H), 7.70 (s, 8 H; *o*-H).

$^{1}H\{^{31}P\}$ NMR (400.1 MHz, CD_2Cl_2, 183 K): δ –27.6 (br. d, $^{1}J_{HRh}$ ~ 48 Hz, 2 H; terminal Rh-H), –4.70 (br. tt, $^{1}J_{HRh}$ ~ 30 Hz, $^{2}J_{HH}$ ~ 25 Hz, 2 H; bridging Rh-H), 1.18 (s, 18 H; ^{t}Bu), 1.27 (s, 18 H; ^{t}Bu), 2.00 (br. s, 2 H; CH_2), 2.12 (br. s, 2 H; CH_2), 7.52 (s, 4 H; *p*-H), 7.70 (s, 8 H; *o*-H).

$^{13}C\{^{1}H\}$ SSNMR (100.6 MHz, 10 kHz spin rate, 298 K): δ 22.3 (dtbpe CH_2), 29.1 (^{t}Bu CH_3), 37.6 (^{t}Bu C_Q), 117–136 (BAr^{F}_4), 161.8 (BAr^{F}_4 C-B).

$^{31}P\{^{1}H\}$ NMR (161.9 MHz, CD_2Cl_2, 298 K): δ 123.0 (dm, $^{2}J_{PRh}$ ~ 108 Hz, $^{2}J_{PP'}$ ~ 20 Hz).

$^{31}P\{^{1}H\}$ NMR (161.9 MHz, CD_2Cl_2, 183 K): δ 121.9 (dm, $^{2}J_{PRh}$ ~ 108 Hz, $^{2}J_{PP'}$ ~ 20 Hz).

$^{31}P\{^{1}H\}$ SSNMR (161.9 MHz, 10 kHz spin rate, 298 K): δ 117.7 (br. d, $^{1}J_{PRh}$ ~ 180 Hz).

$^{19}F\{^{1}H\}$ NMR (376.5 MHz, CD_2Cl_2, 298 K): δ –62.8 (Ar^{F}-CF_3).

$^{19}F\{^{1}H\}$ NMR (376.5 MHz, CD_2Cl_2, 183 K): δ –62.2 (Ar^{F}-CF_3).

$^{11}B\{^{1}H\}$ NMR (128.4 MHz, CD_2Cl_2, 298 K): δ –6.63 ($BAr^{F}_4^{-}$).

$^{11}B\{^{1}H\}$ NMR (128.4 MHz, CD_2Cl_2, 183 K): δ –6.87 ($BAr^{F}_4^{-}$).

ESI-MS (CH_2Cl_2) m/z found (calculated) for $C_{36}H_{80}P_4Rh_2$ $[M]^{2+}$: 423.1853 (423.1811).

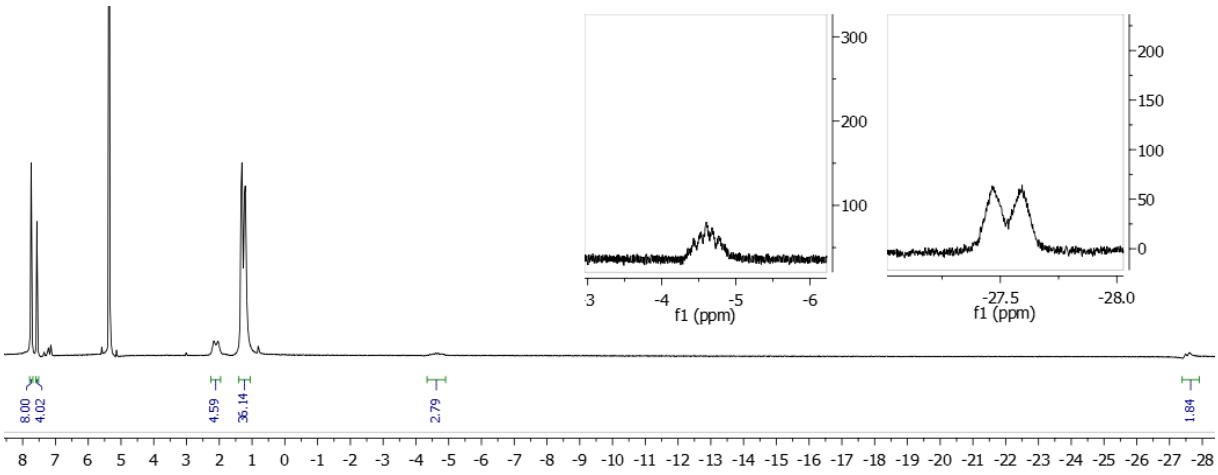

Figure S48: *^{1}H NMR spectrum of complex **14** (400.1 MHz, 183 K, CD_2Cl_2). The metal hydrides are detailed.*

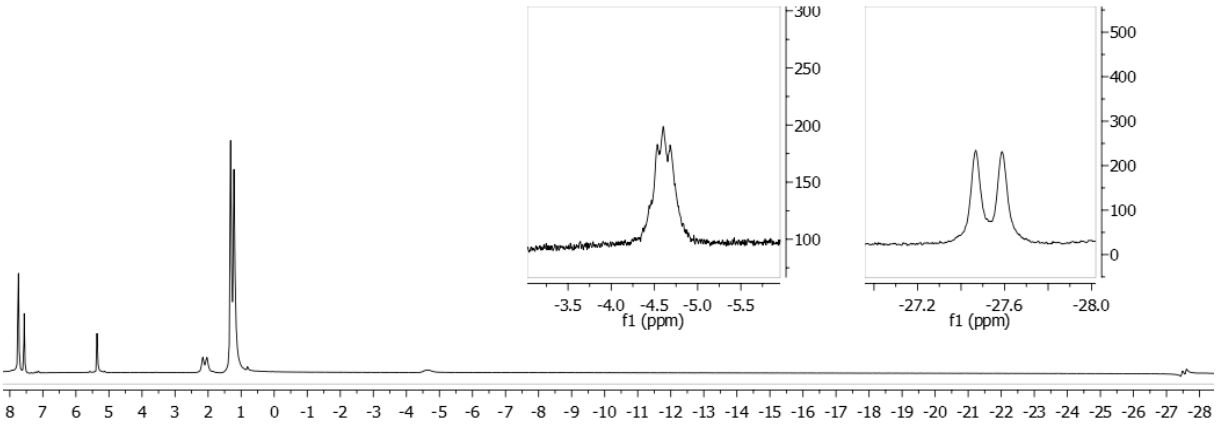

Figure S49: *$^{1}H\{^{31}P\}$ NMR spectrum of complex **14** (400.1 MHz, 183 K, CD_2Cl_2). The metal hydrides remain detailed.*

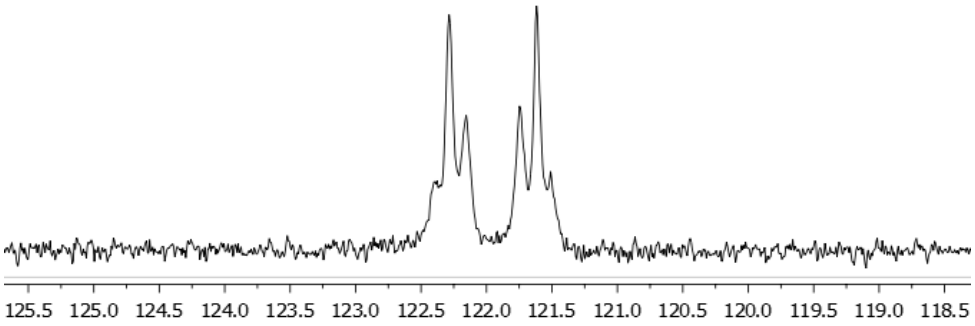

Figure S50: *$^{31}P\{^{1}H\}$ NMR spectrum of complex **14** (161.9 MHz, 183 K, CD_2Cl_2).*

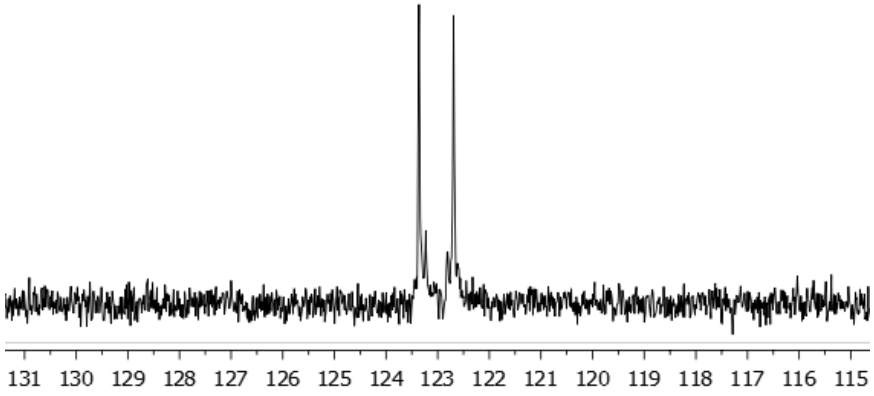

Figure S51: *$^{31}P\{^{1}H\}$ NMR spectrum of complex **14** (161.9 MHz, 298 K, CD_2Cl_2).*

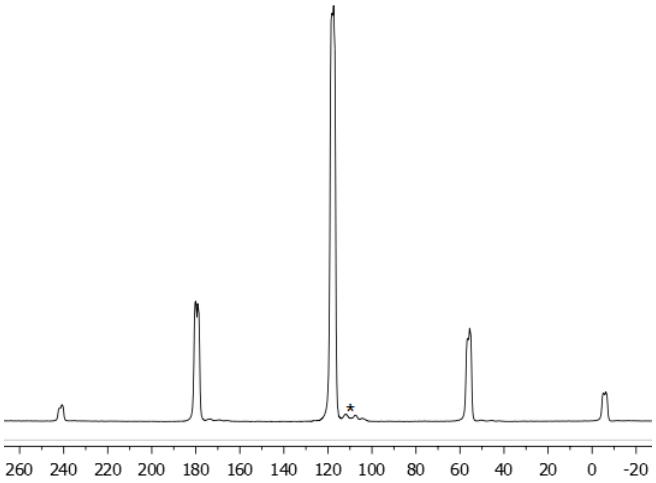

Figure S52: *$^{31}P\{^{1}H\}$ SSNMR spectrum of recrystallized complex **14** (161.9 MHz, spinning speed 10 kHz, 298 K). * indicates an unknown impurity.*

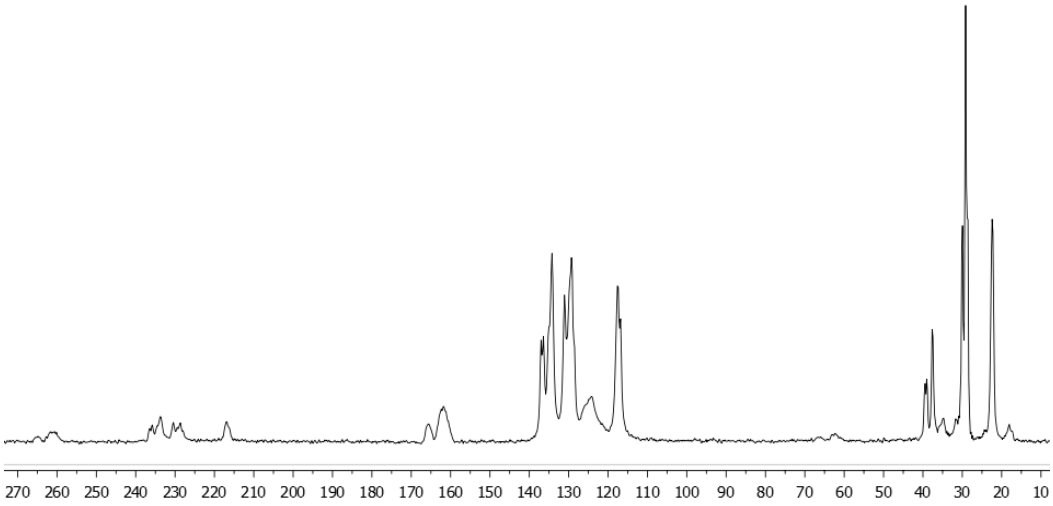

Figure S53: *$^{13}C\{^{1}H\}$ SSNMR spectrum of recrystallized complex **14** (100.6 MHz, spinning speed 10 kHz, 298 K).*

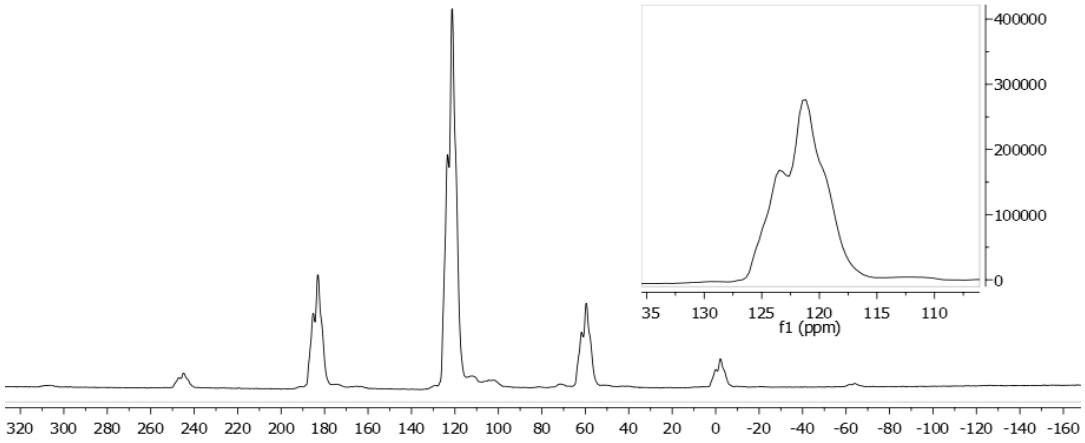

Figure S54: *$^{31}P\{^{1}H\}$ SSNMR spectrum of* in situ-*prepared complex **14** (161.9 MHz, spinning speed 10 kHz, 298 K; Method I).*

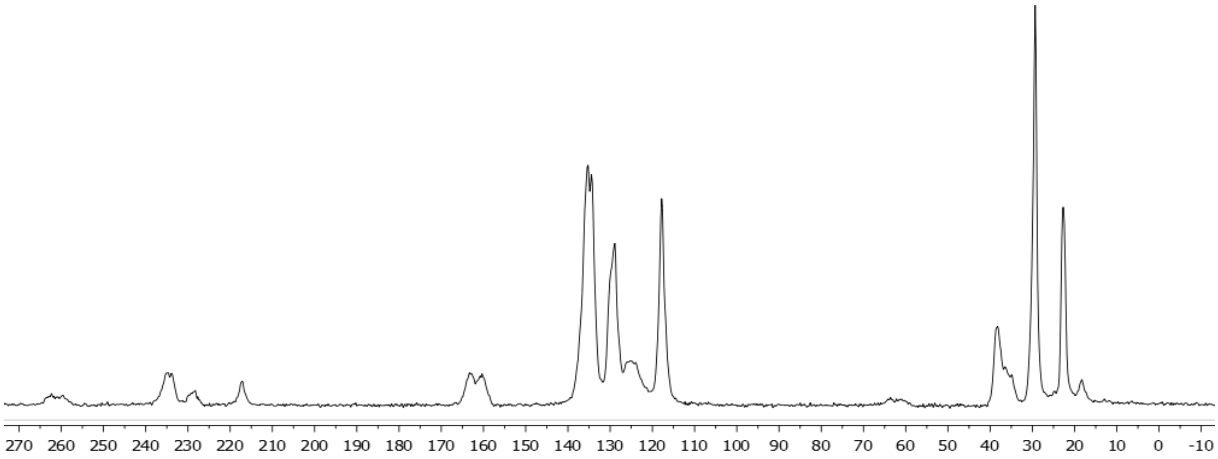

Figure S55: *$^{13}C\{^{1}H\}$ SSNMR spectrum of* in situ-*prepared complex* ***14*** *(100.6 MHz, spinning speed 10 kHz, 298 K; Method I).*

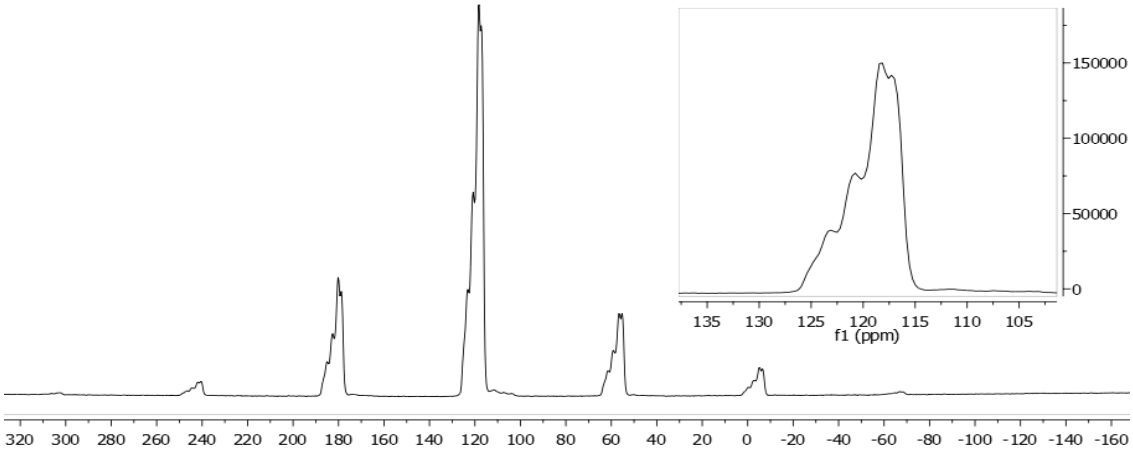

Figure S56: *$^{31}P\{^{1}H\}$ SSNMR spectrum of* in situ-*prepared complex* ***14*** *(161.9 MHz, spinning speed 10 kHz, 298 K; Method II).*

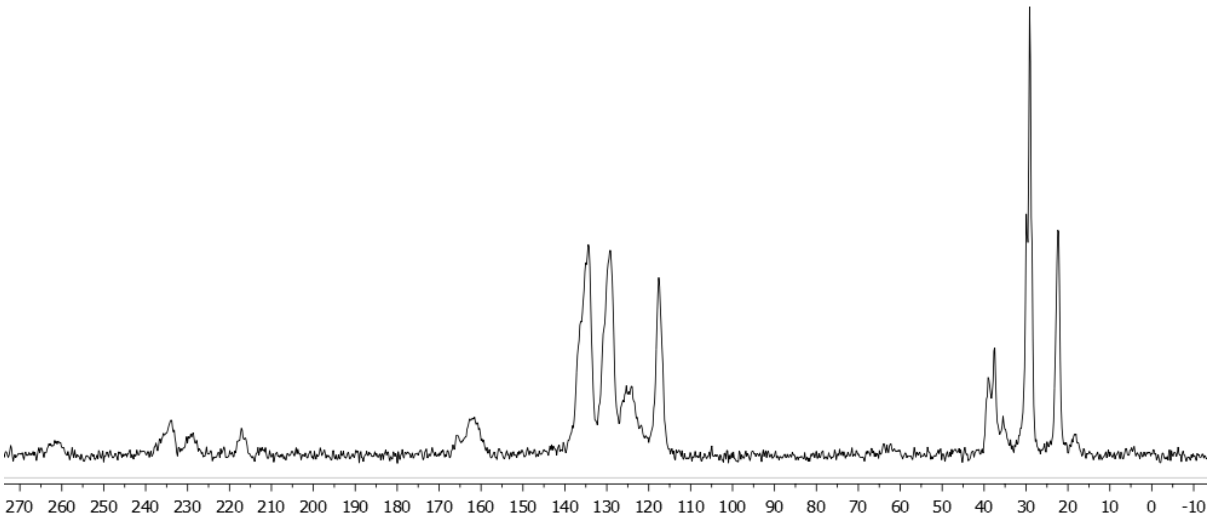

Figure S57: *$^{13}C\{^{1}H\}$ SSNMR spectrum of* in situ-*prepared complex* ***14*** *(100.6 MHz, spinning speed 10 kHz, 298 K; Method II).*

S3.7.1 Selected Crystallographic and Refinement Data for Complex 14

Crystal data for 14 (CCDC 1945341): $C_{50}H_{53.94}BF_{24}P_2Rh$, M = 1286.52 g/mol, triclinic, *P*-1, a = 13.4962(5), b = 15.0316(4), c = 15.0479(3) Å, α = 86.520(2), β = 82.231(2), γ = 64.563(3)°, V = 2731.48(15) Å^3, Z = 2, λ(Cu-Kα) = 1.54184 Å, T = 150(1) K, yellow plate, ρ(calcd, g cm^{-3}) = 1.564, μ (mm^{-1}) = 4.143, 33491 reflections collected, 11281 independent measured reflections (R_{int} = 0.0347), F^2 refinement, R_1(obs, $I > 2\sigma(I)$) = 0.0413, wR_2(all data) = 0.1094, 10152 independent observed reflections [$|F_o| > 4\sigma(|F_o|)$, $2\vartheta_{max}$ = 152.5°], 1438 restrains, 959 parameters, GOF = 1.020 and residual electron density (e Å^{-3}) = 0.739/-0.579.

checkCIF/PLATON report

Alert level B

PLAT315_ALERT_2_B Singly Bonded Carbon Detected (H-atoms Missing).

PLAT780_ALERT_1_B Coordinates do not Form a Properly Connected Set

In answer to checkCIF/PLATON alert level B: The origin of this singly bonded carbon and the set of coordinates can be obviated as it relates to a disordered minor component for the cationic Rh fragment (chemical occupancy = 3.3%). This can be removed by removing the disordered component, but this results in an elevated R-factor and high electron density spots. This model is best described as disordered.

S3.7.2 Supplementary Analysis of the Solid-State Molecular Structure of Complex 14 by Single-Crystal X-ray Diffraction

The crystals yielded above were amenable to single crystal X-ray diffraction studies. The fragment $\{[(dtbpe)RhH(\mu\text{-}H)]_2\}^{2+}$ is disordered over two main domains with chemical occupancies 0.97:0.03 (*Figure S57*) and is surrounded by 12 $BAr^F{}_4^-$ counteranions, with six nearest neighbours arranged into a distorted octahedron. The hydrides belonging to the major disordered component (97%) of the cationic fragment $\{[(dtbpe)RhH(\mu\text{-}H)]_2\}^{2+}$ were located in the difference Fourier map and refined. Only the major component is shown and discussed below.

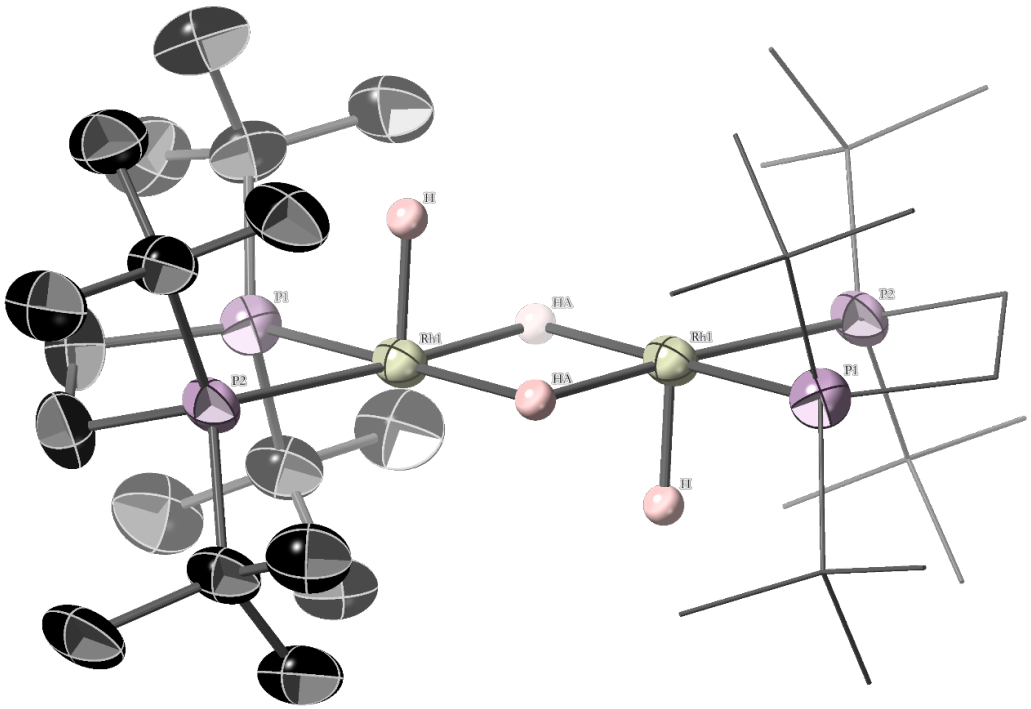

Figure S58: *Major disordered component (97%) of cationic fragment {[(dtbpe)RhH(μ-H)]$_2$}$^{2+}$ of* ***14****. 50% displacement ellipsoids. H atoms omitted for clarity excepting metal hydrides. Selected bond lengths (Å) and angles (deg): Rh1–H, 1.42(4); Rh1–HA, 1.74(5); Rh1–P2, 2.2809(7); Rh1–P1, 2.2973(8); P2–Rh1–H, 92.5(16); P1–Rh1–H, 93.8(19); P2–Rh1–HA, 96.7(14); P1–Rh1–HA, 96.3(17).*

S4 Solid-Gas Chemistry with Single-Crystalline Molecular Organometallics, In Batch

S4.1 Optimisation of Conditions: Solid-State Hydrogenation of Single-Crystalline Complex 7

A series of high-pressure NMR tubes fitted with Young's taps were each charged with fine crystalline **7** (*c.* 5 mg). The atmospheres of each tube were evacuated and replaced with H_2 for time *t* (1 bar) before evacuation and distillation of CD_3CN into the headspace. Upon melting and displacement of weakly-bound NBA with CD_3CN to give the acetonitrile complex, ^1H and $^{31}P\{^1H\}$ NMR studies were conducted at 298 K. The CD_3CN adduct is known in the form of the triflate $[(dtbpe)Rh(NCCH_3)][OTf]$.[16] Conversion surpassed 95% by *t* = 20 min.

S4.2 Solid-Gas Catalytic Isomerisation of 1-butene

S4.2.1 NMR-Scale Solid-Gas Catalytic Isomerisation of Butenes with SMOMs

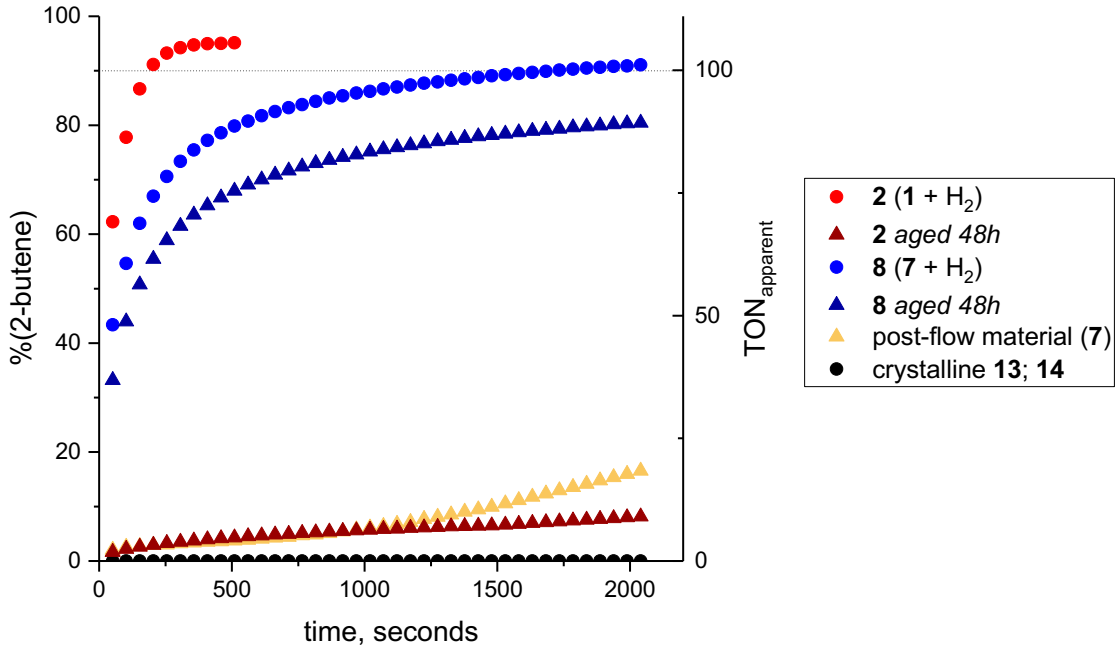

Figure S59: *Conversion of starting pure 1-butene to 2-butenes over time by crushed samples (2 mg,* c. *1.8 µmol), as well as post-flow material approximately corresponding to 2 mg of organometallic, within a high-pressure NMR tube.* p *= 1 bar,* T *= 298 K,* V_{NMR} *= 2 mL (*c. *90 µmol 1-butene). Percentages computed from gas-phase* ^1H *NMR integrals.*

A sample of finely powdered single-crystalline complex **7** (1 mg) was introduced to a series of high-pressure NMR tubes (*V* = 2 mL) fitted with Young's taps (controlled atmosphere valves). The tubes were evacuated, re-pressurised with H_2 (1 bar), and left for 45 min at room temperature.

Following this, the tube was evacuated and re-pressurised with a pure butene isomer atmosphere (*p* = 1 bar; 1-butene, *cis*-2-butene, *trans*-2-butene) for the specified time, after which the atmosphere was withdrawn into the GC dilution glassware as previously detailed (*see Section 1*) before gas chromatography on each sample was undertaken.

A near-thermodynamic distribution of isomers was obtained regardless of the starting straight-chain isomer of butene (*Figure S60*). Halting the reaction after 2 min, however, results in incomplete conversion of 1-butene (<50%) and a reversed cis-trans ratio. The reversed cis-trans ratio is similarly seen under flow conditions (see below).

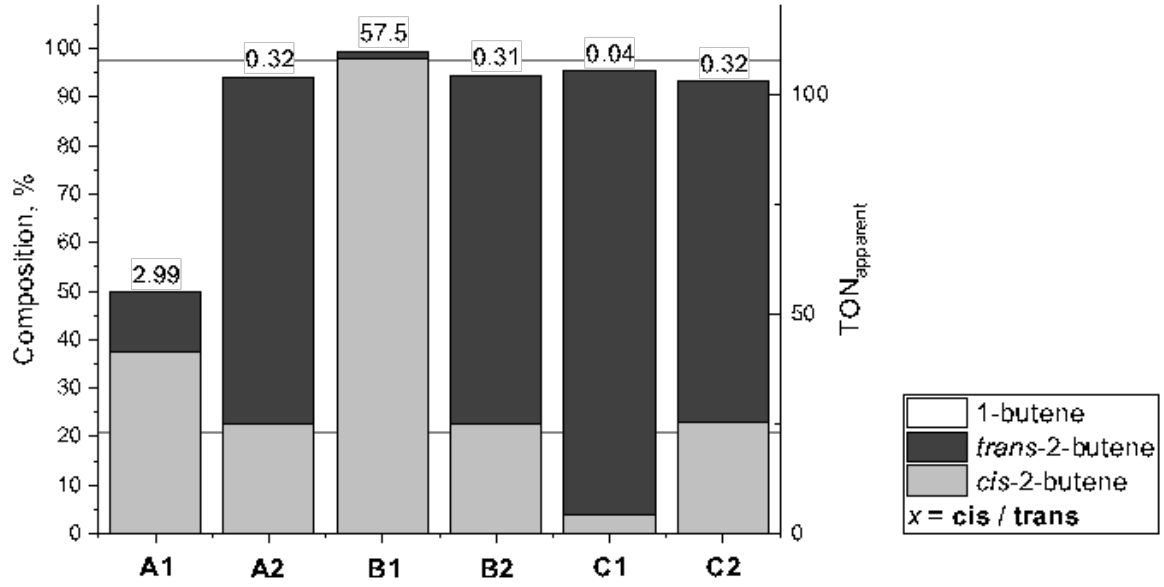

Figure S60: *Conversion of the starting pure butene isomer to a mixture of straight-chain butene isomers over time (**A**, 1-butene; **B**,* cis*-2-butene; **C**,* trans*-2-butene; **1**,* t *= 2 minutes; **2**,* t *= 24 hours) by a crushed and hydrogenated single crystalline sample of **7** (1 mg,* c. *0.9 µmol) within a high pressure NMR tube, with proportions of, 1-,* cis*-2- and* trans*-2-butene detailed as calculated from GC analysis. The expected thermodynamic proportions[17] of each isomer are also shown as reference lines (20.9%* cis*-2-butene, 76.8%* trans*-2-butene (∑ = 97.7%), 2.3% 1-butene).* p *= 1 bar,* T *= 298 K,* V_{NMR} *= 2 mL (*c. *90 µmol 1-butene).*

S4.2.2 Large-Scale Batch Solid-Gas Catalytic Isomerisation of 1-butene with Complex 7

A single crystal of **7** (*c.* 1 mg) was placed inside a *c.* 75 mL reactor vessel fitted with two Young's taps, the second of these in turn connected to a junction where an NMR tube adapter and a third Young's tap were fitted (*Figure S61*). The vessel was evacuated and placed under a pressure of H_2 (1 bar) for 45 min, after which this atmosphere was evacuated and replaced with 1-butene (*p* = 1.4 bar). Every 24 hours, an aliquot of gas was removed into a high-pressure NMR tube fitted with a Young's tap, to be analysed by gas-phase ^{1}H NMR and gas chromatography. After this, the atmosphere of butene was removed and recharged.

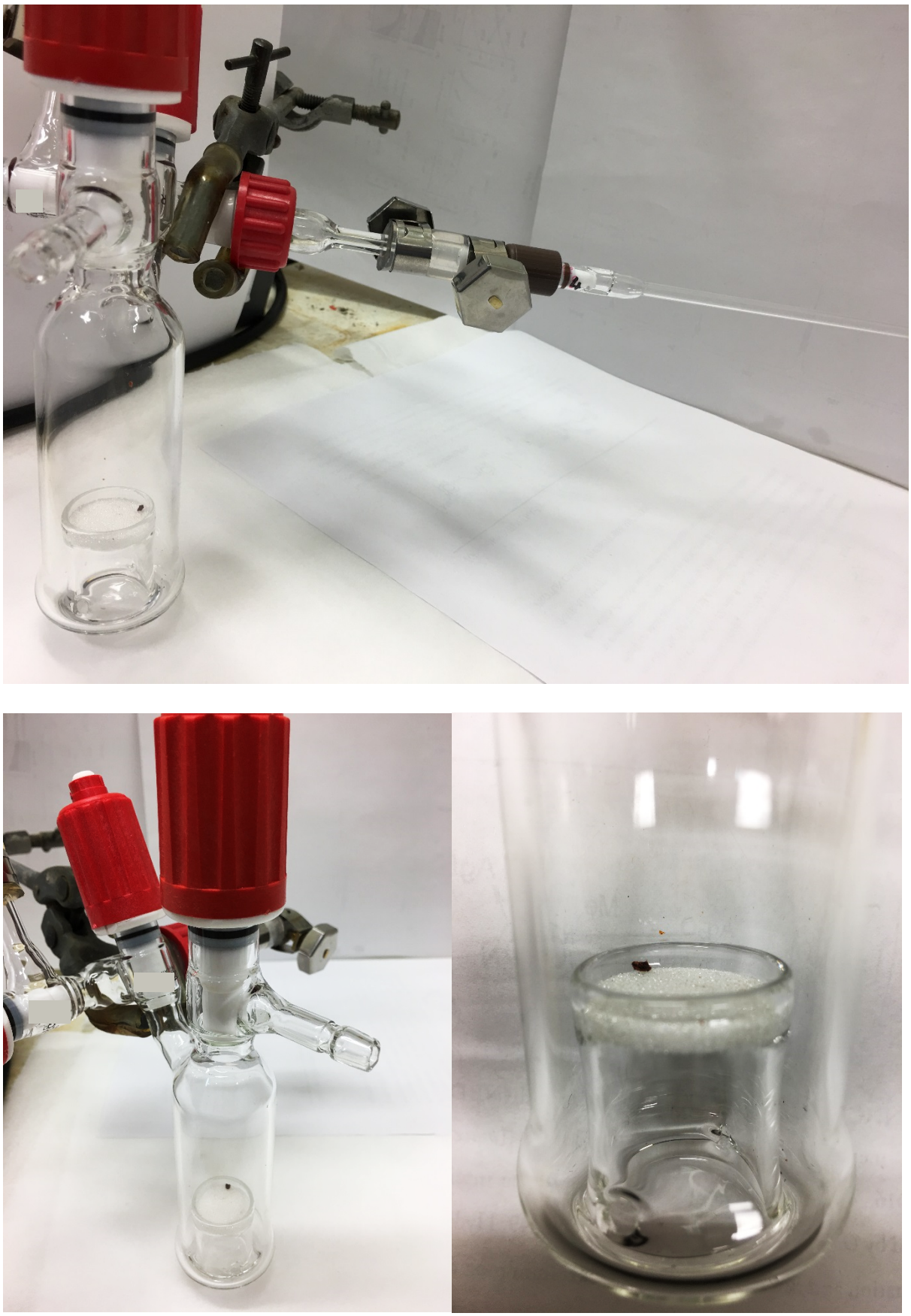

Figure S61: *Custom reactor vessel, with high-pressure NMR tube fitted (top), and mounted single-crystal detailed (bottom right).*

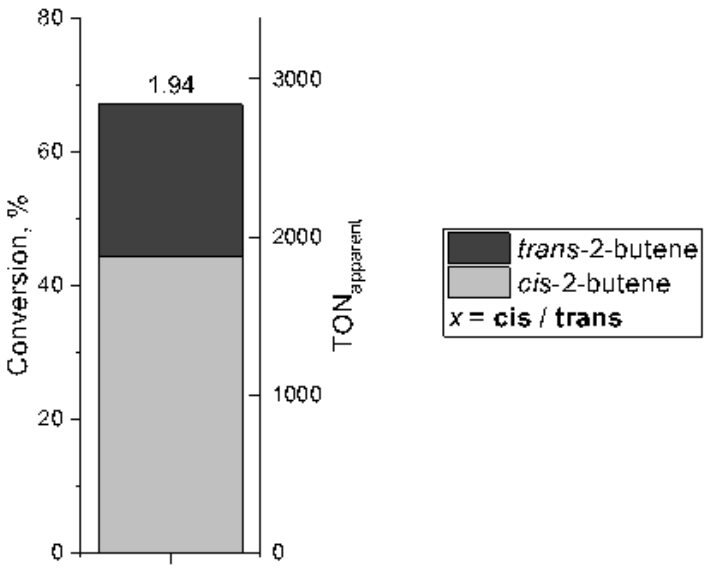

Figure S62: *Conversion of 1-butene to 2-butene after 24 hours by a hydrogenated single crystal of complex **7** (1 mg,* c. *0.9 µmol) within a bespoke reactor vessel, with proportions of* cis- *and* trans-*2-butene detailed as calculated from GC analysis.* p *= 1.4 bar,* T *= 298 K,* $V_{reactor}$ *~ 75 mL (*c. *4,250 µmol 1-butene).*

Under these conditions, a clear bias towards *cis*-2-butene is demonstrated, indicating that on this scale 24 hours is not sufficient time to achieve thermodynamic equilibrium. The first charge is presented in *Figure S62*.

S4.3 *In Situ* Solid-State NMR Studies *versus* X-ray Diffraction Studies 7; 8; 10/11

Complexes **8** and **10**/**11** (from complex **8**) were prepared *in situ* inside a 100 µl solid-state NMR rotor and interrogated by solid-state $^{31}P\{^{1}H\}$ and $^{13}C\{^{1}H\}$ NMR spectroscopy at each stage. The results were compared with **7** and its respective low-angle and high-angle Bragg reflections, as achieved from the appropriate single crystal X-ray diffraction experiments (*Figure S63*).

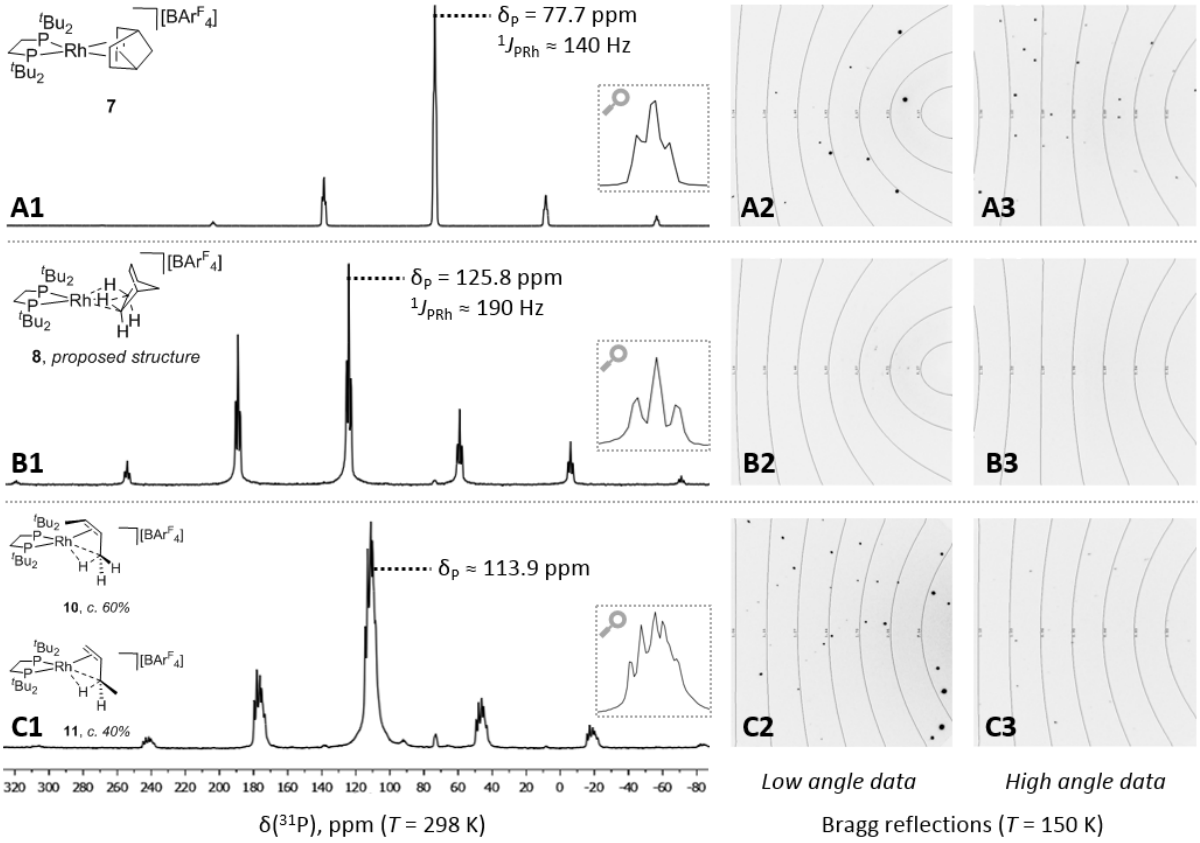

Figure S63: *$^{31}P\{^{1}H\}$ SSNMR spectra (ν = 10 kHz) of complexes **7** (**A1**), **8** (**B1**), and **10/11** (**C1**) compared with frames showing the Bragg reflections of complexes **7** (**A2-3**), **8** (**B2-3**), and **10/11** (**C2-3**).*

It is apparent that while diffraction is lost and subsequently regained *via* hydrogenation and subsequent exposure to 1-butene, short-range order is maintained throughout the process, as determined by $^{31}P\{^{1}H\}$ solid-state NMR spectroscopy.

S5 Solid-Gas Chemistry with Single-Crystalline Molecular Organometallics, In Flow

S5.1 Solution-Phase NMR Characterisation of Post-Flow Material, Complex 1

After catalysis in flow, columns into which complex **1** (15 mg) had been packed were unpacked of their contents inside a glovebox. It was noted that the material had significantly reddened over the course of the experiment. Post-flow samples of glass wool mixed with organometallic were loaded into NMR tubes fitted with Young's taps. CD_2Cl_2 was distilled into the headspace of these tubes, and the tubes were shaken so as to dissolve the organometallic.

$^{31}P\{^1H\}$ NMR analysis was then undertaken at 298 K, revealing a doublet at δ_P = 81.9 ppm ($^2J_{PRh}$ = 169 Hz), indicative of the butadiene complex **5**. This is consistent with experiments in batch.[23]

S5.2 Solution-Phase NMR, Solid-State NMR, Mass Spectrometric, Powder X-ray Diffraction, and SEM Characterisation of Post-Flow Material, Complex 7

As above, columns into which complex **7** (15 mg) had been packed, reporting a <2% conversion at the end of an experiment after *c.* 100 hours on stream at 6.4 mL min^{-1} 1-butene (2% in N_2) and 1.2 mL min^{-1} isobutene (2% in N_2), were unpacked of their contents inside a glovebox. Material which had only been run for one hour at the same flow rates was also unpacked. Both sets of material had been pressurised under H_2 (1 bar) for 10 min.

S5.2.1 Mass Spectrometry

Samples of glass wool mixed with organometallic were soaked in CH_2Cl_2 (neat) and CH_2Cl_2 (*c.* 1% CH_3CN) from which mass spectra were obtained. In this case, the inactive compounds produced in flow appeared to decompose immediately in neat CH_2Cl_2 solution, producing a similar decomposition pattern to the butenes complexes **10**/**11** at 298 K.

S5.2.2 Solution-Phase $^{31}P\{^1H\}$ NMR Spectroscopy

Material which had been on-stream for one hour and *c.* 100 hours was loaded into NMR tubes fitted with Young's taps. CD_2Cl_2 was distilled into the headspace of these tubes such that $^{31}P\{^1H\}$ NMR studies could be undertaken at 183 K (*Figure S64*).

For the post-flow (*c.* 100 hours on stream) material, a range of Rh-bound products were observed between δ_P = 40–120 ppm.

The $^{31}P\{^1H\}$ resonance visible at $\delta_P \sim$ 115 ppm suggested the butene (**10**/**11**)/isobutene complexes; $\delta_P \sim$ 86 ppm suggested a minority of NBD complex **7**. Otherwise, the resonances observed did not correspond to any complex hitherto synthesised. These resonances converged to C-Cl activation product **12** after 72 hours in solution at 298 K.

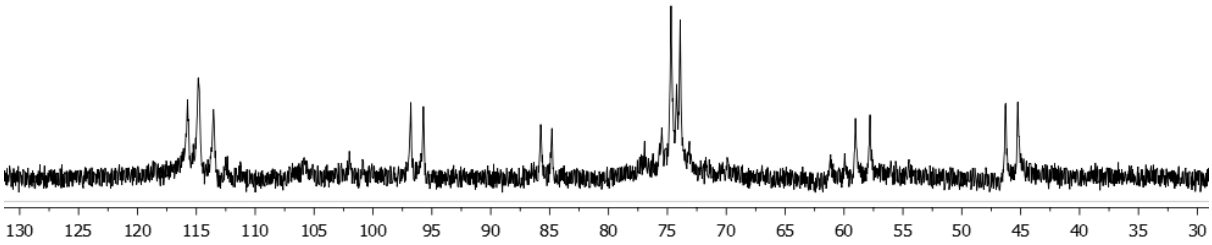

Figure S64: *An exemplar $^{31}P\{^{1}H\}$ NMR spectrum of post-flow (*c. *100 hours on-stream) material (162 MHz, 183 K, CD_2Cl_2).*

Quenching post-flow (*c.* 100 hours on-stream) material with 1,2-difluorobenzene, followed by resting at 298 K for 4 hours before $^{31}P\{^{1}H\}$ NMR spectroscopy was undertaken, revealed conversion to 1,2-difluorobenzene complex **9** (*Figure S65*).

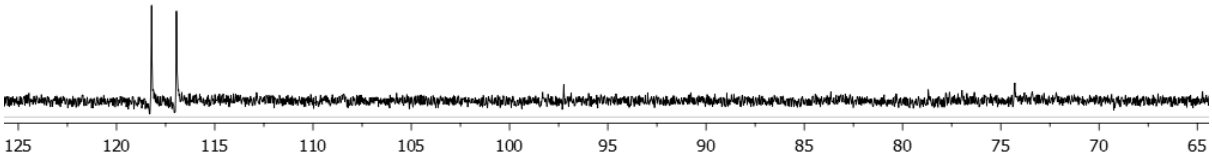

Figure S65: *An exemplar $^{31}P\{^{1}H\}$ NMR spectrum of post-flow (*c. *100 hours on-stream) material (162 MHz, 298 K, 1,2-difluorobenzene).*

Material which had only been on-stream for one hour, when dissolved in CD_2Cl_2 at 183 K, gave a range of products not including the butene (**10**/**11**)/isobutene complexes, also ultimately converging to the C-Cl activation product **12** after 72 hours in solution at 298 K.

S5.2.3 Solid-State $^{31}P\{^{1}H\}$ NMR Spectroscopy

Material which had only been on-stream for one hour, when interrogated by $^{31}P\{^{1}H\}$ solid-state NMR at 298 K, confirmed the presence of a majority of NBA complex **8**, accompanied by incipient butenes (**10**/**11**)/isobutene complexes and a minority of unreacted **7** (*Figure S66*).

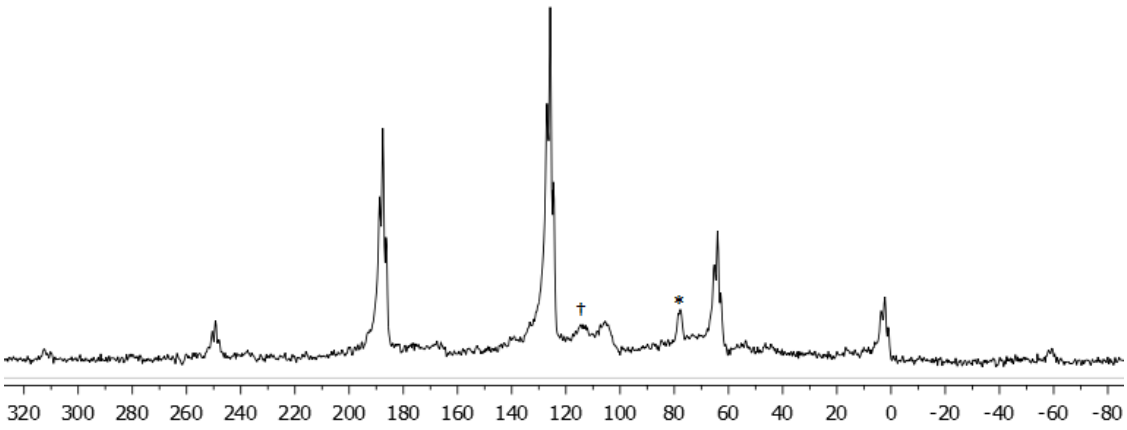

Figure S66: *$^{31}P\{^{1}H\}$ SSNMR spectrum of material on-stream for one hour (161.9 MHz, spinning speed 10 kHz, 298 K).* indicates unreacted **7**, † **10/11**.*

Post-flow (*c.* 100 hours on-stream) material, when interrogated *via* $^{31}P\{^{1}H\}$ solid-state NMR, revealed a mixture of products with three major components, at $\delta_P \sim 113$, 78 and 71 ppm (*Figure S67*). The first likely corresponds to butenes complexes **10**/**11**, and the third to a complex hitherto unknown. $\delta_P \sim 78$ ppm, a relatively sharp peak, suggests NBD complex **7**. Compared to the minor presence of this resonance in the $^{31}P\{^{1}H\}$ SSNMR for material on-stream for one hour (*Figure S66*), this suggests the loss of short-range order in the bulk of the sample.

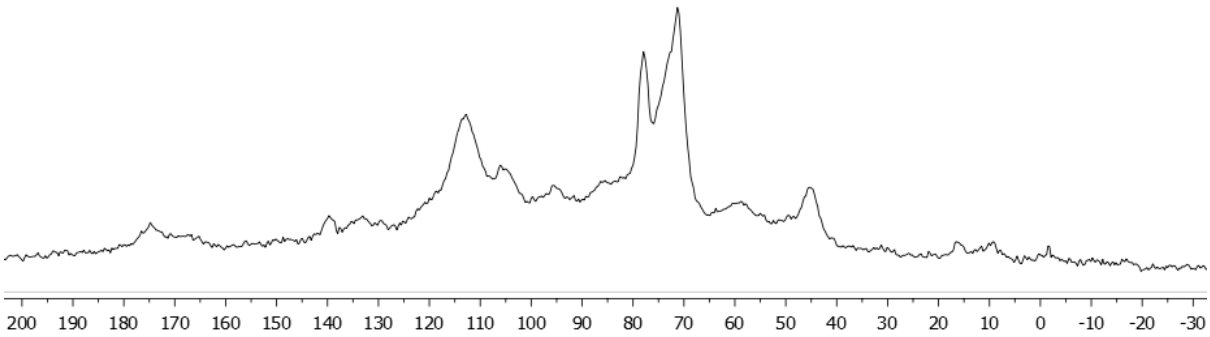

Figure S67: *$^{31}P\{^{1}H\}$ SSNMR spectrum of post-flow material on-stream for* c. *100 hours (161.9 MHz, spinning speed 10 kHz, 298 K).*

S5.2.4 Powder X-ray Diffraction

Due to the dilute nature of the organometallic/glass wool combination used in flow, flow conditions were simulated *ex situ* on neat samples, or conducted on crushed crystalline **7** in flow with glass wool plugs only present to enclose the sample (i.e. to avoid diluting the sample with glass wool). *Ex situ* samples were prepared as follows: crushed crystalline **7** (*c.* 25 mg) was introduced to a Young's flask (volume *c.* 60–100 mL) before evacuation, hydrogenation (1 bar, 45 min), evacuation, and re-pressurisation with 1-butene (1 bar). The simulated ageing process took place over the course of four days with the 1-butene atmosphere recharged twice every 24 hours for a total of at least eight recharges. On the fourth day, the atmosphere was evacuated and replaced with argon. The resulting material was then interrogated by powder x-ray diffraction, alongside a sample of unreacted crushed **7** of equal mass. Post-flow samples were prepared as follows: in a glovebox, a column was packed with a glass wool plug before crushed crystalline **7** (*c.* 30 mg) was introduced *without* glass wool segmentation as normal, followed by another glass wool plug. This column was then ran as above until activity registered <2% conversion, before unpacking inside a glovebox. The material received from the unpacked column, having removed any uncoated glass wool, was then interrogated by powder x-ray diffraction. The results are presented on the following page (*Figure S68*). While some peaks are retained, some broadening/loss of information is apparent from **7** (measured, **B**) to the material aged *ex situ* (**C**) as produced above, suggesting a reduction in crystallinity. This phenomenon is observed more severely for the material achieved post-flow (**D**), with almost total loss of information after 100 hours on-stream.

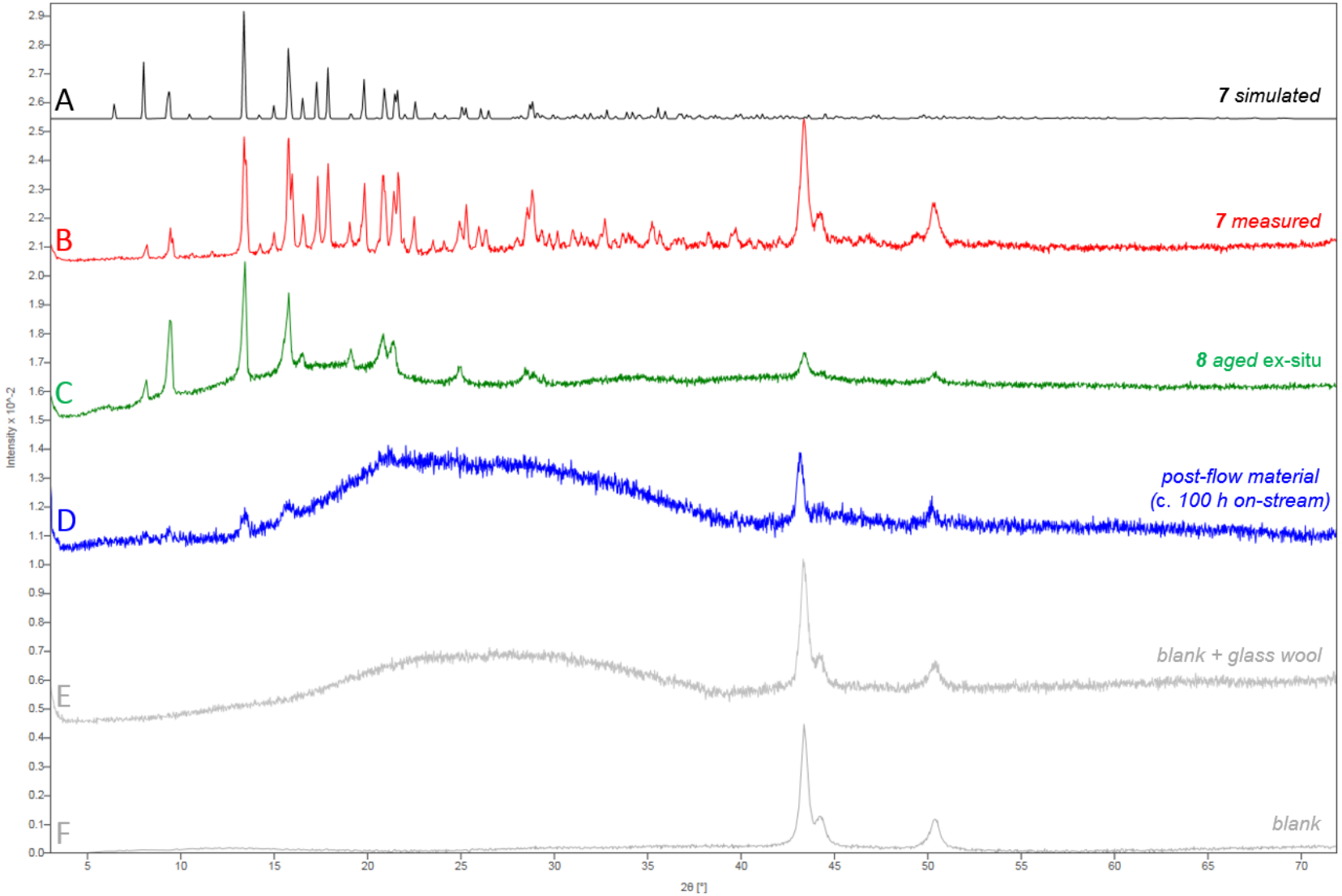

Figure S68: *Powder x-ray diffraction patterns of complex **7** (simulated, **A**; measured **B**), complex **8** aged* ex situ *as detailed in the text (**C**), unpacked post-flow material* (c. *100 hours on-stream, **D**), and a blank sample holder (with glass wool, **E**, and without, **F**).*

S5.2.5 Scanning Electron Microscopy

Post-flow (*c.* 100 hours on stream) and one-hour material, alongside material intended for flow that had *not* been exposed to H_2 or 1-butene, were all analysed *via* SEM (*Figure S69, Figure S70).* Organometallic material was unambiguously differentiated from glass wool using EDX. The materials were visibly different under SEM.

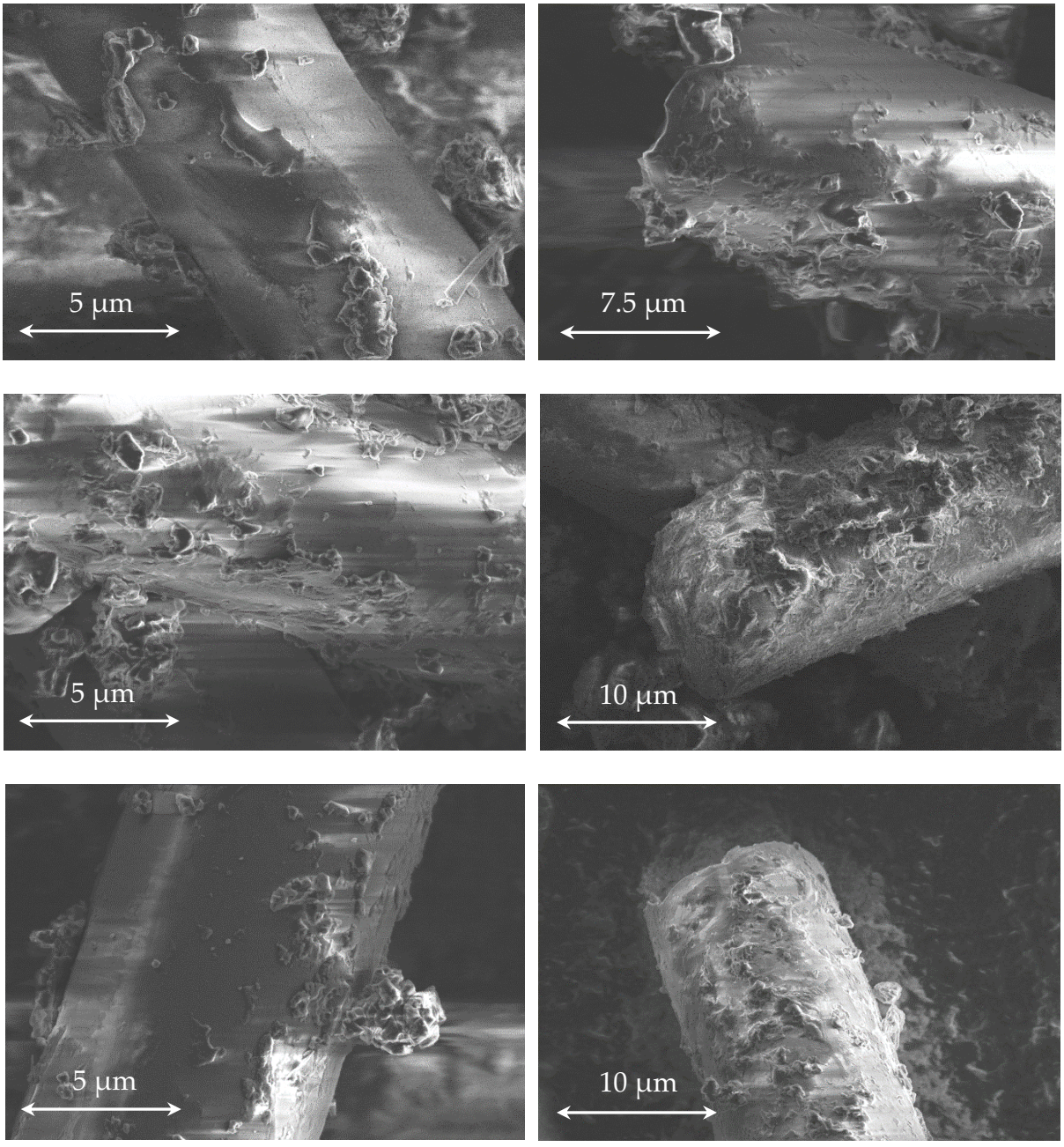

Figure S69: *Scanning electron microscopy on post-flow (*c. *100 hours on-stream) material.*

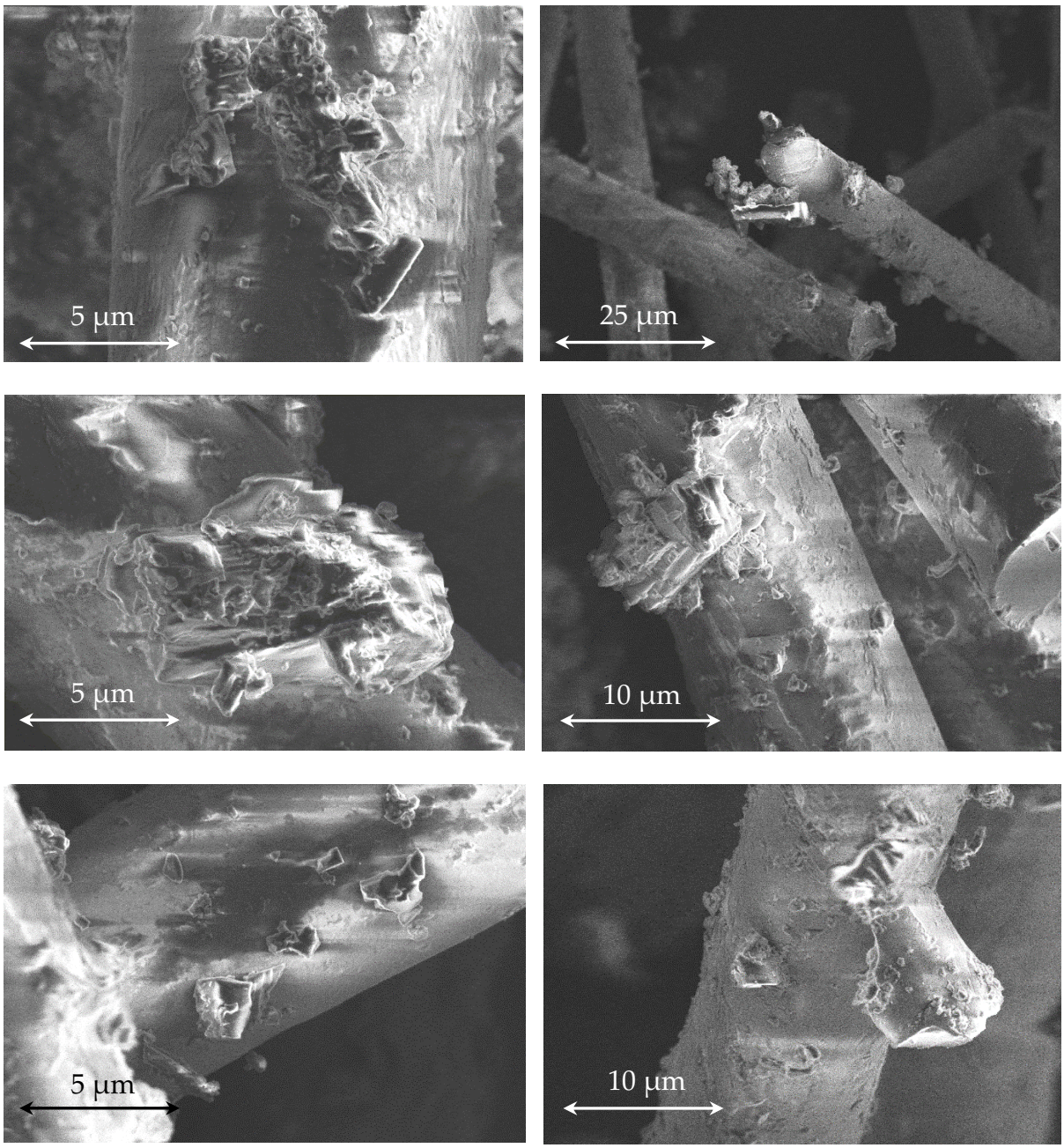

Figure S70: *Scanning electron microscopy on one hour on-stream material.*

Post-flow organometallic (*Figure S69*) appeared poorly-defined. Most crystallites possessed smoothened edges, of which there were few examples >5 μm across. Moreover, organometallic appeared to have spread out and coated much of the glass surface.

One hour on-stream organometallic (*Figure S70*) and unexposed organometallic (*Figure S71*) were mostly in the form of well-defined, distinct crystallites, many of them large (*ℴ* 5–25 μm across). Furthermore, unexposed organometallic contained numerous examples of very large (>25 μm) crystallites. On-stream crystallites appeared occluded or damaged compared to similar-sized examples among unexposed crystallites. This is congruent with observations of crystal fracturing upon hydrogenation (*see Section S2*).

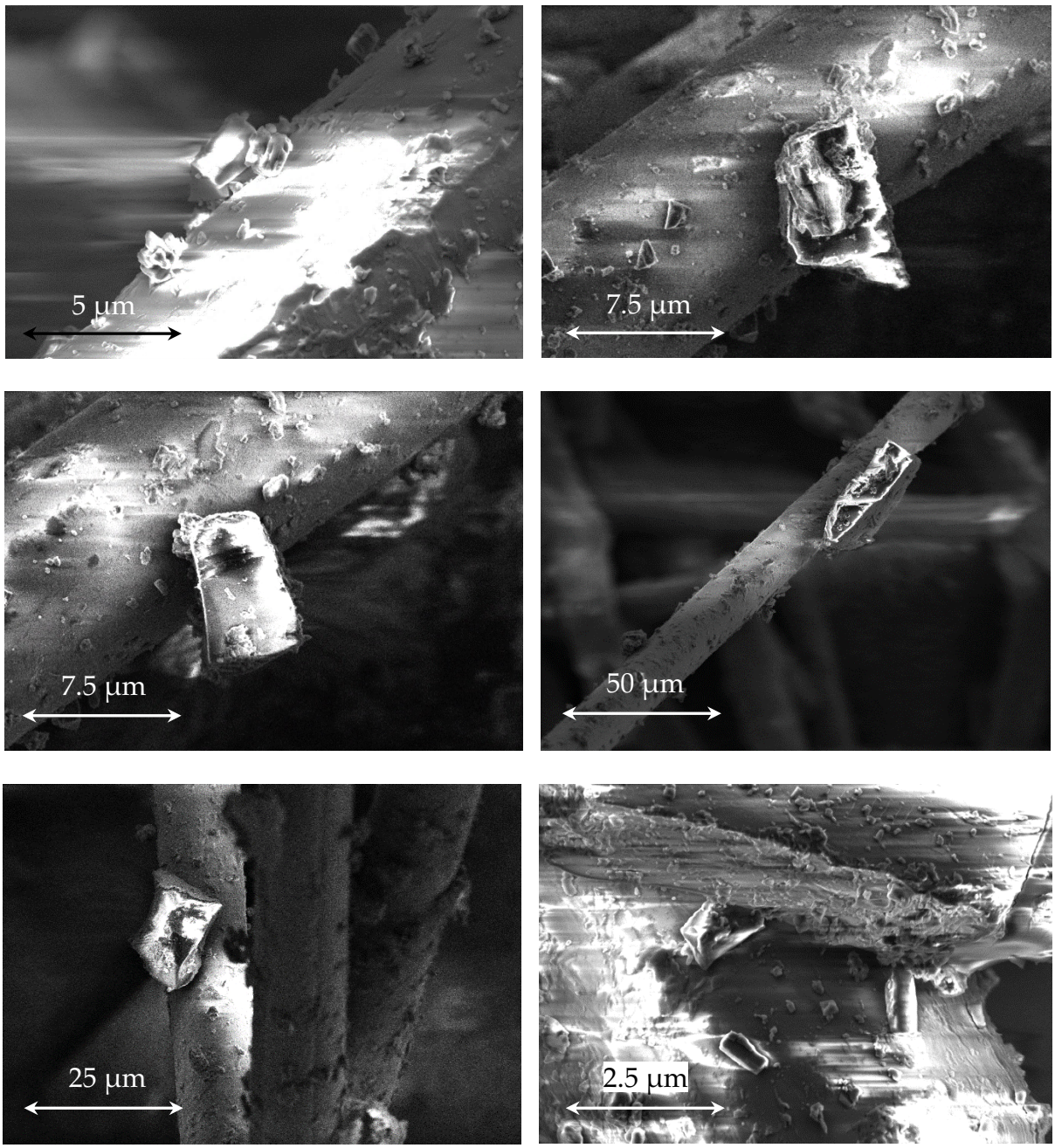

Figure S71: *Scanning electron microscopy on material that had not been exposed to either H_2 or 1-butene.*

S5.3 Continuous Flow Data: 1-Butene Isomerisation Catalysis by Complex 7 (90+ Hours on Stream)

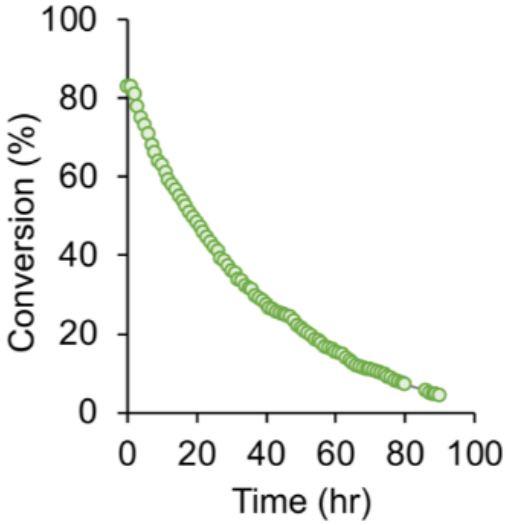

Figure S72: *On stream catalytic performance of 1-butene isomerisation catalysis in solid/gas flow, 298 K, 1 atm, complex **7** (15 mg, pre-activated with H_2 for 10 minutes* – see Section S1*). Data plotted are total 2-butenes (GC conversion). 1-butene (2% in N_2, 6.4 mL min^{-1})/isobutene co-feed (2% in N_2, 1.2 mL min^{-1}, 15% relative to 1–butene).*

S5.4 Reproducilibilty Studies Under Continuous Flow Conditions, Complex 1

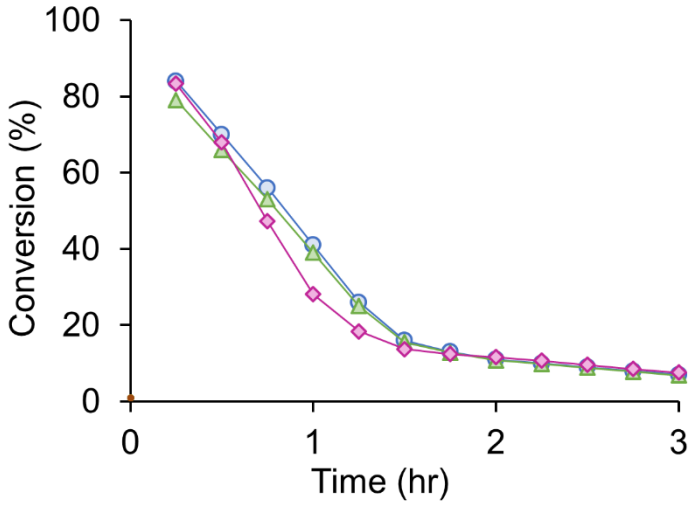

Figure S73: *On stream catalytic performance of 1-butene isomerisation catalysis in solid/gas flow, 298 K, 1 atm: three separate experimental catalytic runs of 1-butene isomerisation under continuous flow conditions from three different batches of pre-catalyst complex **1** (6 mg, pre-activated with H_2 for 10 minutes* – see Section S1*) by three different operators. Data plotted are total 2-butenes (GC conversion). 1-butene (2% in N_2, 6.4 mL min^{-1})/isobutene co-feed (2% in N_2, 1.2 mL min^{-1}, 15% relative to 1–butene).*

The reproducilibity of the column pack methodology and the experiemntal procedure is highlighted in *Figure S73* above. Three separate catalytic runs was conducted by three separate users using three different batches of the pre-catalyst (complex **1**).

S5.5 Particle Size Studies Under Continuous Flow Conditions, Complex 1

The effects of the particle size of the pre-catalyst (complex **1**) is demonstrated in *Figure S74* below. The particle sizes were separated using Endecott sieves.

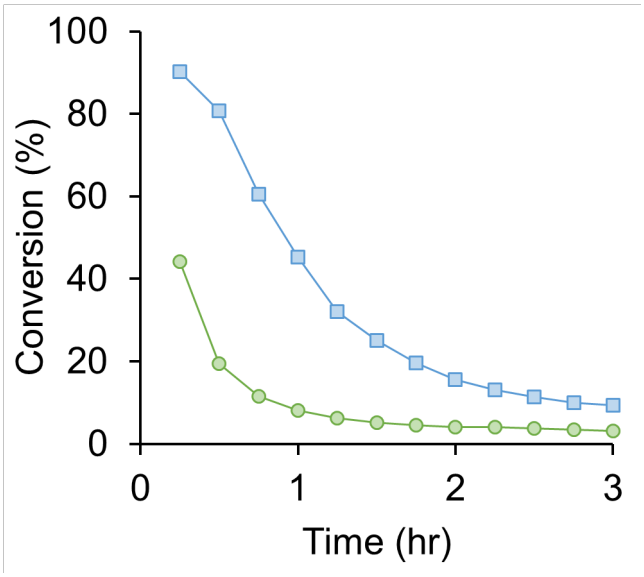

Figure S74: *On stream catalytic performance of 1-butene isomerisation catalysis in solid/gas flow, 298 K, 1 atm, complex **1** (6 mg, pre-activated with H_2 for 10 minutes* – see Section S1*). Data plotted are total 2-butenes (GC conversion). 1-butene (2% in N_2, 6.4 mL min^{-1})/isobutene co-feed (2% in N_2, 1.2 mL min^{-1}, 15% relative to 1–butene). Particle sizes <150 µm across (blue squares); ≥150 µm across (green circles).*

S6 References

(1) Pike, S. D.; Chadwick, F. M.; Rees, N. H.; Scott, M. P.; Weller, A. S.; Krämer, T.; Macgregor, S. A. Solid-State Synthesis and Characterization of σ-Alkane Complexes, $[Rh(L_2)(\eta^2,\eta^2\text{-}C_7H_{12})][BArF_4]$ (L_2 = Bidentate Chelating Phosphine). *J. Am. Chem. Soc.* **2015**, *137* (2), 820–833. https://doi.org/10.1021/ja510437p.

(2) Chadwick, F. M.; McKay, A. I.; Martinez-Martinez, A. J.; Rees, N. H.; Krämer, T.; Macgregor, S. A.; Weller, A. S. Solid-State Molecular Organometallic Chemistry. Single-Crystal to Single-Crystal Reactivity and Catalysis with Light Hydrocarbon Substrates. *Chem. Sci.* **2017**, *8* (9), 6014–6029.

(3) Martínez-Martínez, A. J.; Tegner, B. E.; McKay, A. I.; Bukvic, A. J.; Rees, N. H.; Tizzard, G. J.; Coles, S. J.; Warren, M. R.; Macgregor, S. A.; Weller, A. S. Modulation of σ-Alkane Interactions in $[Rh(L_2)(Alkane)]^+$ Solid-State Molecular Organometallic (SMOM) Systems by Variation of the Chelating Phosphine and Alkane: Access to η^2,η^2-σ-Alkane Rh(I), η^1-σ-Alkane Rh(III) Complexes, and Alkane Encapsulation. *J. Am. Chem. Soc.* **2018**, *140* (44), 14958–14970.

(4) Giordano, G.; Crabtree, R. H.; Heintz, R. M.; Forster, D.; Morris, D. E. Di-μ-Chloro-Bis (η^4-1,5-Cyclooctadiene) Dirhodium (I). *Inorg. Synth.* **1979**, *19*, 218–220.

(5) Pörschke, K.-R.; Pluta, C.; Proft, B.; Lutz, F.; Krüger, C. Bis(Di-Tert-Butylphosphino)Ethan-Nickel(0)-Komplexe / Bis(Di-Tert-Butylphosphino)Ethane-Nickel(0) Complexes. *Z. Naturforsch. B*. 1993, p 608.

(6) Martínez-Martínez, A. J.; Weller, A. S. Solvent-Free Anhydrous Li^+, Na^+ and K^+ Salts of $[B(3,5\text{-}(CF_3)_2C_6H_3)_4]^-$, $[BArF_4]^-$. Improved Synthesis and Solid-State Structures. *Dalton Trans.* **2019**, *48* (11), 3551–3554.

(7) Peersen, O. B.; Wu, X. L.; Kustanovich, I.; Smith, S. O. Variable-Amplitude Cross-Polarization MAS NMR. *J. Magn. Reson. Ser. A* **1993**, *104* (3), 334–339.

(8) Earl, W. L.; Vanderhart, D. L. Measurement of ^{13}C Chemical Shifts in Solids. *J. Magn. Reson.* **1982**, *48* (1), 35–54.

(9) Pike, S. D.; Krämer, T.; Rees, N. H.; Macgregor, S. A.; Weller, A. S. Stoichiometric and Catalytic Solid–Gas Reactivity of Rhodium Bis-Phosphine Complexes. *Organometallics* **2015**, *34* (8), 1487–1497.

(10) Lubben, A. T.; McIndoe, J. S.; Weller, A. S. Coupling an Electrospray Ionization Mass Spectrometer with a Glovebox: A Straightforward, Powerful, and Convenient Combination for Analysis of Air-Sensitive Organometallics. *Organometallics* **2008**, *27* (13), 3303–3306.

(11) Cosier, J. t; Glazer, A. M. A Nitrogen-Gas-Stream Cryostat for General X-Ray Diffraction Studies. *J. Appl. Crystallogr.* **1986**, *19* (2), 105–107.

(12) VandeVondele, J.; Hutter, J. Gaussian Basis Sets for Accurate Calculations on Molecular

Systems in Gas and Condensed Phases. *J. Chem. Phys.* **2007**, *127* (11), 114105.

(13) Sheldrick, G. M. SHELXT–Integrated Space-Group and Crystal-Structure Determination. *Acta Crystallogr. Sect. A.* **2015**, *71* (1), 3–8.

(14) Sheldrick, G. M. A Short History of SHELX. *Acta Crystallogr., Sect. A.* **2008**, *64* (1), 112–122.

(15) Dolomanov, O. V; Bourhis, L. J.; Gildea, R. J.; Howard, J. A. K.; Puschmann, H. OLEX2: A Complete Structure Solution, Refinement and Analysis Program. *J. Appl. Crystallogr.* **2009**, *42* (2), 339–341.

(16) Whited, M. T.; Kosanovich, A. J.; Janzen, D. E. Synthesis and Reactivity of Three-Coordinate (Dtbpe)Rh Silylamides: CO_2 Bond Cleavage by a Rhodium(I) Disilylamide. *Organometallics* **2014**, *33* (6), 1416–1422.

(17) Aston, J. G.; Szasz, G.; Woolley, H. W.; Brickwedde, F. G. Thermodynamic Properties of Gaseous 1,3-Butadiene and the Normal Butenes above 25°C Equilibria in the System 1,3-Butadiene, N-Butenes, and N-Butane. *J. Chem. Phys.* **1946**, *14* (2), 67–79.